

A Thesis on
**Material Cutting Through Wire EDM by Using
Taguchi Method**

Submitted for partial fulfillment of the requirement for the degree of

MASTER OF TECHNOLOGY
In Mechanical Engineering with specialization in
“**Production & Industrial Engineering**”

By
MOHAMMAD FAIZAN
Enrollment no- **1300100338**

Under the Supervision of
Er. FAIZAN HASAN
Assistant professor

INTEGRAL UNIVERSITY LUCKNOW



Department of Mechanical Engineering
Integral University, Lucknow–226026(U.P.)
2020

CERTIFICATE

Certified that the thesis entitled “**Material Cutting Through Wire EDM by Using Taguchi Method**” is being submitted by **Mr. MOHAMMAD FAIZAN (Enrollment No. 1300100338)** in partial fulfillment of the requirement for the award of degree of Master of Technology (Production & Industrial) of Integral University, Lucknow, is a record of candidate’s own work carried out by him under my supervision and guidance.

The results presented in this thesis have not been submitted to any other university or institute for the award of any other degree or diploma.



Er. Faizan Hasan

Assistant professor

Department of Mechanical Engineering

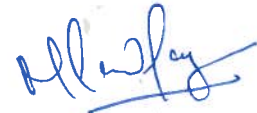
Integral University, Lucknow

DECLARATION

I declare that the research thesis entitled “**Material Cutting Through Wire EDM by Using Taguchi Method**” is the bonafide research work carried out by me, under the guidance of **Er. Faizan Hasan Assistant Professor, Department of Mechanical Engineering, Integral University, Lucknow**. Further I declare that this has not previously formed the basis of award of any degree, diploma, associate-ship or other similar degrees or diplomas, and has not been submitted anywhere else.

Date: 10/07/2020

Place: Lucknow



Name of Student
MOHAMMAD FAIZAN
Enrollment No. 1300100338
Department of Mechanical Engineering,
Integral University, Lucknow

ACKNOWLEDGEMENT

I am very much thankful to **Er. Faizan Hasan** for their valuable suggestions, without which it is not possible to complete the thesis. I honestly admit that these feeling of indebtedness are due to his affable co-operation and companionship he has extended despite his busy schedule and scarcity of time.

I am sincerely thankful to **Er. Faizan Hasan (Assistant Professor)** for his valuable suggestion and guidance during work. I am thank full to him for providing necessary facilities which were needed from time to time to complete the work. He always spared his precious time for me whenever I needed his help and guidance I am indeed fortunate to get an opportunity of working with him.

I am also obliged to **Er. Faizan Hasan** "Integral University Lucknow" for the valuable information provided by them in their respective field. I am grateful for their cooperation during period of my project.

I am also grateful to all my teachers for their kind encouragement during my work. This thesis is the result of approximately six months of work whereby I have been accompanied and supported by many people. It is a pleasant aspect that I have the opportunity to express my gratitude for all of them.

Lastly, I thank Almighty, my parents and friends for their constant encouragement without which this project would not be possible.



Mohammad Faizan

Enrollment No. 1300100338

ABSTRACT

This study investigates the wire electrical discharge machining (WEDM) of Ti-48Al intermetallic alloys. Ti-48Al is intermetallic alloys which are categorized as lightweight material, possess greater strength and toughness are usually known to create major challenges during conventional and non-conventional machining. Wire electrical discharge machining (WEDM) which is very prominent amongst the non-conventional machining methods is expected to be used quite extensively in machining titanium aluminides (Ti-Al) alloys due to favorable features and advantages that it can offer. This project was undertaken to study the machining performance of WEDM on Ti-48Al by using 0.2mm brass wire. The machining parameter was studied including pulse on time, pulse off time, peak current, servo reference voltage and servo feed rate. The effect of those varying parameters on the machining responses such as cutting speed, material removal rate (MRR), surface finish and width of kerf was investigated. This study presents an attempt to determine the optimum combinations of WEDM process parameters in machining Ti-48Al intermetallic by using the Taguchi Methodology as parametric design tool. An L_8 orthogonal array was employed in this study and the results were statistically evaluated using analysis of variance (ANOVA). Result showed that servo feed rate was the most significant parameter that influence the machining responses of Ti-48Al.

CONTENTS

CHAPTER	TITLE	PAGE
	TITLE PAGE	i
	DECLARATION	ii
	CERTIFICATE	iii
	ACKNOWLEDGEMENT	iv
	ABSTRACT	v
	TABLE OF CONTENTS	vii
	LIST OF TABLES	xiii
	LIST OF FIGURES	xv
	NOMENCLATURE	xix
1	INTRODUCTION	1
	1.1 General review	1
	1.2 Objective	3
	1.3 Scope	3
	1.4 Background of the problem	4
2	LITERATURE REVIEW	5
	2.1 Wire Electro Discharge Machining	5
	2.2 Equipment	9
	2.2.1 Positioning	9
	2.2.2 Wire movement	10
	2.2.3 Power supply	12
	2.2.4 Dielectric System	13
	2.3 Operation parameters	14

2.3.1	Cutting rates	14
2.3.2	Surface Roughness characteristics	15
2.3.3	Tolerances	16
2.3.4	Dielectric	16
2.3.5	Electrode wire	17
	2.3.5.1 Material of wire(electrode)	17
	2.3.5.2 Size of wire	19
2.4	Effect of machining process	20
2.4.1	Influence of wire material characteristics	20
2.4.2	Effect of wire tension	20
2.4.3	Influence of dielectric(Flushing technique)	21
	2.4.3.1 Function of dielectric fluid	21
	2.4.3.2 Choosing dielectric fluid	22
	2.4.3.3 Flushing method	22
	2.4.3.4 Flushing pressure	23
2.4.4	Effect of frequency	24
2.4.5	Heat affected zone	25
2.4.6	Thickness of the workpiece	26
2.4.7	Material of the workpiece	26
2.5	WEDM machining characteristics	26
2.5.1	Material Removal Rate(MRR)	26
2.5.2	Surface roughness(RA)	27
2.6	An overview on Titanium Aluminides Intermetallic Alloys	28
2.6.1	Introduction	28
2.6.2	Definition of Intermetallic alloy	28
2.6.3	Titanium Aluminides Intermetallic Alloy	29
2.6.4	Applications of Titanium Aluminides Alloys	32
2.6.5	Mechanical Properties	34
2.6.6	Microstructure of Ternary Ti-48Al-4Cr Intermetallic Alloys	36
2.7	WEDM previous research	40

2.7.1	Factor affecting the performance measure	40
2.7.2	Effects of the machining parameter on cutting rates(CR)	41
2.7.3	Effects of the machining parameters on the material removal rate(MRR)	42
2.7.4	Effects of the machining parameters on the surface finish	42
2.8	Taguchi Methods	43
2.8.1	Introduction	43
2.8.1.1	The loss function	44
2.8.1.2	Orthogonal Arrays(OA)	44
2.8.1.3	Robustness	45
2.8.2	Defining the quality characteristic	45
2.8.2.1	Bigger-the-better	45
2.8.2.2	Smaller-the-better	45
2.8.2.3	Nominal-the-best	46
2.8.3	Taguchi Design Method	46
2.8.3.1	Planning the experiment	47
2.8.3.2	Designing the experiment	47
2.8.3.3	Conducting the experiment	47
2.8.4	Steps in designing, conducting and analyzing	49
2.8.4.1	selection of factor	49
2.8.4.2	Selection number of level	51
2.8.4.3	Selection of OA	51
2.8.4.4	assignment of factors and interaction	52
2.8.4.5	conducting the experiment	52
2.8.4.6	analysis the experiment data	53
2.8.4.7	main effects	55
2.8.4.8	confirmation experiment	55

3	EXPERIMENT PREPARATION	56
3.1	Experiment detail	56
3.2	Preparation of the workpiece	57
3.3	Design of experiment based on Taguchi Method	59
3.4	Conducting the experiment	59
3.4.1	Recognition of statement of the problem	59
3.4.2	Identify potential factors	60
3.4.3	Dry run the planned experiment	62
3.4.4	Select appropriate working range	62
3.4.5	Selection of response variable	63
3.4.5.1	Material Removal Rate	63
3.4.5.2	Surface roughness	63
3.4.5.3	Cutting speed	64
3.4.5.4	Width of cut(kerf)	64
3.4.6	Selection of the Orthogonal Arrays	65
3.4.7	Full fledge of experiments	66
3.4.8	Analyze the experiment result	66
3.4.9	Verification run	67
3.5	Investigation Characteristic of the machined Ti-48Al	67
3.5.1	Direct machine Analysis	67
3.5.2	Cross Section Surface Analysis	68
3.6	Measurement equipment	69
3.6.1	Surface roughness tester	69
3.6.2	Balance	69
3.6.3	Optical microscope (Zeiss)	70

4	RESULTS AND ANALYSIS	71
4.1	Introduction	71
4.2	Experiment Results of WEDM of Ti-48Al	72
4.3	Data analysis using Taguchi Method	74
4.3.1	Data analysis for cutting speed	74
4.3.2	Data analysis for Material Removal Rate	82
4.3.3	Data analysis for Surface Roughness	88
4.3.4	Data analysis for Kerf	94
4.4	Interaction	100
4.4.1	Interaction between two factor for cutting speed	100
4.4.2	Interaction between two factor for Material Removal Rate	102
4.4.3	Interaction between two factor for Surface Roughness	105
4.4.4	Interaction between two factor for Kerf	107
4.5	Confirmation Test	109
4.3	Analysis of Surface Characterization of Machined Ti-48Al	112
4.3.1	Direct Machined Surface	112
4.3.2	Cross Sectional Analysis of the Specimen	118
5	DISCUSSION	132
5.1	Parameters and Performance Measure	133
5.1.1	Cutting Speed and Material Removal Rate	133
5.1.2	Surface finish and Kerf	135
5.1.3	Response Optimization	136
5.2	Surface Morphology and Characterization of Ti-48Al	139
5.2.1	Direct Machine Surface	139
5.2.2	Cross Sectional Analysis	142

6 CONCLUSIONS AND RECOMMENDATIONS 145

6.1 Conclusion 145

6.2 Recommendation for further studies 148

REFERENCES 149

LIST OF TABLES

TABLE NO.	TITLE	PAGE
2.1	Typical of WEDM operating parameters	14
2.2	Properties of alloys based on the titanium aluminides Ti ₃ Al and TiAl compared with conventional titanium alloys and nickel-base superalloys	30
2.3	Effects of various alloying elements in two-phase TiAl alloys	35
2.4	Nominal compositions (at%) and microhardness of ternary Ti-48Al-4Cr intermetallic alloy	37
2.5	Layout of experimental table	54
2.6	Main Effect	55
3.1	Sodick AQ537L machining	57
3.2	Initial machining condition	57
3.3	Mechanical properties of Titanium Aluminides	58
3.4	Input parameter and their level	62
3.5	The experiment design L ₈ orthogonal array	65
4.1	Experimental results of WEDM of Ti-48Al in term of cutting Speed	73
4.2	Experimental results of WEDM of Ti-48Al in term of material removal rates.	73
4.3	Experimental results of WEDM of Ti-48Al in term of kerf	74
4.4	Experimental results of WEDM of Ti-48Al in term of Surface Roughness	74
4.5:	S/N ratio for cutting speed	76
4.6	Main effect of the factors in effecting cutting speed	77
4.7	ANOVA results for cutting speed	79
4.8	Estimation of WEDM conditions and predicted performance for fastest cutting speed.	81

4.9	S/N ratio for material removal rates	82
4.10	Main effect of the factors in effecting material removal rates	83
4.11	ANOVA results for material removal rates	85
4.12	Estimation of WEDM conditions and predicted performance for higher material removal rates	87
4.13	S/N ratio for surface roughness	88
4.14	Main effects of the factor in effecting surface roughness	89
4.15	ANOVA results for surface roughness	91
4.16	Estimation of WEDM conditions and predicted performance for finest surface roughness	93
4.17	S/N ratio for kerf	94
4.18	Main effects of the factor in effecting kerf.	95
4.19	ANOVA results for kerf	97
4.20	Estimation of WEDM conditions and predicted performance for better kerf.	99
4.21	Interacting between two factors for cutting speed	100
4.22	Interacting between two factors for material removal rate	103
4.23	Interacting between two factors for surface roughness	105
4.24	Interacting between two factors for kerf	107
4.25	Comparison between the theoretical result and the experimental result for fastest cutting speed	110
4.26	Comparison between the theoretical result and the experimental result for higher material removal rates (MRR).	110
4.27	Comparison between the theoretical result and the experimental result for finest surface roughness	111
4.28	Comparison between the theoretical result and the experimental result for smaller kerf.	111
5.1	The factors and its level after analyze by ANOVA	136
5.2	Comparison responses between experiments (confirmation run) with the predicted.	137
5.3	Summary of the responses obtained throughout this experiment	137

LIST OF FIGURES

FIGURE NO.	TITLE	PAGE
2.1	Basic Features of WEDM Set up	6
2.2	Voltage Pulses	8
2.3	Part-positioning tables, wire delivery and take up system, and three axis taper mechanisms for WEDM.	11
2.4	Complex shapes that can be cut with WEDM	12
2.5	Change in cutting speed with wire tension	21
2.6	Change in cutting speed with purity of dielectric	22
2.7	Influence of flushing pressure on machining speed and Surface roughness.	23
2.8	Effect of current and frequency on surface finish and MRR.	24
2.9	Surface finish as related to frequency and current	24
2.10	WEDM heat affected zone.	25
2.11	Field use with temperature for Ti_3Al and $TiAl$ based intermetallics As well as composites that lines these alloys as the matrix	29.
2.12	Comparison of specific strength of intermetallics, intermetallic matrix composites and different alloys used as structural material for aircraft.	30
2.13	Ti – Al phase diagram	31

2.14	(a) Worldwide market of titanium and its alloy in 2005 (b) Most of Jaguar S-type components made by titanium and its alloy	32
2.15	Parts or components of aircraft and automotive made by Titanium Aluminides	34
2.16	Plot of weight change during cyclic thermal exposure in air at 850°C of four γ alloys	35
2.17	Vickers hardness and tensile elongation at room temperature as a function of Al content for single phase and two-phase TiAl alloys	35
2.18	Optical micrographs of unoxidized ternary alloys of Ti-48Al-4Cr (a) at 100x, (b) at 200x and (c) at 500x	38
2.19	Secondary electron (SE) image of scanning electron micrographs (SEM) with the corresponding energy dispersive (EDX) spectrum of the surface morphology for ternary Ti-48Al-4Cr alloys isothermally oxidized at 700°C in flowing dry air for (a) 150hr and (b) 500hr	39
2.20	Secondary electron (SE) image of scanning electron micrographs (SEM) with the corresponding energy dispersive (EDX)	39
2.21	Procedure in conducting the experiment	48
3.1	WEDM Sodick AQ537L	56
3.2	Workpiece material	58
3.3	Cause and effect diagram for WEDM process	60
3.4	The controllable and uncontrollable factors affecting WEDM	61
3.5	(a) and (b): Kerf profile	64
3.6	The flowchart process in conducting the experiment	68
3.7	Taylor Hobson surface roughness tester	69
3.8:	Presica Balance	70
3.9	Optical microscope	70
4.1	Graphs show average effect of various factors (in affecting cutting speed) at different level	78
4.2	Significant factor affecting WEDM cutting speed	80

4.3	Graphs show average effect of various factor (in affecting material removal rates) at different level	84
4.4	Significant factor affecting WEDM material removal rates	86
4.5	Graphs show average effect of various factor (in affecting surface roughness) at different level	90
4.6	Significant factor affecting WEDM surface roughness	92
4.7	Graphs show average effect of various factor (in affecting kerf) at different level	96
4.8	Significant factor affecting WEDM of kerf	98
4.9	Interacting between 2 factors for cutting speed	101
4.10	Interaction severity index for cutting speed	102
4.11	Interacting between 2 factors for material removal rate	104
4.12	Interaction severity index for material removal rate	104
4.13	Interacting between 2 factors for surface roughness	106
4.14	Interaction severity index for surface roughness	107
4.15	Interacting between 2 factors for kerf	108
4.16	Interaction severity index for kerf	109
4.17	(a), (b) and (c): Microstructure of Ti-48Al before machining at magnification of 10x, 20x and 50x before machined by wire-cut process.	112
4.18	FESEM micrographs of surface morphology of WEDM Ti-48Al at 500x with WEDM condition	114
4.19	FESEM micrographs of surface morphology of WEDM Ti-48Al at various magnifications where crystal observed	115
4.20	FESEM micrographs of WEDM Ti-48Al surface with corresponding EDX spectrum	116
4.21	FESEM micrographs of WEDM Ti-48Al surface with corresponding EDX spectrum at various features	117
4.22	FESEM micrographs of cross sectioned specimen identify the recast layer	119
4.23	FESEM micrographs of cross sectioned specimen identify the	

	recast layer with the thickness ranging from 2 μ m to 6 μ m	120
4.24	FESEM micrographs of cross sectioned specimen observed the micro crack penetrate deeper than recast layer as deep as 25 μ m	121
4.25	FESEM micrographs of cross sectioned specimen observed the micro crack penetrate deeper than recast layer as deep as 7 μ m	122
4.26	EDX line-scan profile of the elements present along the recast layer	124
4.27	EDX line-scan profile of the elements present along the recast layer and base-alloy of the cross-sectional	125
4.28	EDX line-scan profile of the elements present along the recast layer base-alloy of the cross-sectional surface	126
4.29	EDX line-scan profile of the elements present along the recast layer and base-alloy	127
4.30	EDX spot-scan profile of the element present in the point was taken on the in the cross-sectional surface	128
4.31	EDX spot-scan profile of the element present in the point was taken on the cross-sectional surface	129
4.32	EDX spot-scan profile of the element present in the point was taken on the in the cross-sectional	130
4.33	EDX spot-scan profile of the element present in the point was taken on the in the cross-sectional surface of WEDM Ti-48Al	131
5.1	The existence of oxide layer on the top of machined surface analyzed by EDX line scan.	140
5.2	Pores or voids found and formed on the surface	141
5.3	Oxide layer formed on the top surface	143

LIST OF SYMBOLS / NOMANCLATURES

A	-	ampere
ANOVA	-	Analysis of variance
CS	-	Cutting Speed
DOE	-	Design of Experiment
DOF	-	Degree of Freedom
EDM	-	Electrical Discharge Machining
EDX/EDS	-	Energy Dispersive Spectroscopy Microanalysis
FESEM	-	Field Emission Scanning Electron Microscope
gm	-	gram
HAZ	-	Heat affected zone
in.	-	inch
IP	-	Peak current
Min	-	minutes
Mm	-	millimeter
MRR	-	Material Removal Rate
MSD	-	Mean Square deviation
OA	-	Orthogonal array
OFF	-	Off time
ON	-	On time
QC	-	Quality characteristic
Ra	-	Surface roughness mean deviation
S/N	-	Signal to noise ratio

SEM	-	Scanning Electron Microscope
SF	-	Servo Feed Rate
SV	-	Servo Reference Voltage
TiAl	-	Titanium aluminide
V	-	Voltage
WEDM	-	Wire Electrical Discharge Machining
WK	-	Flushing rate
WS	-	Wire speed
WT	-	Wire Tension
α	-	Alpha
γ	-	Gamma
μm	-	Micrometer
μs	-	Microsecond

CHAPTER 1

INTRODUCTION

1.1 General Review

Wire electrical discharge machining (WEDM) has been found to be an extremely potential electro-thermal process in the field of conductive material machining. Owing to high process capability it is widely used in manufacturing of cam wheels, special gears, stators for stepper motors, various press tools, dies and similar intricate parts. Selection of optimum machining parameter combinations for obtaining higher cutting efficiency and other dimensional accuracy characteristics is a challenging task in WEDM due to presence of large number of process variables and complicated stochastic process mechanism. Hence, there is a demand for research studies which should establish a systematic approach to find out the optimum parametric setting to achieve the maximum process criteria yield for different classes of engineering materials. An effective way to solve this state of problem is to focus on establishing the relationship between machining input parameters and machining criteria performances. A number of research works has been carried out on different materials to study the influence of different process parameters on EDM and WEDM [1].

In the present research study wire electrical discharge machining of γ -titanium aluminide alloy (Ti-48 Al-4Cr (at. %)) has been considered. The material is attracting considerable interest now a day due to their high temperature strength retention, low-density, excellent resistance to ignition and good creep and oxidation resistance. TiAl-based alloys are potential candidates for replacing Ti-based and Ni-based superalloys for structural applications in the range of 400 °C–800 °C [2]. This alloy is of great interest in aerospace and automobile industries. Most of these components have performed well in laboratory tests as well as in the field. Engine valves, turbine blades, airframes, seal supports and cases are some examples [3]. But like other intermetallics these alloys are not ductile and have low fracture toughness at room temperature which makes them difficult to fabricate [4]. Further it is found that it is extremely difficult to machine by conventional method due to its excellent strength property.

Wire electrical discharge machining (WEDM) is a specialized thermal machining process capable of accurately machining parts with varying hardness or complex shapes, which have sharp edges that are very difficult to be machined by the main stream machining processes. This practical technology of the WEDM process is based on the conventional EDM sparking phenomenon utilizing the widely accepted non-contact technique of material removal. Since the introduction of the process, WEDM has evolved from a simple means of making tools and dies to the best alternative of producing micro-scale parts with the highest degree of dimensional accuracy and surface finish quality. Over the years, the WEDM process has remained as a competitive and economical machining option fulfilling the demanding machining requirements imposed by the short product development cycles and the growing cost pressures. However, the risk of wire breakage and bending has undermined the full potential of the process drastically reducing the efficiency and accuracy of the WEDM operation. A significant amount of research has explored the different methodologies of achieving the ultimate WEDM goals of optimizing the numerous process parameters analytically with the total elimination of the wire breakages thereby also improving the overall machining reliability.

The purpose of the research project is to investigate the machinability of Titanium Aluminides intermetallic alloys (Ti-Al) using wire-cut EDM process. By using the selected parameters WEDM such as pulse on-time, pulse off-time, peak current, servo reference voltage, servo speed, wire speed and dielectric pressure flushing as a factor to get the good performance machining of the Ti-48Al-4Cr ternary alloys. The resulting surface roughness of the Wire EDM surface and material removal rate (MRR) will be investigated to determine the optimum wire EDM conditions for obtaining Taguchi techniques of experimental design process were developed to predict the effect of wire EDM parameters on surface roughness, cutting speed and material removal rates.

1.2 Objective

To establish the optimum combinations of WEDM process parameters which are able to provide high material removal rate, fastest cutting speed, finest surface finish and smaller width of slit (kerf) in machining of Ti-48Al and investigate the surface characteristic due to the WEDM process of Ti-48Al.

1.3 Scope

The scope of this project is as follows:

1. Ternary alloys Ti-48Al will be studied using 0.2 mm brass wire

2. To investigate quality attributes of wire EDM machining including surface roughness, material removal rates, cutting speed, kerf, recast layer and microcracks.
3. The machining variables to be investigate include on time, off time, peak current, servo feed rate and servo reference voltage
4. To apply the Taguchi method in the designation of experiment.

1.4 Background of the problem

WEDM process is used to achieve high accuracy, fine surface finish, high removal rate and increased productivity. However there are some problems that might occur when we do WEDM process such as bad surface finish, wire breakage, microcracks and others. The problem still happened even the skilled operator is used. It is difficult to achieve the optimal performance machining. These problems made the product have bad surface finish, low mechanical strength and other problems.

In Present, most of the WEDM machine manufacturers are able to provide machining condition guidelines, but it is found that these guidelines are only applicable to common material such as steel, copper and aluminium. Advance material like titanium intermetallic is still new and rare in the industry; therefore it is difficult to obtain suitable guidelines which will result in good accuracy and fine surface finish.

It is useful to understand the parameter optimization clearly when machining intermetallic titanium aluminides alloys by using brass wire diameter 0.2 mm. The Taguchi method is used as a tool for experimental design and analysis the result to find optimum condition for observed value of machining characteristics.

CHAPTER 2

LITERATURE REVIEW

2.1 Wire Electro Discharge Machining

Wire-electro discharge machining is a process of material removal of electrically conductive materials by the thermo-electric source of energy. The material removal by controlled erosion through a series of repetitive sparks between electrodes, i.e. work piece and tool.

Figure.2.1 shows the basic features of the wire cut EDM machine. In the WEDM process there is no relative contact between the tool and work material, therefore the work material hardness is not a limiting factor for machining materials by this process. In this operation the material removal occurs from any electrically conductive material by the initiation of rapid and repetitive spark discharges between the gap of the work and tool electrode connected in an electrical circuit [5] and the liquid dielectric medium is continuously supplied to deliver the eroded particles and to provide the cooling effect. A small diameter wire ranging from 0.05 to 0.25 mm is applied as the tool electrode. The wire is continuously supplied from the supply spool through the work-piece, which is

clamped on the table by the wire traction rollers. A gap of 0.025 to 0.05 mm is maintained constantly between the wire and work-piece [5]. Deionized water of 15 micro semen/cm is applied as the dielectric fluid [5]. A collection tank that is located at the bottom is used to collect the used wire and then discard it. The wires once used cannot be reused again due to the variation in dimensional accuracy. The dielectric fluid is continuously flashed through the gap along the wire, to the sparking area to remove the byproducts formed during the erosion [5]. Brass wire is most commonly used for wire cutting, and zinc or aluminum coatings are employed for high-speed cuts.

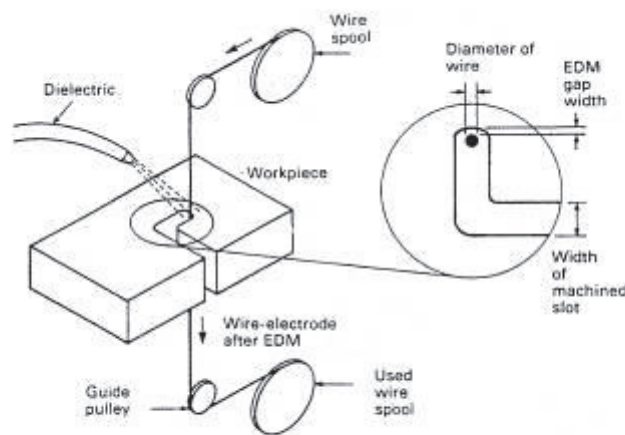


Figure 2.1 Basic Features of WEDM Set up

Wire-Electro Discharge Machining (WEDM) has become an important non-traditional machining process, widely used in the aerospace, nuclear and automotive industries. This is because the WEDM process provides an effective solution for machining hard materials (like titanium, nimonics, zirconium etc.) with intricate shapes, which are not possible by conventional machining methods. In WEDM the cost of machining is rather high due to high initial investment for the machine and cost of the wire–electrode tool. The WEDM process is more economical, if it is used to cut difficult to machine materials with complex, precise and accurate contours in low volume and greater variety. The selection of optimum machine setting parameters plays an important role for obtaining higher cutting speed or good surface finish. Improperly selected

parameters may also result in serious consequences like short-circuiting of wire and wire breakage. Wire breakage imposes certain limits on the cutting speed that in turn reduces productivity. As surface finish and cutting speed are most important parameters in manufacturing, various investigations have been carried out by several researchers for improving the surface finish and cutting speed of WEDM process. However the problem of selection of cutting parameters in WEDM process is not fully solved, even though the most up to date CNC-WEDM machine are presently available. WEDM process involves a number of machine setting parameters such as applied voltage (V), pulse on-time (ON), pulse off time (OFF), servo-control reference mean voltage (SV), wire speed (WS), wire tension (WT), and high pressure flushing (WP). The material of work piece and its height (H) also influence the process. All these parameters influence surface finish and cutting speed to varying degree [6].

EDM machining utilizes a voltage across the two electrodes, which is greater than the breakdown voltage across the gap between the work piece and the wire. This breakdown voltage is a function of the distance between the wire and work piece, the insulating properties of the dielectric (fluid separating the electrodes), and the degree of pollution of the gap.

Now imagine that there is a point on the work piece, which protrudes farther than the rest of the work piece surface. When a voltage is applied, the electric field is strongest at this location and will thus be the location of a discharge. This discharge is the culmination of the following process:

- The electric field causes electrons and positive free ions to be accelerated to high velocities between the wire and the high point on the workpiece. An ionized channel is formed across the gap between this point and the wire.
- At this stage, current can flow and the spark takes place between the electrodes.
- A bubble of gas forms due to vaporization of the electrodes and the dielectric. The pressure caused by the bubble rises until it becomes very high.

- A plasma zone is formed, which very quickly reaches extremely high temperatures (~8000-12000 degrees C). This causes instantaneous local melting of a certain amount of material at the surface of both the wire and the workpiece.
- The voltage is now dropped. The sudden reduction in temperature causes implosion of the bubble. This implosion creates dynamic forces which pull the melted material away from the two conductors.
- This eroded material then re-solidifies in the dielectric and is swept away.

This process occurs over and over about once every 2 microseconds. The initial voltage can be set as high as 200 V. The figure 2.2 shows a simplified representation of how this is implemented. At the beginning of each pulse, the machine applies a high voltage to create the bubble. It then drops the voltage to implode the bubble. It maintains the lowered voltage as the material is ejected. Finally, the voltage is returned to ground state and the process is begun again.

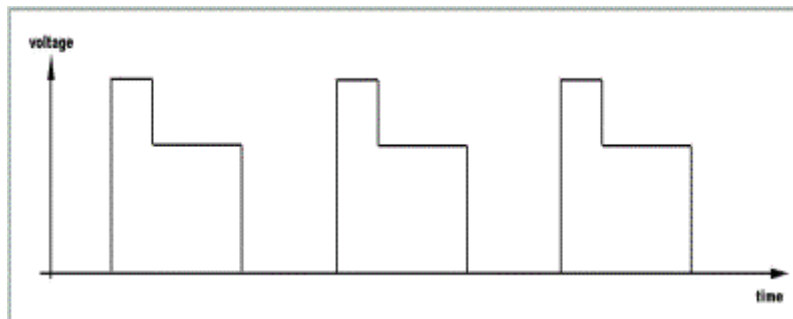


Figure 2.2 Voltage Pulses

The EDM moves the wire through the work piece eroding material away. There is always a gap present between the wire and the work piece, thus there is no contact and very little force on the work piece. A basic model based on heat transfer and melting is available to predict the crater depth when a spark occurs between two points on a flat surface. Material is removed by the overlap of craters formed due to the spark. This

produces an undulating surface whose roughness is characterized by Ra defined as the difference between the crest and valley of a surface averaged over the sample length.

The distribution of the sparks is not known. Thus the material removal rate is not just the product of the volume of the crater and the sparking frequency. Moreover as the radius of the cut section is not easily predictable, the cutting velocity cannot be determined. It can be assumed that the probability of sparking between two points increases as the points are brought closer.

2.2. Equipment

A WEDM machine consists of four subsystems:

1. Positioning
2. Wire movement
3. Power supply
4. Dielectric

All four of these subsystems have distinct differences from conventional EDM.

2.2.1. Positioning.

WEDM positioning systems usually consist of a CNC two-axis table and in some cases, an additional multi-axis wire positioning system. Two-axis machines cut straight and taper cuts automatically; 4 ½-axis machines have the ability to position the upper

wire guide automatically depending upon the thickness of material. The CNC system receives program instructions either through a simple keyboard or by punched tape. Mirror image cutting is providing. A digitizer may be used to obtain X and Y coordinates of shapes not defined geometrically.

The most unique feature of the CNC system is that it must operate in an adaptive control mode to always insure the consistency of the gap between the wire and the work piece. If the wire should come in contact with the workpiece or if a small piece of material bridges the gap and causes a short circuit, the positioning system must sense this condition and back up along the programmed path to reestablish the proper cutting gap condition.

Linear cutting rates with WEDM are slow, typically less than 100 mm/hr in 25 mm thick steel. Therefore the block processing time of the CNC system is not as important as it is no unusual for jobs to be run continuously for 10-20 hrs unattended. To facilitate unattended operation, WEDM CNC systems are usually provided with a battery powered backup system in case a power failure occurs during a run. If a power failure occurs, the system will automatically restart itself at the proper location so that work can be resuming without human intervention.

2.2.2. Wire movement

The function of the wire drive system is to continuously deliver fresh wire under constant tension to the work area. The need for constant wire tension is important to avoid such problems as taper, machining streaks, wire breaks, and vibration marks. Several stages of preparation are incorporated into wire delivery systems to ensure wire straightness. After the wire leaves the supply spool, it passes through several wire feed

and wire removal capstan rollers. These act to buffer the eroding zone from any disturbing influences created by the wire supply. Changes in part contour produce different cutting conditions requiring the drive system to modify the speed of cutting. This requires sophistication within the drive system and the computer power supply interface. The diagram introduced in **Figure 2.3** illustrates a taper mechanism. A CNC offset wire guide which position able in the U, V, and Z axes is used to actively change the wire angle, and hence the taper, during the cutting process.

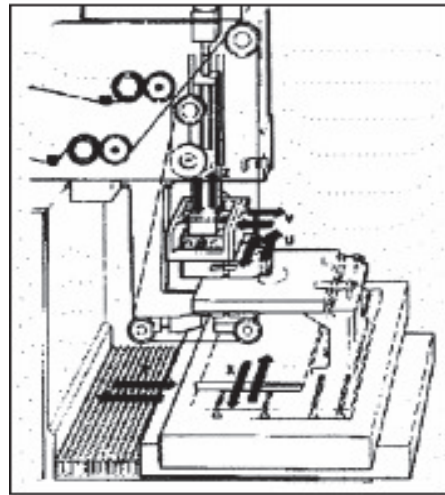


Figure 2.3: Part-positioning tables, wire delivery and take up system, and three axis taper mechanisms for WEDM.

Taper cutting techniques provide the ability to generate extremely difficult to produce shapes and irregular taper patterns, such as a square at the top of the taper and a circle on the bottom. **Figure 2.4** shows an example of some of the shapes that can be produced with taper cutting.

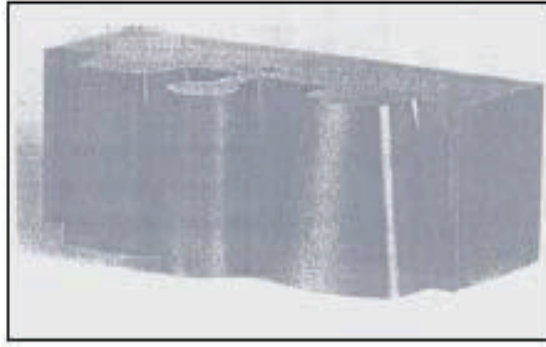


Figure 2.4: Complex shapes that can be cut with WEDM.

As the wire passes through the work piece, it is guided by a set of sapphire or diamond wire guides. Before being collected by the take up spool, it passes through a series of tensioning rollers. Many WEDM systems use a massive granite slab as the machine base to further guarantee wire accuracy and stability. The wire is no longer round after one pass through the work piece and it is discarded because the major portion of the spark discharge occurs at the leading surface of the wire as the wire passes through the work piece. Nowadays some company using the wire backs for roughing cutting, it is for economic objectives.

2.2.3. Power Supply

Power supplies for WEDM machines are varied in design and technology. The most pronounced differences between the power supplies used for wire-EDM and the conventional EDM are the frequency of the pulse used and the current. To achieve the smoothest surface finish, it possible maintains the pulse frequencies at high positions (1 MHz) may be used with WEDM. Such a high frequency ensures that each spark removes as little material as possible, thus reducing the size of the craters. Current carrying capability is limited by the diameter of the wire, which is used in cutting operation.

Because of this limitation, WEDM power supplies are rarely built to deliver current more than 20 Amp. There are two types of power supplies, pulse-type and capacitor discharge models. Pulse-types power supplies require fewer adjustments and are easier to operate; however, capacitor discharge models do offer some cutting advantages on certain materials.

2.2.4. Dielectric System

The dielectric systems are critical to successful operation. A constant supply of filtered, de-ionized water ensures unattended operation. System generally includes a deionization canister and a circuit to hold the level of de-ionization constant. Deionized water is used for three reasons: no fire hazard, low viscosity, and high cooling rate. Many users run their most time-consuming jobs overnight or over the weekend unattended. With conventional EDM, the use of flammable dielectric oils presents a fire hazard. When using water for the dielectric, the fire hazard problem is eliminated. De-ionized water dielectric systems reuse the water to minimize operating cost. This is accomplished by first filtering the collected water with 5 disposable paper filters. After filtration, the water resistivity is corrected by passage through a mixed-bed deionizer cartridge. For an extended period process, special additives can be mixed with the water to avoid rust formation on the part surfaces. If rust forms, an extra polishing operation is generally required to remove the oxides.

2.3 Operation Parameters

Table 2.1: Typical of WEDM operating parameters

Power supply Type:	55 to 60 V (open circuit volts to 300)
Frequency:	Pulse time controlled 1 to 100 μ s in time or 180 to 300 kHz with 300 kHz most frequent.
Current:	1 to 32 A
Electrode wire Type:	Brass, copper, tungsten, molybdenum
Diameter:	0.2mm,0.25mm,0.3mm
Speed:	0.1 to 6 in/s(2.5 to 150mm/s)
Dielectric	Deionized water, oil, or rarely, air, gas or plain water
Overcut (working gap)	0.0005 to 0.0020 inch (0.02 to 0.05 mm): usually 0.001 in(0.025mm)

2.3.1 Cutting Rates

A rule that is commonly employed to predict cutting rates in WEDM operations is for materials up to 6 in. (152mm) thick, about 1 in² (645 mm²) of cross-sectional material per hour can be removed. Cutting rates as high as 4.2 feet/min (1.28 m/min) can be achieved when thin materials are being cut. Cutting speed is a direct result of the type of material, thickness of material, and size of wire used and to some degree, flushing. The

linear-cutting rate for WEDM is approximately 38-115 mm/hr in 25 mm thick steel (1.5-4.5 in. /hr in. 1 in. thick steel), or approximately 20 mm/hr in 76 mm steel (0.8 in. /hr in 3-in. steel). The linear speed is dependent upon the thickness of the material not upon the shape of the cut. The linear cutting rate is the same whether a straight cut or complex curves are being generated. Special precautions must be taken when cutting sintered carbides and various cutting tool insert materials. These materials must be machined with as little voltage as possible to avoid electrolysis from selectively removing the cobalt binder at the cut edge [7].

2.3.2 Surface Roughness Characteristics

Surface roughness using WEDM can be held to about 30-50 μ in. (0.76-1.27 μ m) Ra. Under special conditions, surface roughness can be held to about 15- μ in. (0.38 μ m) Ra [8]. As is the case with all EDM processes, WEDM produces a shallow recast layer or heat-affected zone, which may be detrimental to the functional performance of work pieces that will be subjected to possible fatigue in service. Low spark intensities minimize the heat-affected zone. Materials such as steel, aluminum and brass show no appreciable surface impairment. The affected surface layer, however, is relatively thin (<10 μ m) and can be compared more to "fine-sparking" EDM [9]. Normally there are no observable cracks in the eroded surface after wire erosion. But in certain cases another problem has been experienced. After heat-treating through hardening steel the part contains high stresses (the higher the tempering temperature, the lower the stresses). These stresses take the form tensile stresses in the surface area and compressive stresses in the center and are in opposition to each other. During the wire erosion process a greater or smaller amount of steel is removed from the heat-treated part. Where a large volume of steel is removed, this can sometimes lead to disturbed and tries to reach equilibrium again. The problem of crack formation is usually only encountered in

relatively thick cross section, e.g. over 50 mm (2") thick. With such heavier sections, correct hardening and double tempering is important.

2.3.3 Tolerances

Many WEDM machines are available with a positioning resolution of 0.001 mm (0.000040 in.) and can routinely obtain accuracies of ± 0.007 mm (± 0.003 in.). With special care, accuracies of ± 0.0025 mm over 152 mm (± 0.0001 in. over 6 in.) are possible. However to achieve the best result, caring should be taken to ensure the uniformity of the wire diameter and the temperature and resistivity of the dielectric must be closely controlled.

2.3.4 Dielectric Fluid

De-ionized water is the dielectric fluid which is generally used for WEDM. Water was used because it can flow better into the small slots than other dielectrics and provides good cooling. Some machines submerge the work piece, machine arms, and guides in a dielectric bath to control thermal changes. In some cases, oil was used as a dielectric. Hydrocarbon dielectrics have been applied in laboratory environments to investigate the cutting performances during finishing stages [10]. In other cases, air, gas, or plain water is used. The major advantage of water is formed by its good cooling qualities, which are needed for the energy transmission during the wire cutting process.

Most machines will cool the dielectric to keep thermal problems to a minimum, sometimes using water jackets to cool heat-producing motor connections.

2.3.5 Electrode Wire

Cutting performance of the WEDM process depends on a combination of electrical and mechanical characteristics. Surface finish and tolerance control are strongly related to the quality of the electrode, which must possess electrical conductivity, close size tolerance (generally 0.00004 in.), and strength to allow tensioning to limit bow or taper in a work piece.

2.3.5.1 Material of Wire (electrode)

The evolution of new materials for the wire used in WEDM has kept pace with the development of the machining technology to advance the overall capabilities of the process. Brass, copper, tungsten, and more rarely, molybdenum wire are used as electrode material in WEDM [8]. The most popular wire materials are chosen partly by the diameter of the wire being used. When wire diameter is relatively large, i.e., 0.15-0.30 mm (0.006-0.012 in.), copper or brass is used. However when very fine wire, approximately 0.03-0.15 mm (0.001-0.006 in.) in diameter, is required, the additional strength derived from molybdenum steel wire is necessary. The first WEDM machines were relatively slow cutting and used readily available spooled copper wire from copper-

cable manufacturers [8]. Copper is an excellent conductor with a 100 IACS value - a common electrical-conductivity scale.

However, copper wears rapidly and has a poor tensioning ability in thicker work piece. (For example, 400 g.in 0.010 in. diameter wire). Brass alloy wire consisting of 63 % copper and 37 % zinc was developed in 1974 to improve the cutting speed. It has a 29 IACS value and was produced with a tensioning ability of 1000-1500 g on 0.010in diameter wire. Tensions of up to 4500g with 0.010 in diameter wire are currently available. A brass or copper wire electroplated with a 3 to 5 /lm zinc coating was found, around 1980 by university research in the Federal Republic of Germany in conjunction with Charmilles, capable of attaining significant cutting speed increase [7]. Zinc's low melting temperature and vapor pressure allows faster ionization. Its annealed surface has a somewhat rough, oxidized finish, which aids flushing and promotes speed while keeping guide wear low. It has an IACS of 29, and a 0.010in diameter wire has a tension of 1800 g. Zinc-coated wire with a copper core with an IACS of 84 was introduced around 1980 by Charmilles [7]. This shiny-coated wire is annealed on the machine and has a maximum tension of 1700 g on 0.010 in diameter wire. In 1985, a slightly higher strength wire, 1850 g, was introduced. It doesn't require machine annealing.

Molybdenum wire is widely used in fine detail applications in which multiple skim cuts are needed to hold tight tolerances. It is slow cutting compared with brass. Molybdenum has about twice the tensioning ability of soft brass and an IACS of 34. It is useful when no zinc contamination can be allowed on the work piece, such as in some aerospace and medical applications. It also exhibits less effect from gas bubbles than copper alloy.

2.3.5.2 Size of Wire

The most commonly used EDM wire is 0.010 or 0.012 inch in diameter, usually made of plain brass. Other commonly used wire sizes are 0.008 and 0.006 inch. Brass wire coated with zinc or other alloys is also popular because it allows faster cutting. Steel core wire also has advantages because it is exceptionally resistant to breakage. Wire 0.004 inch in diameter and smaller is considered fine wire. To use the small wire, most machines require the special wire guides should be installed. Some machines cannot use wire smaller than 0.002 inch. Maroney Company has worked with wire 0.001 inch which is made of a special tungsten alloy and is imported from Japan [9]. Tungsten has much higher tensile strength than brass, so it can be pulled harder without stretching or breaking. Wire that is a fraction of this dimension is difficult to see with the naked eye, so it is a very practical reason for reliable operation of automatic wire threading when fine wire is used. Not only is wire this fine so difficult to see, it is also almost impossible to feel with the fingertips. Automatic operation minimizes the need to manipulate the wire by hand, cutting down on the frustration and wasted motion the operator will experience. Maroney Company has also worked with wire 0.0005 inch in diameter with very exciting results. During the years, the wire diameter has been varying towards larger diameter but also towards smaller ones. Where in the early seventies, brass wires with "non standardized diameter" were used (180 μm diameter), today, and wires of 250 to 300 μm are currently used [10]. The most important reason for wire diameter increase is the pulse power to be delivered in the gap. Micro WEDM applications require small pulse energies (less than 20 μJ) and geometrical precisions of tenths of microns. The use of ultra fine wires (30 μm diameters) is therefore absolutely required.

2.4 Effected of machining process

2.4.1 Influence of wire material characteristics

As WEDM use a thin wire as a single electrode, it is not necessary to make different shape of tool electrode to achieve the complex contours. However, to prevent the wire break becomes critical to obtain a continuous machining process. Research has been conducted to improve the technology of the tool by overcoming the thermal effects to prevent the wire from breaking during the process. The optimal selection of wire properties would also determine its final performance and success.

2.4.2 Effect of wire tension

Within a considerable range, an increase in wire tension significantly increases the cutting speed. The higher tension decreases the wire vibration amplitude and hence decreases the cut width, so that the speed is higher for the same discharge energy. However, if the applied tension exceeds the tensile strength of the wire, it leads to wire breakage (**Figure 2.5**).

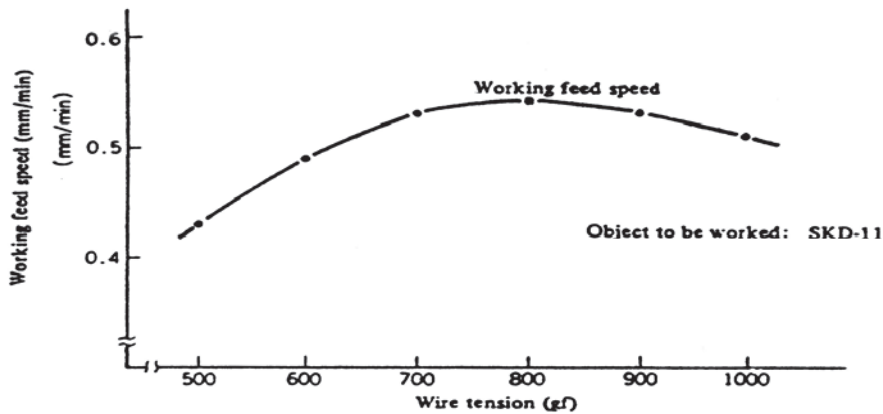


Figure 2.5 Change in cutting speed with wire tension [11].

2.4.3 Influence of dielectric (Flushing technique)

2.4.3.1 Function of dielectric fluid

The dielectric fluid and the flushing perform the following function:

- To insulate the gap before a large amount of energy is accumulated and to concentrate the discharge energy to a small area.
- To recover a desired gap condition after the discharge by cooling the gap and deionizing.
- To flushes away the debris of the workpiece that was removed by the spark discharges.

2.4.3.2 Choosing dielectric liquid

Most WED machines use very pure deionized water for dielectric liquids (purity is usually measured by ratio resistance). The major advantage of water is formed by its better cooling qualities, which were needed for the energy transmission during the wire cutting process. **Figure 2.6** explains the relation between the purity of the dielectric and the material removal rates (MRR).

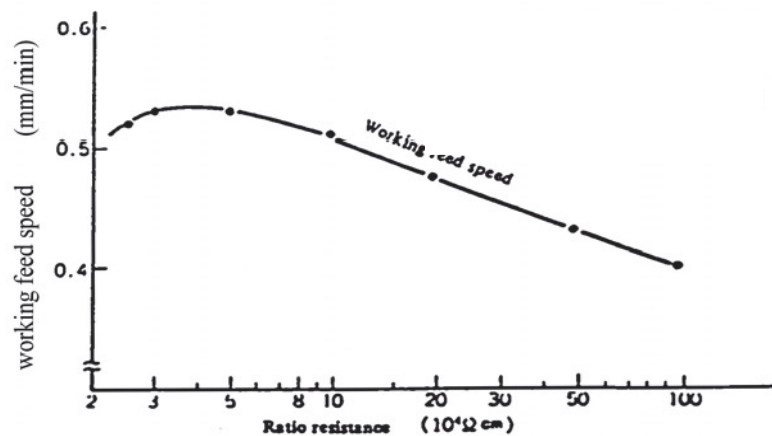


Figure 2.6 Change in cutting speed with purity of dielectric [11].

High MRR are observed at lower specific resistance of the dielectric liquid. Very low ratio resistance is not recommended, however. Some organic additives in the dielectric water may also improve the cutting speed.

2.4.3.3 Flushing method

Different flushing methods can be used; the commonly used methods are immersion flushing, spray or jet flushing [12].

2.4.3.4 Flushing Pressure

Figure 2.7 shows the curve of influence of flushing pressure on machining speed and surface roughness. The cutting performances during roughing cuts have been improved since the removed particles in the machining gap are evacuated more efficiently (The pressure must be turned down during finishing in order to avoid geometrical part errors) [13].

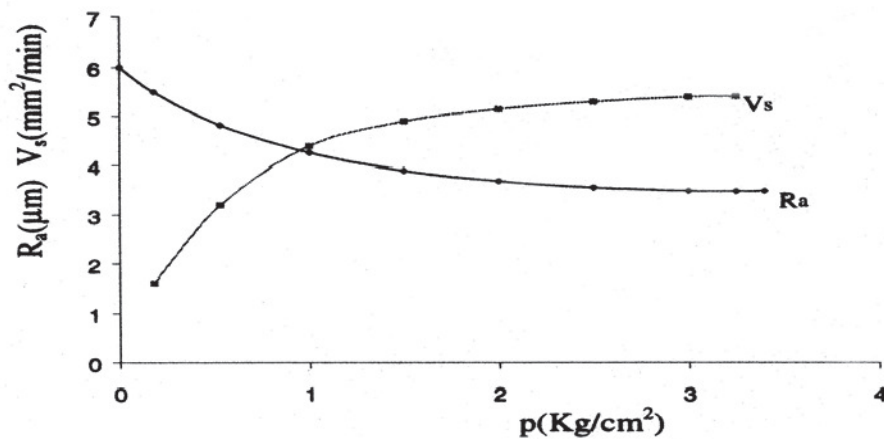


Figure 2.7 Influence of flushing pressure on machining speed and surface roughness [13].

It can be seen that when flushing pressure is less than certain pressure, it is impossible to do any machining. Along with increased flushing pressure the machining speed also increases, but when it is over 1 kg/cm², the increased trend slows down while the surface roughness is improved gradually with increased flushing pressure. When flushing pressure is less than 0.3 kg/cm², high temperature is easily registered electric discharge area [14].

2.4.4 Effect of frequency

As illustrated in **Figure 2.8**, increased discharge frequency can improve the surface finish. Within limits, by doubling the amperage and frequency, the metal removal rate will double without changing the finish [15].

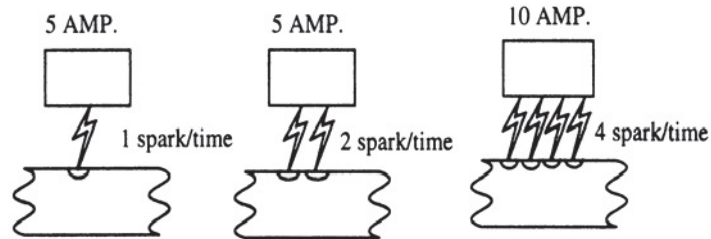


Figure 2.8 Effect of current and frequency on surface finish and MRR [15].

At high frequencies, the amperage is reduced due to inductance, thereby reducing the metal removal rate. The economics involved, therefore, set a practical limit on surface finish. The relationship between current and frequency on surface finish is shown in **Figure 2.9** [15].

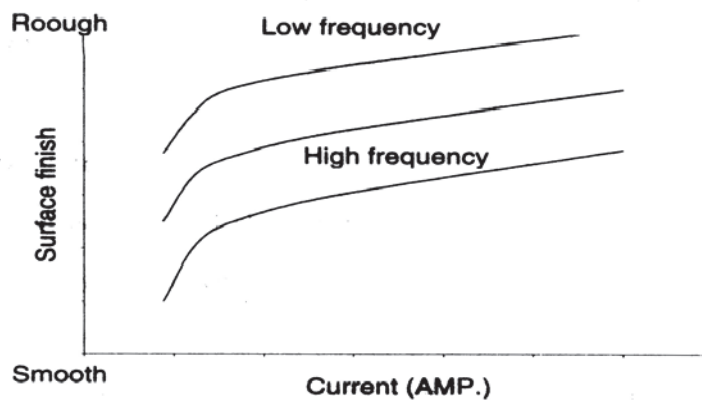


Figure 2.9 Surface finish as related to frequency and current [15].

2.4.5 Heat affected zone

The Wire EDM process is a thermal process and, therefore, some annealing of the workpiece can be expected in a zone just below the machined surface. In addition, not all of the workpiece material melted by the discharge is expelled into the dielectric. The remaining melted material is quickly chilled, primarily by heat conduction into the bulk of the workpiece, resulting in an exceedingly hard surface.

The depth of the annealed layer is proportional to the amount of power used in the cutting operation. It will range from 0.002 in. for finish cutting, to approximately 0.008 in. for high metal removal rates. The amount of annealing is usually about 2 points of hardness below the parent metal for finish cutting. In the roughing cuts, the annealing effect is approximately 5 points of hardness below the parent metal. **Figure 2.10** shows the relationship of the heat-affected zone to the cutting conditions.

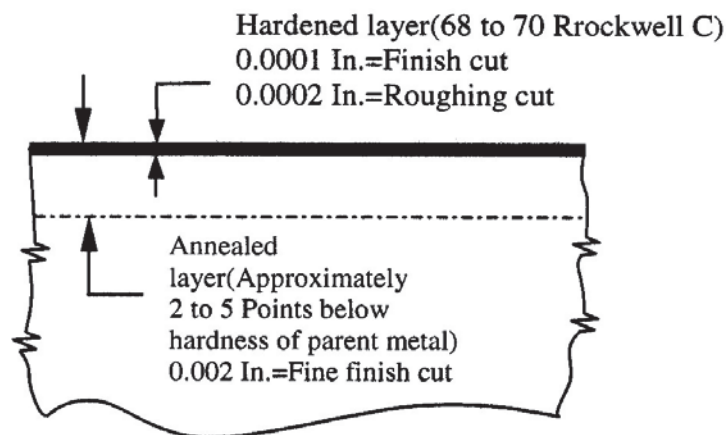


Figure 2.10 WEDM heat affected zone [15].

Since The annealing effect is most common when unstable machining conditions exist, it can be reduced by choosing conditions that produce better stability [15], for example, chose electrodes that produce more stable machining, machining at lower rates. It can

also be reduced by using a finish cut to remove the annealed material left by the previous high-speed roughing cut.

2.4.6 Thickness of the Workpiece

In the WEDM process, cutting speed decreases as the thickness of the workpiece increases. Normally, WEDM uses a transistor controlled capacitor circuit in which the cutting speed is controlled by a capacitor value. When using a fixed capacitor to machine a thicker workpiece, the cutting speed is decreased.

2.4.7 Material of the Workpiece

Specific properties of the workpiece material also influence the process. These properties include how well the metal is polished, its magnetic condition, and how the metal was removed from the heat treatment process when it was produced. One must also consider expansion and contraction according to the temperature of the material. For material processed by EDM or WEDM, the initial surface condition affects the results. A low melting point in the material increases the MRR, and improper heat treatment of the metal results in distortion and breakage of the mold.

2.5 WEDM machining characteristics

2.5.1 Material Removal Rate, MRR

The amount of material removed in a given unit of time during WEDM process is called material removal rate (MRR). Material removal rate for WEDM are somewhat

slower than conventional machining methods. The rate of material removal is dependent on the following factor:

- Amount of current of each discharge
- Frequency of the discharge
- Wire material
- Workpiece material
- Dielectric flushing conditions

As the current increases, metal removal rate increase. A spark of 1 ampere (A) erodes a certain amount of metal. When the current is doubled, the energy in the discharge is also doubled and approximately twice the amount of metal is removed. Modern WEDM machine have power supplies capable generating more than 100A to material per hour for every 20A of machining current. However material removal rates of up to 245 cm³/h are possible for roughing cuts with special power supply.

2.5.2 Surface roughness, Ra

The surface finish is controlled by number of discharge per second, more often referred to as the frequency sparks. The greater amount of energy applied the greater amount of material removed. However, when greater amount of current are used, larger craters are eroded from the work, causing a rougher surface finish. To maintain increased metal-removal rates and at the same time improve the surface finish, it is necessary to increase the frequency of the discharge.

2.6 An Overview on Titanium Aluminides Intermetallic Alloy

2.6.1 Introduction

TiAl intermetallic compound have been intensively investigated for the potential applications of aerospace and automotive engine components due to their attractive properties such as high strength, low density and excellent creep resistance. Titanium aluminides have generally proved difficult to process, have limited heat treatability, and generally low ductility at room temperature. They have a density of 5.5g/cm^3 (0.2lb/in^3), which makes them lighter than steels or nickel based alloys they would be likely to replace. They do not suffer from the poor ductility and fracture toughness of gamma based alloys, and possess better burn resistance compared to traditional titanium alloys.

2.6.2 Definition of Intermetallic alloy

An intermetallic can generally be define as a compound formed by combination of two or more metallic (or metalloid) elements, generally (but not always) falling at or near the stoichiometric ratio and order on at least two or more sublattices [16, 17]. According to schulze (1967) and Girgis (1983), the crystal structures of intermetallics are different from those of constituent metals, and thus intermetallic phases and order alloys are included. The main difference between alloys and intermetallic compound is the metal in alloys can be separated by purely physical process, like heating and cooling the alloy, whereas intermetallic compounds cannot be separated easily. Intermetallic compound are strong, hard and brittle. The properties are strength at elevated temperature, good oxidation resistance, low density and high melting points temperature.

Most materials considered for high temperature applications belong to the aluminide, silicide or beryllide systems [18]. These systems are considered either as base materials or coatings, in part because of the protective scales that form on such systems. The scales that form are Al_2O_3 , SiO_2 and BeO and are known to be the most protective

oxide scales during oxidation under high temperature conditions. These three systems are examples of intermetallics [19]. Intermetallic include materials that exhibit a wide range of useful properties for applications such as resistors, magnets superconductors, heating elements, structural alloys and corrosion resistant coatings [19]. There are different types of intermetallic phases, many of which have not been investigated for useful properties.

2.6.3 Titanium Aluminides Intermetallic Alloy

The first intensive and successful structural materials developments of intermetallics were based on the titanium aluminides Ti_3Al and $TiAl$, and were started at the beginning of the 1970s [53]. Titanium aluminides is an intermetallic compound, which is a distinct material from any of the metals that comprise it. Ti_3Al and $TiAl$ aluminides, have been examined and developed for high temperature applications as shown in **figure 2.11**.

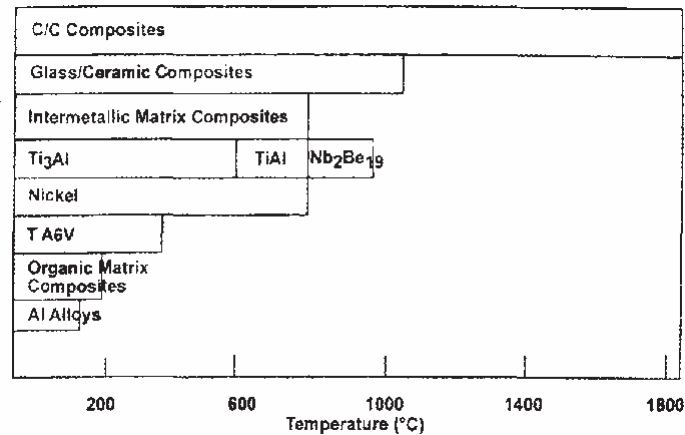


Figure 2.11 Field use with temperature for Ti_3Al and $TiAl$ based intermetallics as well as composites that lines these alloys as the matrix [19, 20].

The excellent high temperature properties and low density (see Table 2.2 and figure 2.12) have made titanium aluminides as an attractive candidate for use in both engine and airframe applications in the aerospace industry. Titanium aluminides offer a

lowest density ($3.73 - 3.9 \text{ g/cm}^3$) and a higher temperature limit ($900 - 1000^\circ\text{C}$) compared to the titanium alloys. The major concern of titanium aluminides is the low ductility and toughness at low temperature, which make the difficult to processing.

Table 2.2: Properties of alloys based on the titanium aluminides Ti_3Al and TiAl compared with conventional titanium alloys and nickel-base superalloys [54].

Property	Ti-base	Ti_3Al -base	TiAl -base	Superalloys
Structure	A3/A2	$\text{D0}_{19}/\text{A2/B2}$	$\text{L1}_0/\text{D0}_{19}$	Al/L1_2
Density (g/cm^3)	4.5	4.1-4.7	3.7-3.9	7.9-9.1
Young's modulus (GPa)	95-115	100-145	160-180	195-220
Yield strength (MPa)	380-1150	700-990	400-650	250-1310
Tensile strength (MPa)	480-1200	800-1140	450-800	620-1620
Creep Limit ($^\circ\text{C}$)	600	760	1000	1090
Oxidation Limit($^\circ\text{C}$)	600	650	900	1090
Ductility, % at room temperature	10-25	2-26	1-4	3-50
Ductility, % at high temperature	12-50	10-20	10-60	8-125
Fracture toughness K_{Ic} ($\text{MN/m}^{3/2}$)	high	13-42	10-20	25

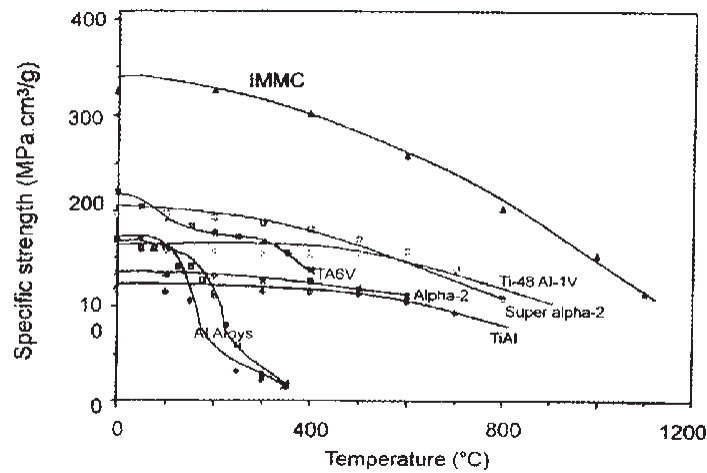


Figure 2.12 Comparison of specific strength of intermetallics, intermetallic matrix composites and different alloys used as structural material for aircraft [20].

The phase diagram of titanium aluminides is shown in figure 2.13. Basically, there are two main phases of titanium aluminides:

- a) Ti_3Al (α_2 alloys)
- b) TiAl (γ alloys)

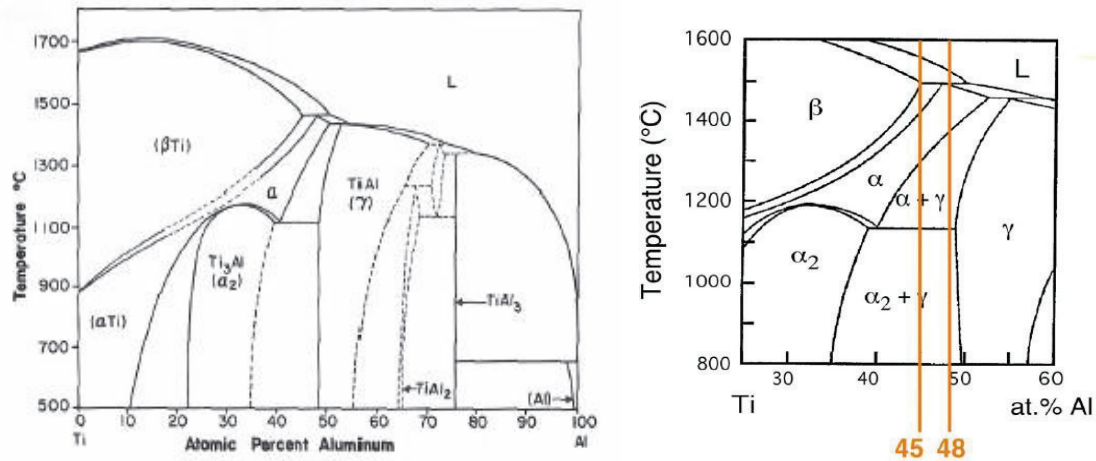
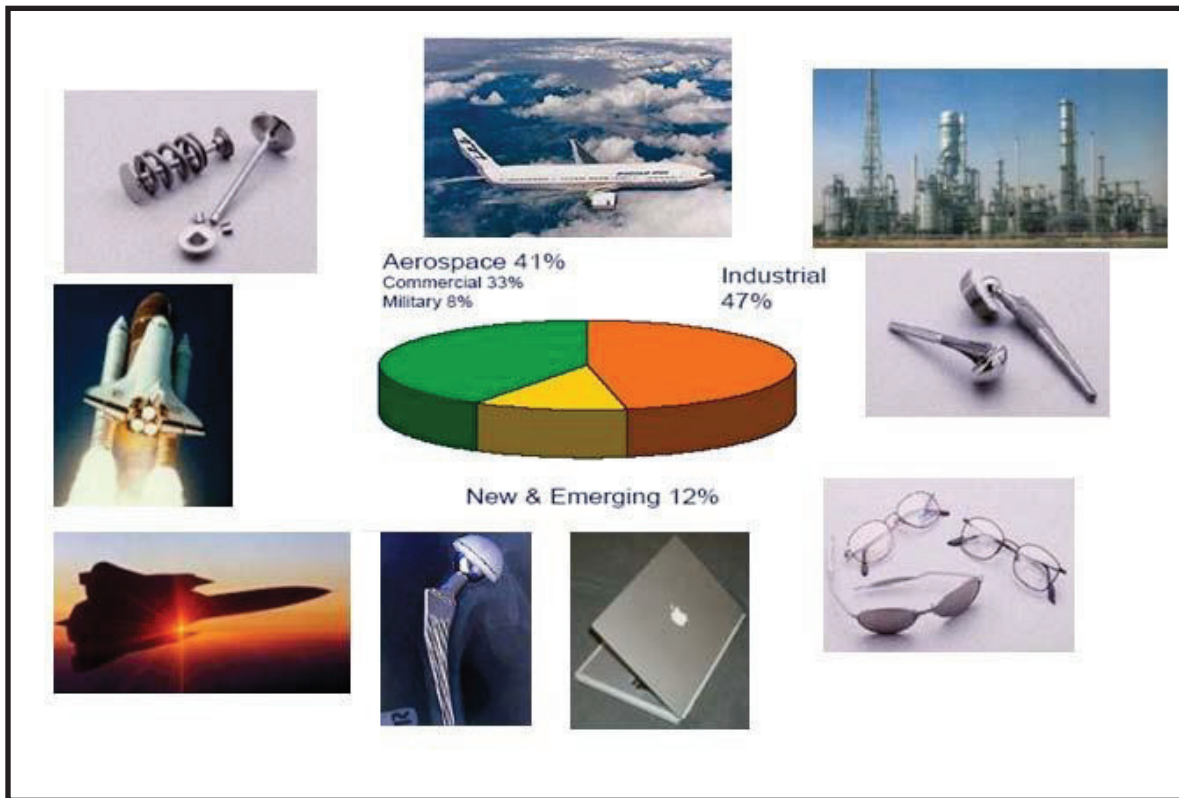


Figure 2.13: Ti-Al phase diagram [55].

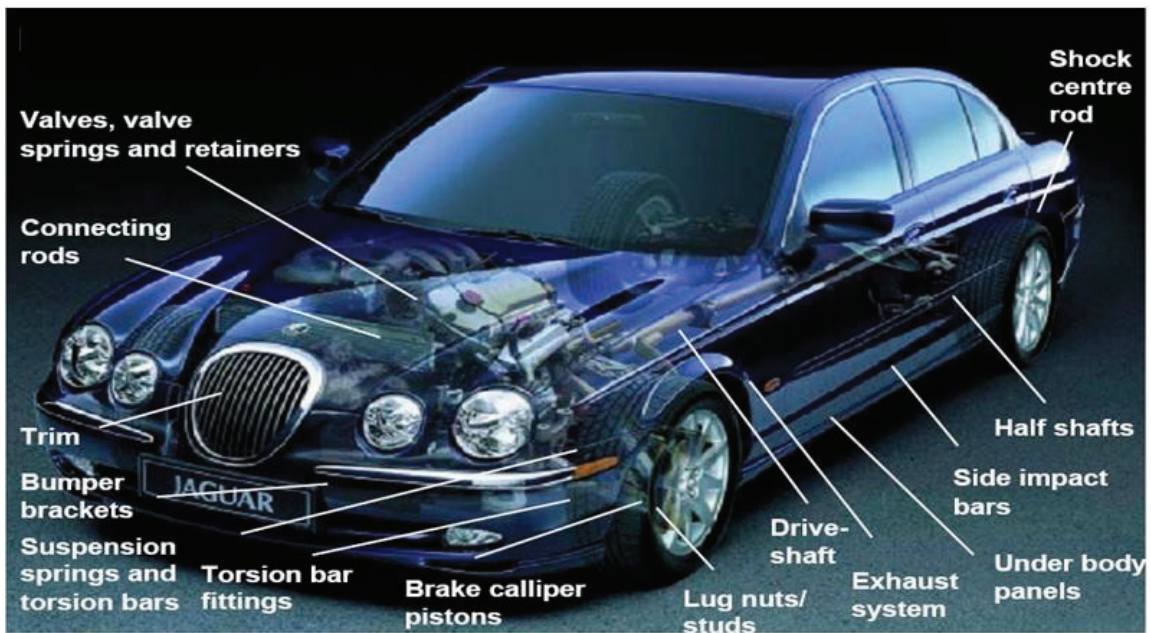
Based from the phase diagram in figure 2.13, it is observed that the workpiece material (Ti-48Al intermetallic) location.

2.6.4 Applications of Titanium Aluminides Alloys.

Titanium aluminides alloys offer many attractive properties and are being considered for space, aerospace, military and commercial applications [19]. The combination of high strength to weight ratio, excellent mechanical properties and corrosion resistance make this alloys the best choice for many critical applications. Titanium aluminide has enhanced high temperature strength, good oxidation and burn resistance, high elastic stiffness, and low density. The high strength to weight ratio makes it especially appealing; its density is approximately half of the nickel alloys, which is currently used as turbine airfoils. Some of titanium aluminides application will be describe below (also see figure 2.14):



(a)



(b)

Figure 2.14: (a) Worldwide market of titanium and its alloy in 2005 (b) Most of Jaguar S-type components made by titanium and its alloy [56].

a) Aircraft Industries

Titanium is increasing greater preference compare with aluminium and stainless steel in aircraft utilization. Titanium has a high temperatures strength advantages at temperature up to 800⁰F (426⁰C); such elevated temperatures occur at high speeds due to aerodynamic heating; and weight reduction with no loss in strength [22]. In fact, titanium alloys are used only in cooler engine parts because above 600⁰C, it oxidation and make material damage. For temperature between 600⁰C to 700⁰C, nickel-base superalloys are the best materials. However, intermetallic compounds based on Ti₃Al and TiAl based could be used in engine technology in aerospace and aircraft fields to overcome these strong thermal and mechanical loads, in some components, nickel-based superalloys may have been substituted by intermetallic compounds if such materials were not disadvantaged by their low toughness and ductility [19], for examples in rotative components, such as blades, rings, discs, centrifugal loads generate a large part of mechanical loading [20].

b) Automotive Industries

Decreased fuel consumption or increased pay load and better fatigue strength in piston rods and transmissions are possible advantages by the titanium for materials used in automobile industries [31]. The use of Ti₃Al and TiAl based alloys in the automotive components such as turbine rotors, blades or turbochargers and exhaust valves can provide benefits such as increased power output and decreased fuel consumption of the reciprocal thermal automotive engines, which is vital to boost rotation speed and to reduce friction force loss (see figure 2.15). For example, the service temperature of the intake valve is about 1043⁰C while, for the exhaust it reaches 1343⁰C, therefore Ti₃Al and TiAl based materials are suitable materials ; a burst speed over 210,000 rpm can be reached for the TiAl rotor, which make them suitable for high speed cars [19].



Figure 2.15: Parts or components of aircraft and automotive made by titanium aluminides [56].

2.6.5 Mechanical Properties

Alloys based on the TiAl (γ) composition have higher elastic modulus, lower density, enhanced elevated-temperature capabilities, and are less likely to ignite than Ti₃Al (α_2) alloys. However, generally room-temperature ductility and fracture resistance can only be classed as “poor” [57]. The corresponding range of tensile ductilities is 0.5-3% elongation. A general trend to increase the ductility is by alloying with small amounts (1-3%) of various elements. Table 2.3 illustrates effects of various alloying elements in TiAl alloys. The additions of Nb and Cr are beneficial to the oxidation behaviour and this relationship is shown in Figure 2.16 [58]. The reason for this improvement appears to be the stabilization of the Al₂O₃ scale when elements are present. The content of Al in TiAl alloys has an important effect in the mechanical properties of TiAl alloys as shown in Figure 2.17. The Ti-52%Al alloy demonstrates the lowest hardness value at room temperature, while Ti-48%Al shows a maximum value of tensile elongation at room temperature.

Table 2.3: Effects of various alloying elements in two-phase TiAl alloys.

Elements	Effects
V, Cr and Mn	Increase the ductility significantly [54].
Nb, Cr, Ta and Mn	Improve oxidation resistance and strength [59].

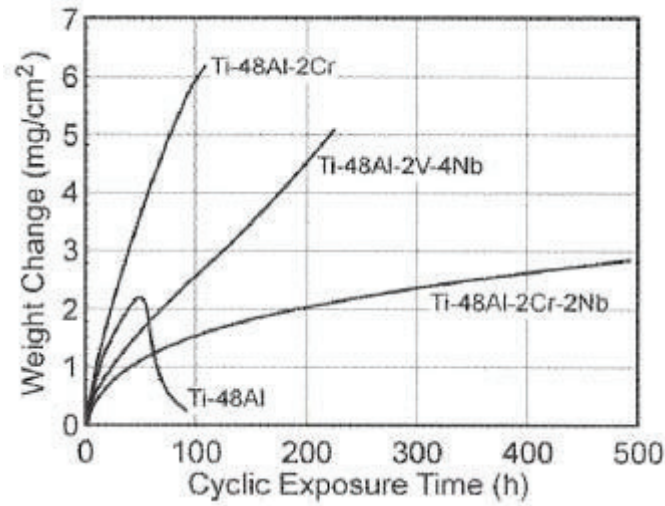


Figure 2.16: Plot of weight change during cyclic thermal exposure in air at 850°C of four γ alloys [58].

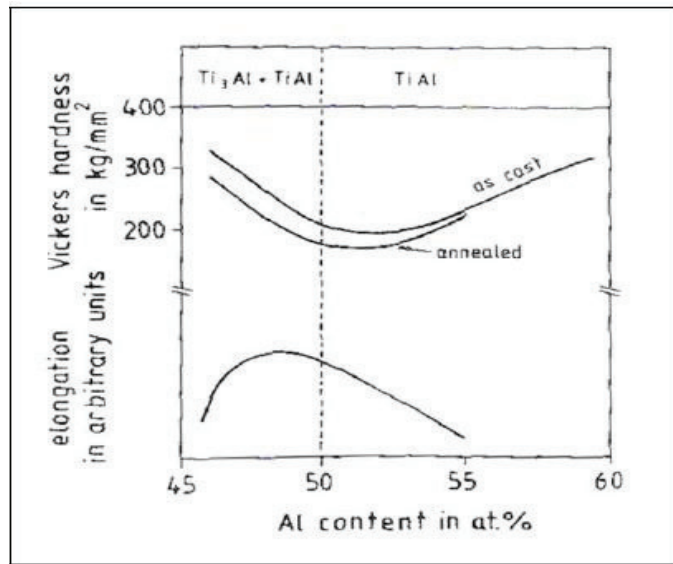


Figure 2.17: Vickers hardness and tensile elongation at room temperature as a function of Al content for single phase and two-phase TiAl alloys [54].

2.6.6 Microstructure of Ternary Ti-48Al-4Cr Intermetallic Alloy

TiAl alloys in present are in the range Ti-(46-52)Al-(1-10)M, with M being at least one element from V, Cr, Mn, Nb, Ta, W, and Mo. These alloys can be divided into single-phase (γ) alloys and two-phase ($\gamma+\alpha_2$) alloys. Single-phase γ alloys contain third alloying elements such as Nb or Ta that promote strengthening and additionally enhance oxidation resistance. The role of third alloying elements in two-phase alloys is to increase ductility (V, Cr, Mn), oxidation resistance (Nb, Ta), or combined properties (Froes and Suryanarayana, 1994).

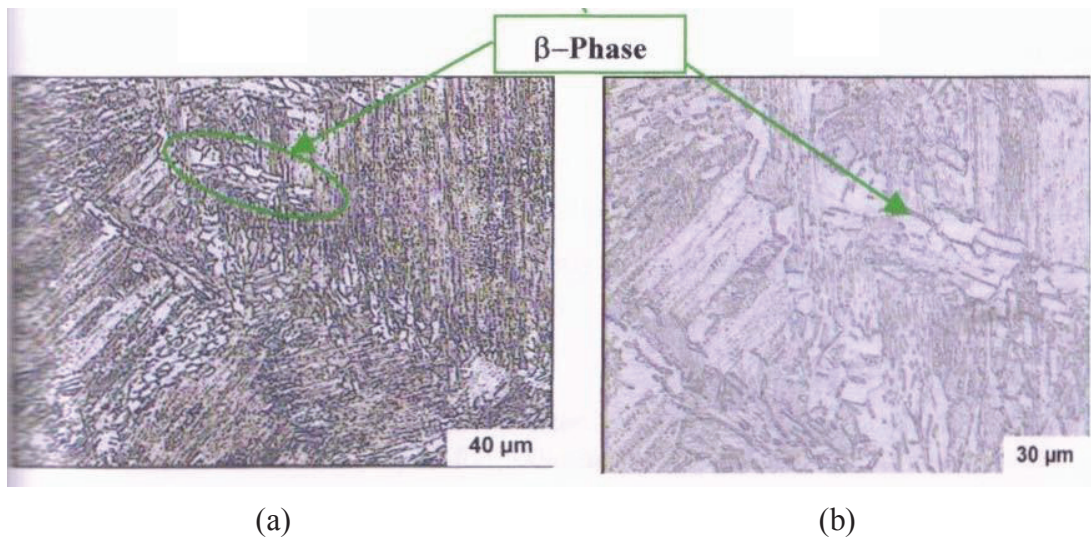
The alloys of technical interest contain 48 at% aluminium and addition of a ternary element (4 at% of Cr). Ternary addition of Chromium (Cr), appeared to increase the ductility of two phase Ti-48Al base alloys [19] and good oxidation resistance; a ternary element also reduces the grain size of γ alloys [18].

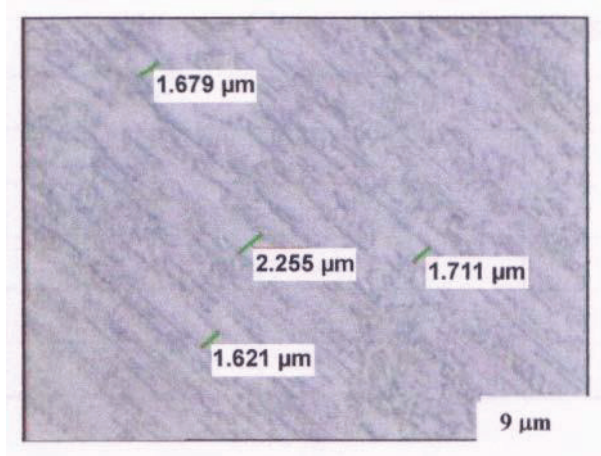
The microstructures of the ternary Ti-48Al-4Cr intermetallic alloy characterized using low magnification optical microscopy. Prior to observation, the following etching solution was used: 1ml HF, 3ml HNO₃ and 96ml distilled water. The chemical composition of the bulk alloy was analyzed by energy dispersive x-ray analysis (EDX). The microhardness was measured using Shimadzu HVM-2 series microhardness tester (see **table 2.4**) [19]. It is found that the increment in aluminium content resulted in a decrease of the microhardness in the alloys, and also, chromium addition exhibits improvement in ductility [19, 18]. This is due to aluminium being soft and ductile metal and will certainly have an effect on the hardness of the intermetallics [19].

Table 2.4 Nominal compositions (at%) and microhardness of ternary Ti-48Al-4Cr intermetallic alloy [18].

Sample	Ti	Al	Cr	Microhardness (H _v)
Ti-48Al-4Cr	53.01	42.12	4.39	317

The microstructure of the alloys strongly depends on the composition. Ternary alloys of Ti-48Al-4Cr; the presence of the ternary element of chromium decreases the grain diameter from 14.6 μm to 12.1 μm and improves the mechanical properties of the alloys [19]. The (β)-phase restricts the grain growth of the primary α_2 and can be considered as a grain-size controlling agent. Figure 2.18 (a) to (c) show the optical microstructures of the unoxidized ternary alloys of Ti-48Al-4Cr [19].

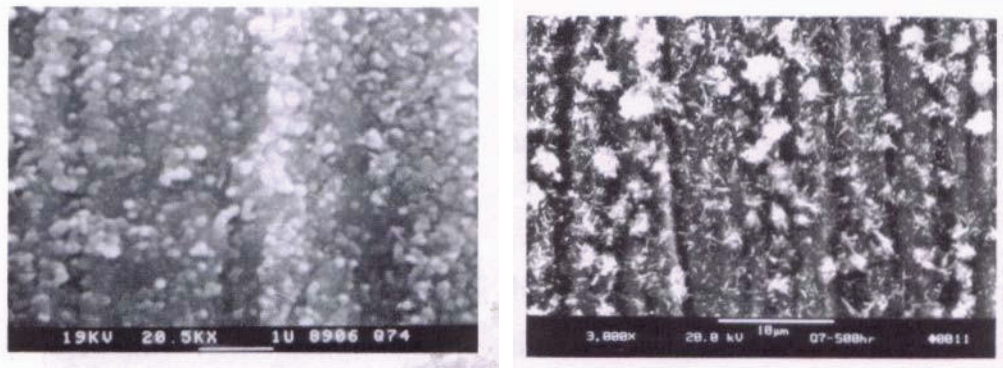




(c)

Figure 2.18 Optical micrographs of unoxidized ternary alloys of Ti-48Al-4Cr (a) at 100x, (b) at 200x and (c) at 500x [19].

The isothermal and thermal cycling oxidation behaviour in flowing dry air as well as in high-purity oxygen of the ternary Ti-48Al-4Cr alloys have been studied at temperatures of 700°C, 900°C and 1100°C. Based on the experimental results [19]; the kinetics of the isothermal oxidation at 700°C alloys show protective oxidation. The chromium containing ternary alloys exhibited the faster oxidation rates with parabolic behaviour at 900°C compared to the binary alloys. Increasing the aluminium content of the alloy improved their oxidation behaviour. During oxidation at higher temperature of 1100°C, the ternary alloys exhibited protective oxidation showing slower rates and the fastest rate is in alloys Ti-45Al. At the lower temperature a higher concentration of chromium may be needed to provide better oxidation resistance; SEM analysis after isothermal oxidation in flowing dry air, chromium has a significant influence on the oxide scale formation at all temperature for the isothermal oxidation in flowing dry air. The microstructural development of ternary Ti-48Al-4Cr alloys oxidised at 700°C and 900°C for 150hr and 500hr in flowing dry air are shown in **figures 2.19 and 2.20**.



(a)

(b)

Figure 2.19: Secondary electron (SE) image of scanning electron micrographs (SEM) with the corresponding energy dispersive (EDX) spectrum of the surface morphology for ternary Ti-48Al-4Cr alloys isothermally oxidized at 700°C in flowing dry air for (a) 150hr and (b) 500hr [19].

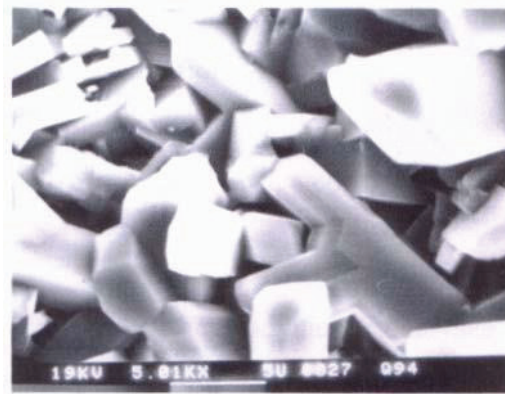


Figure 2.20: Secondary electron (SE) image of scanning electron micrographs (SEM) with the corresponding energy dispersive (EDX) spectrum of the surface morphology of ternary Ti-48Al-4Cr alloys after isothermally oxidized at 900°C in flowing dry air for (a) 150hr and (b) at 350x for 500hr [19].

The thermal cyclic oxidation in flowing dry air at temperatures of 700°C exhibited poor oxidation resistance. Oxidation kinetics upon at 900°C demonstrated linear weight loss in all alloys indicating a severe oxide scales spallation. The presence of chromium in the ternary alloys was not sufficient to provide the cyclic oxidation resistance but could influence the spallation rate.

2.7 WEDM previous research

Today, the most effective machining strategy is determined by identifying the different factors affecting the WEDM process and seeking the different ways of obtaining the optimal machining condition and performance. This section provides a study on the numerous machining strategies involving the design of the process parameter.

The settings for the various process parameters required in the WEDM process play a crucial role in producing an optimal machining performance. This section shows some of the analytical and statistical methods used to study the effects of the parameters on the typical WEDM performance measures such as CR, MRR and SF.

2.7.1 Factors affecting the performance measure

WEDM is a complex machining process controlled by a large number of process parameters such as the pulse duration, discharge frequency and discharge current intensity. Any slight variations in the process parameters can affect the machining performance measures such as surface roughness and CR, which are two of the most significant aspects of the WEDM operation [23]. Suziki and Kishi [24] studied the reduction of discharge energy to yield a better surface roughness, while Luo [25] discovered the additional need for a high energy efficiency to maintain a high machining rate without damaging the wire. Several authors [26] have also studied the evolution of the wire tool performance affecting the machining accuracy, costs and performance measures.

The selection of appropriate machining conditions for the WEDM process is based on the analysis relating the various process parameters to different performance measures namely the CR, MRR and SF. Traditionally, this was carried out by relying heavily on the operator's experience or conservative technological data provided by the WEDM equipment manufacturers, which produced inconsistent machining performance. Levy and Maggi [27] demonstrated that the parameter settings given by the

manufacturers are only applicable for the common steel grades. The settings for machining new materials such as advanced ceramics and MMCs have to be further optimised experimentally.

2.7.2 Effects of the machining parameters on cutting rate (CR).

Many different types of problem-solving quality tools have been used to investigate the significant factors and its inter-relationships with the other variables in obtaining an optimal WEDM CR. Konda et al. [28] classified the various potential factors affecting the WEDM performance measures into five major categories namely the different properties of the workpiece material and dielectric fluid, machine characteristics, adjustable machining parameters, and component geometry. In addition, they applied the design of experiments (DOE) technique to study and optimize the possible effects of variables during process design and development, and validated the experimental results using noise-to-signal (S/N) ratio analysis. Tarng et al. [29] employed a neural network system with the application of a simulated annealing algorithm for solving the multi-response optimization problem. It was found that the machining parameters such as the pulse on/off duration, peak current, open circuit voltage, servo reference voltage, electrical capacitance and table speed are the critical parameters for the estimation of the CR and SF. Huang et al. [52] argued that several published works [29, 30,31] are concerned mostly with the optimization of parameters for the roughing cutting operations and proposed a practical strategy of process planning from roughing to finishing operations. The experimental results showed that the pulse on-time and the distance between the wire periphery and the workpiece surface affect the CR and SF significantly. The effects of the discharge energy on the CR and SF of a MMC have also been investigated [32].

2.7.3 Effects of the machining parameters on the material removal rate (MRR).

The effects of the machining parameters on the volumetric MRR have also been considered as a measure of the machining performance. Scott et al. [30] used a factorial design requiring a number of experiments to determine the most favorable combination of the WEDM parameter. They found that the discharge current, pulse duration and pulse frequency are the significant control factors affecting the MRR and SF, while the wire speed, wire tension and dielectric flow rate have the least effect. Liao et al. [31] proposed an approach of determining the parameter settings based on the Taguchi quality design method and the analysis of variance. The results showed that the MRR and SF are easily influenced by the table feed rate and pulse on-time, which can also be used to control the discharging frequency for the prevention of wire breakage. Huang and Liao [33] presented the use of Grey relational and S/N ratio analyses, which also display similar results demonstrating the influence of table feed and pulse on-time on the MRR. An experimental study to determine the MRR and SF for varying machining parameters has also been conducted [34]. The results have been used with a thermal model to analyze the wire breakage phenomena.

2.7.4 Effects of the machining parameters on the surface finish (SF).

There are also a number of published works that solely study the effects of the machining parameters on the WEDM surface. Gökler and Ozanozgu [35] studied the selection of the most suitable cutting and offset parameter combination to get a desired surface roughness for a constant wire speed and dielectric flushing pressure. Tosun et al. [36] investigated the effect of the pulse duration, open circuit voltage, wire speed and dielectric flushing pressure on the WEDM workpiece surface roughness. It was found that the increasing pulse duration, open circuit voltage and wire speed increases with the surface roughness, whereas the increasing dielectric fluid pressure decreases the surface roughness. Anand [37] used a fractional factorial experiment with an orthogonal array layout to obtain the most desirable process specification for improving the WEDM

dimensional accuracy and surface roughness. Spedding and Wang [38] optimized the process parameter settings by using artificial neural network modelling to characterize the WEDM workpiece surfaces, while Williams and Rajurkar [40] presented the results of the current investigations into the characteristics of WEDM generated surfaces.

2.8 TAGUCHI METHOD

2.8.1 Introduction

Quality is always been an important aspect in the manufacturing of products and processes. Taguchi method is normally used as a tool to design experiment that have multiple factors and different levels and is also known as factorial design. The conventional methods of evaluating an experiment involve the consideration of all the possible design configurations. If an experiment involves six (6) factors and two levels in each of the factors, then 2^6 trials have to be carried out. In actual experiments, it would cost too much to attain high reliability by testing all the relevant inner factors, so the experiment should be conducted with a more limited range of factor [41]. By using Taguchi, fractional factorial experiments are used to lessen the number of trials that have to be conducted. Fractional factorial experiments investigate only a fraction of all the possible combinations and this saves time and cost. Taguchi used this technique but simplified and standardized the fractional factorial designs in such a manner that two engineers conducting tests thousands of mile apart, will always use similar designs and tend to obtain similar results [42].

Dr Taguchi realized the importance of quality improvement and thus invented the Taguchi's experiment designation to identify those key factors that have the greatest contribution to variation and to ascertain those settings or values that result in the least variability. In developing methods to understand better the influences upon the functionality of products and associated processes, Dr Taguchi is recognized for three major contributions to the field of quality as follows:

2.8.1.1 The Loss Function

Dr Taguchi used the Taylor expansion series to develop a mathematical model which loss is a quadratic function of the deviation of the quality of interest from its target value. Although many others approaches developed by academia were valid and statistically correct, the profitability and loss was not considered. Based on the Taguchi methodology, sound management decisions can be made on the true worth of quality improvement efforts.

2.8.1.2 Orthogonal Arrays

The designing of experiments is by using specially constructed tables known as “orthogonal arrays” (OA) .The use of these tables make the design of experiments very easy and consistent. There are different types of array including an L_2 , L_4 , L_8 , L_{16} and so on. For example an L_8 array contain 7 factors at 2 levels each and only 8 trials are needed to be conducted with different levels of each factor. The experiment description is determined by reading numerals 1 and 2 appearing in the rows of the trial run. Dr Taguchi used the OAs not only to measure the effect of a factor on the average result, but to determine the variation from the mean as well. The advantage of using OAs is the relationship among the factors under investigation. For each level of any one factor, all levels of the other factors occur an equal number of times. This constitutes a balanced experiment and permits the effect of one factor under study to be separable from the effects of other factors. This makes the findings of the result reproducible.

2.8.1.3 Robustness

The definition of robustness from both a product and a process related standpoint as follows:

Product: The ability of the product to perform consistently as designed with minimal effects from changes in uncontrollable influences.

Process: The ability of the process to produce consistently good product with minimal effect from changes in uncontrollable manufacturing process.

2.8.2 Defining the quality characteristics

The quality characteristic of a product should be stated such as heavy, light, low, high and so on. The measure of quality for a certain product can be categorized as follows:

2.8.2.1 Bigger-the-better

The goal of bigger-the-better characteristics is to achieve the highest value possible. Infinity is the ultimate objective. Examples of this type of characteristics are strength, pull strength, shelf life, corrosion resistance and melting point.

2.8.2.2 Smaller-the-better

The objective characteristics of smaller-the-better type problems are non-negative and should be as small as possible [43]. Just the opposite of bigger-the-better, the

objective of small-the-better is to obtain a measure of zero. The examples are percent shrinkage, machine wear, residue and loudness.

2.8.2.3 Nominal-the-best

The term refers to characteristics with a specific numerical goal or target value such as dimension. Specific examples includes height, length, diameter, viscosity and voltage.

2.8.3 Taguchi's Design Method

Taguchi's approach to enhance quality in the design phase involves two steps as follows:

1. Optimizing the design of the product/process (system approach).
2. Making the design insensitive to the influence of uncontrollable factors (robustness).

An optimum condition is reached when it performed best under the operating conditions. This condition is reached when there is a right combination of the parameter involved.

Taguchi try to attain quality by the reducing the variation around the target by searching techniques that allow variability to be reduced without necessarily eliminating the cause of the variation. To determine the optimum combination, Taguchi developed a special table that is called Orthogonal Array (OA). An OA is a table developed for two level factors so that column contains two sets of all possible combination of levels and is amenable to statistical analysis with a high degree of confidence.

By using an OA experiment design, variations in the process could be reduced because of controllable factors. Uncontrollable factors or noise factors can be handled by repeating the experiment trials at different noise conditions or the noise factors can be

included in a second OA which is used in conjunction with the array of controllable factors.

To achieve a successful experiment and obtain reproducible results calls for a well-organized and executed effort, requiring careful planning and faithful execution to the plan. The essential steps for properly performing an experiment is categorized into for distinct phases as follow:

2.8.3.1 Planning the experiment

Experiment planning is the first step to performing an experiment and this includes conscientious planning in identifying the quality characteristic, determining measuring requirements, selecting factors for study and associated settings, and laying experimentation strategy.

2.8.3.2 Designing the experiment

In the second phase, the experiment layout is constructed and includes selection of the most efficient experimental matrix to provide meaningful results and contain all of the required information. This phase also involve the proper assignment of the factors and interactions of interest to the appropriate locations within the experimental matrix.

2.8.3.3 Conducting the experiment

The experiment is conducted as developed in the planning and design phases. Beside that, this phase also includes development of the test plan and the preparations and coordination essential for conducting the study. These preliminary efforts are essential for executing the experiment smoothly and in a short time.

Failure to consider these aspects of conducting an experiment can lead to erroneous measurements, biased results, or even no data at all. The complete procedures in conducting an experiment flow diagram are shown in **figure 2.21**.

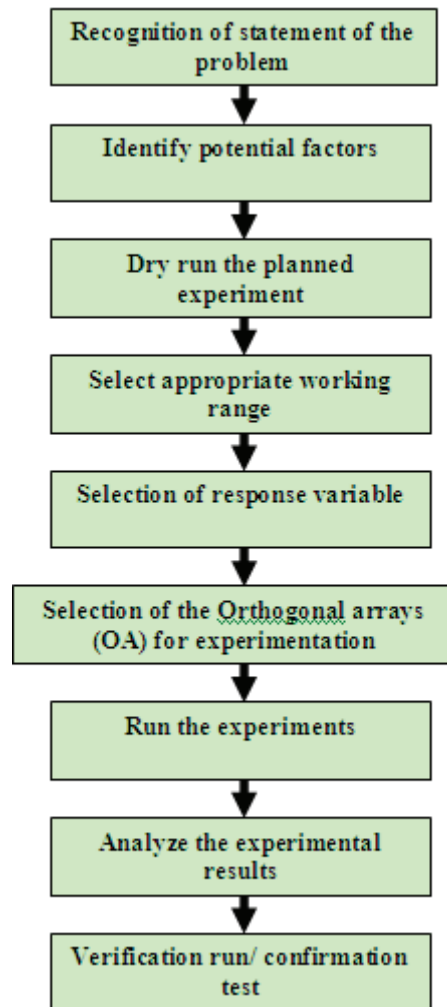


Figure 2.21: Procedure in conducting the experiment

2.8.4 Steps in designing, conducting and analyzing an experiment by Taguchi technique

The complete procedure is shown but only the major steps are followed. These are:

2.8.4.1 Selection of factor and/or interactions

To select the factors that influence the result of the performance characteristics of the product, several methods can be used to determine factors that can be included in the initial experiments. These methods are:

Brainstorming

Brainstorming is the bringing together a group of people associated with the particular problems and soliciting their advice concerning what to investigate. Brainstorming is a necessary and important step in the application process. The nature and content of the brainstorming is dependent on the type of project and there are no specific guidelines. Taguchi recommends the participation of all relevant functional organization such as the product or process experts, statistically oriented people to discuss the factors and the structure of the experiment. Brainstorming promotes creativity by drawing from the participant's ideas that are free from bias and restraint mindsets. By fostering an atmosphere of open-mindedness with the group, effective brainstorming is likely to help the members expands the horizons of their thinking and particularly helps quite members of the team to make a larger contribution .Besides facilitating the determination of the experiment objective, brainstorming also can be used to define alternative quality characteristics and direct the listing.

Flowcharting

In the case of a process, flowcharts are particularly useful in the determination of factor affecting the process results. In the event that the process is too immense or complex to include all variables of interest in one experiment, the flowchart can help determine the most appropriate dividing line between experiment segments [44]. The purpose of the flowchart is to help to understand the sequence of events that lead to the finished product.

Cause-effect diagram

The cause-effect diagram is also known as the fish bone diagram. The effect of causes (quality attributes) is placed on the right side meanwhile the causes of the effect are placed on left side. A cause and effect diagram can be classified into one of the three groups:

a) Dispersion analysis type

Dispersion analysis is helpful in developing the thought process and for developing the relationship among potential causes. Major categories of potential causes are developed first and these causes can be divided into subgroups and the subgroups into more specific causes. This type of diagram provide a simple structured technique for generating ideas concerning potential causes of the specific end results that you are concerned with and organizing them into a logical order.

b) Production process classification type

The production process classification can be helpful in giving those not as familiar of the process a better idea of the relationship between each stage and of the impact of potential factors would be felt. The limitation is the tendency to identify repetitive causes at different process steps that can result in a large and expensive

experiment and difficulty in detecting potential interactions between factors identified at different process steps.

c) Cause enumeration type

The cause enumeration diagram is a particularly effective tool in promoting team brainstorming efforts. Cause enumeration begins with brainstorming open to any type of potential cause linked to the effect that are being investigated. After all of the ideas have been listed, they can be clustered into subgroups, and related subgroups can be combined into major categories. The final result will resemble the dispersion analysis diagram but the difference is the steps to get there.

2.8.4.2 Selection of number of levels.

Initially, the first few rounds of experiments should involve many factors at few levels in order to minimize the size of experiments. Degree of freedom (DOF) for a factor is the number of level minus one, thus increasing the number of levels for a factor increases the total degree of freedom in the experiment. The increase of the DOF would increase the total numbers of test that had to be conducted. Therefore by using two level for each factor, the DOF would be 1, reducing the number of test. The initial round of experimentation will eliminate many factors from contention and the few remaining can then be investigated with multiple levels without causing an undue inflation in the size of the experiment, which causes increase in time and cost.

2.8.4.3 Selection of the OA

The selection of OA to be used would depend upon:

- The number of factors and interactions of interest.
- The numbers of level for the factors of interest.

These two items determine the DOF required for the entire experiment. The number in the array designation indicates the number of trials in the array, for example an L_{16} has 16 trials. The total DOF available in an OA is equal to the number of trials minus one.

$$V_{LN} = N - 1$$

The following inequality must be satisfied when a particular OA is selected:

$$V_{LN} \geq V_{\text{required for factors and interactions}}$$

2.8.4.4 Assignment of Factors and Interactions

Before getting into detail of using some methods or assigning factors and interactions, a demonstration of a mathematical property of OA is in order. OA's have several columns available for assignment of factors and some columns subsequently can estimate the effect of interactions of those factors.

2.8.4.5 Conducting The Experiments

Once the factors are assigned to a particular column of the selected OA, the test strategy had to be set up and preparation of the test can begin. Decisions need to be made concerning the order of testing the various of trials. Whenever possible, the trials conditions should be run in random order to avoid the influence of experiment setup. For example, 4 trials are to be conducted and each of the trials is, trial 1, 2, 3 and 4. For single runs have to be conducted, then 2 ways can be used:

Replication

Replication, whereby all the trial conditions will be run in a random order. A method to decide the order to randomly pull one trial number at a time from a set of trials numbers including repetitions. This usually requires a new setup and in turn increases the cost of experiments.

Repetition

Repetition, whereby each trial is repeated as planned before proceeding to the next trial. The trial run sequence is selected in a random order. For the trial sequence of 2, 4, 3 and 1, three run of trial number 2 are made followed by trial number 4, 3 and 1. This method reduces the setup costs for the experiment but it is unlikely to detect the effect of external factors.

2.8.4.6 Analysis of Experiments Data

After the trial are conducted, the quality characteristic, for example surface roughness etc, will be measured and recorded on the right most column of the OA of each of the trials. In the Taguchi Method, the results of the experiments are analyzed to achieve one or more of the following objectives:

- To establish the best of the optimum condition for a product or a process
- To estimate the contribution of individual factors.
- To estimate the response under the optimum conditions

In order to determine the optimum condition, the main effects of each of the factor would have to be studied by using minor arithmetic manipulation of the numerical results. By knowing the characteristic of the quality attributes, i.e., whether a higher or lower value is preferred, the levels of factors that produce the best results can be predicted.

The contribution of individual factors can be determine by using analysis of variance (ANOVA) that is most commonly applied to determine the percent contribution of each factors and whether the factors are insignificant to the result and thus, be polled.

An example of an L₈ Orthogonal Array (OA) are shown in **table 2.5** and the main effects shown in **table 2.6**.

Table 2.5: Layout of experimental table

Std order trial no	Factor							Results
	A	B	C	D	E	F	G	
	Column number							
	1	2	3	4	5	6	7	
1	1	1	1	1	1	1	1	X ₁
2	1	1	1	2	2	2	2	X ₂
3	1	2	2	1	1	2	2	X ₃
4	1	2	2	2	2	1	1	X ₄
5	2	1	2	1	2	1	2	X ₅
6	2	1	2	2	1	2	1	X ₆
7	2	2	1	1	2	2	1	X ₇
8	2	2	1	2	1	1	2	X ₈

Table 2.6: Main Effect

No	Column	Level 1 average	Level 2 average	Difference
1	A	A1	A2	A1—A2
2	B	B1	B2	B1—B2
3	C	C1	C2	C1—C2
4	D	D1	D2	D1—D2
5	E	E1	E2	E1—E2
6	F	F1	F2	F1—F2
7	G	G1	G2	G1—G2

2.8.4.7 Main Effects

The important of main effect is in the determination of optimum conditions. When we find the results of the main effects we should know the optimum condition in the process. It means that the machining parameter and the levels, which can be expected to produce the best result. **Table 2.6** as an example to proceed the main effects from the experimentation.

2.8.4.8 Confirmation Experiment

This reason of this experiment is to verify the truth in the estimation of the optimum conditions from the previous round of experimentation. The optimum conditions are set the significant factors and levels and several tests are made under constant conditions. The average result of the quality attribute is then compared to anticipated average based on the factors and levels tested. The successfulness of the whole experiment depends on the result obtained from the confirmation experiment.

CHAPTER 3

EXPERIMENT PREPARATION

3.1 Experiment Detail

Wire electrical discharge machine trials have been carried out with WEDM model Sodick AQ537L as shown in **figure 3.1**. Brass wire was mounted on the spool attached to the machine as a electrode. Workpiece was placed on the machine table, where it was flooded by dielectric fluid stream. During machining, die electric fluid was circulated under pressure by a pump, through a wire. The machining conditions are described on **table 3.1** and the initial machining condition on **table 3.2**.



Table 3.1: Sodick AQ537L machining condition [48].

Machine		CNC Power Supply Unit LQ33W/LQ34W	
Machining tank dimensions (W x D)	1050 x 720 mm	Maximum machining current	60A
X-axis travel	570 mm	Power requirement	200/220V 50/60-Hz
Y-axis travel	370 mm	NC unit	Multi-task OS, Sodick Motion Controller (SMC) system
Z-axis travel	350 mm	User memory capacity	For editing: 100,000 blocks For storage: 30 MB
U-axis x V-axis stroke	120 x 120 mm	Storage media	Hard disk, floppy disk
Taper control angle	±25° (Workpiece thickness: 100 mm)	Input device	3.5-inch floppy disk drive, touch panel, keyboard
Maximum workpiece size (W x D x H)	770 x 520 x 340 (flush machining) mm 770 x 520 x 280 (submerged machining) mm	Display system	15.1-inch TFT-LCD (SVGA)
Maximum workpiece weight	1000 (flush machining) kg	Character set	Alphanumeric characters and symbols
Wire electrode diameter	φ0.15~φ0.33 mm ^{*1}	Keyboard	Standard 101-type keyboard, function keys
Wire tension	3~23 N	Position command system	Incremental/absolute
Wire feed speed	Max. 420 mm/sec	Input data range	±999999.999/±99999.9999 (setting possible)
Distance from the floor to the table top	995 mm	Machining condition registration	1000conditions available (C000 to C999)
Machine dimensions (W x D x H)	2450 x 2570 x 2390mm	Offset function	1000conditions available (H000 to H999)
Machine installation dimensions (W x D)	3550 x 3700 mm	Program sequence number	N000000000 to N999999999 available by setting
Machine weight	4500 kg	Subprogram nesting levels	50
Total electric capacity	3-phase, 50/60 Hz, 10.5 kVA ^{*2}	Q command nesting levels	7
		The number of coordinates	60
		Simultaneous-controlled axis	Maximum 4 axes (LQ34W: maximum 8 axes)
		Minimum command increment	0.1 μm
		Minimum drive increment	0.1 μm
		Maximum feed rate	5m/min
		Position detection system	Full-closed loop (linear scale)
		Drive mechanism	Linear motors
		Compensation function	Pitch error compensation, backlash compensation, torque compensation for each axis
		Editing	Editing during machining, multi-editing of two files on one screen
		Graphics function	XY, YZ, ZX planes, graphics drawing during machining, background graphics drawing

Supply Tank	
External dimensions (W x D)	725 x 2550 mm
Weight (dry)	600 kg
Supply tank capacity	800 lit
Dielectric fluid filtration system	Replaceable paper filter (internal pressure 3-shell type)
Deionizer	Ion exchange resin (18-lit. type)

*1 φ0.1-mm wire available as an option
*2 Indicates the electric capacity when φ0.2-mm wire is used.

Table 3.2: Initial machining condition

On time (μs)	Off time (μs)	Peak current (A)	Servo reference voltage (V)	Voltage (V)
6	4	15	30	8
Servo feed rate (mm/min)	Wire dia. (mm)	Wire speed (m/min)	Wire tension (g)	Flushing rate (bar)
8	0.2 (brass)	10	550	2

Note: MAO was setting at 720

3.2 Preparation of the Workpiece

The Titanium aluminides intermetallic alloy (Ti-48Al) workpiece specimen was prepared by using WEDM and cut the material into bars (12 mm x 10 mm area). The

dimensions of the preparation workpiece shown in **figure 3.2**. As an intermetallic compound, a distinct material from any of the metals that comprise it. The strength of bonding between the Ti atom and Al atom is larger than that between the same atoms and cannot be separated easily. The Al content varies between 46% and 52%. The mechanical properties of Ti-48Al will be described in **table 3.3**

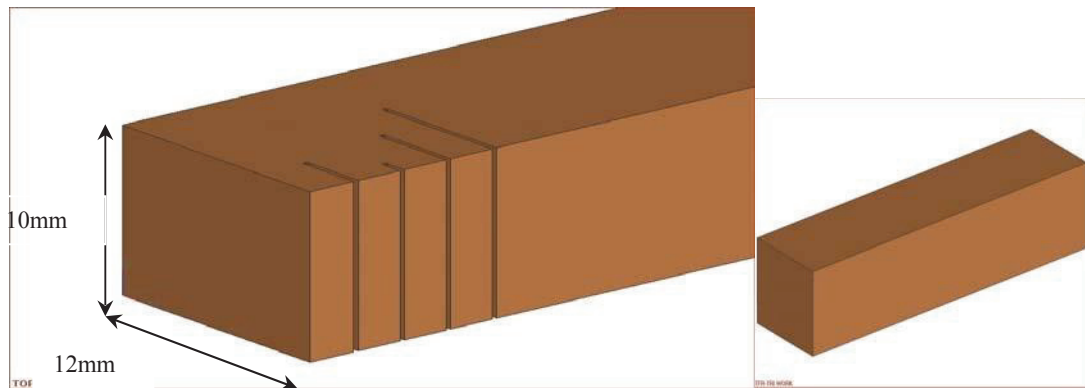


Figure 3.2: Workpiece material

Table 3.3: Mechanical properties of Titanium Aluminides

Properties	TiAl
Density (g/cm ³)	3.7 – 3.9
Young's modulus (GPa)	160 – 180
Yield strength (MPa)	400 – 650
Tensile strength (MPa)	450 – 800
Creep limit (°C)	1000
Oxidation limit (°C)	900
Ductility, % at room temperature	1 – 4
Ductility, % at high temperature	10 – 60
Fracture toughness (MN/m ^{3/2})	10 – 20

3.3 Design of experiment based on Taguchi method

To evaluate the effects of machining parameters on performance characteristics (surface roughness and MRR), and to identify the performance characteristics under the optimal machining parameters, a specially designed experimental procedure is required [45]. Classical experimental design methods are too complex and difficult to use. Additionally, large number of experiments has to be carried out when number of machining parameters increases [45]. In this study, Taguchi method, a powerful tool for parameter design of performance characteristics, was used to determine optimal machining parameters for better surface roughness and maximum MRR in WEDM. In Taguchi method, process parameters which influence the products are separated into two main groups: control factors and noise factors [46]. The control factors are used to select the best conditions for stability in design of manufacturing process, whereas the noise factors denote all factors that cause variation. Taguchi proposed to acquire the characteristic data by using orthogonal arrays, and to analyze the performance measure from the data to decide the optimal process parameters [46]. This method uses a special design of orthogonal arrays to study the entire parameter space with small number of experiments only. In this study, seven machining parameters were used as control factors and each parameter was designed to have two levels, denoted 1 and 2 (**Table 3.4**). According to the Taguchi quality design concept, a L_8 orthogonal arrays table with 8 rows (corresponding to the number of experiments) was chosen for the experiments

3.4 Conducting the Experiment

The flowchart process in conducting the experiment is shown in **figure 3.6**

3.4.1 Recognition of statement of the problem

To investigate and analysis the cutting parameter of WEDM process of Ti-48Al intermetallic alloy and find out the response parameters.

3.4.2 Identify potential factors

As first step in Taguchi technique, a brainstorming and cause and effect analysis was performed and the results are presented in **Figure 3.3**. This Figure shows the various factors within each category; for example, under dielectric fluid, the affecting factors could be the type of dielectric, contamination level of dielectric, flow rate, pressure, and flushing direction.

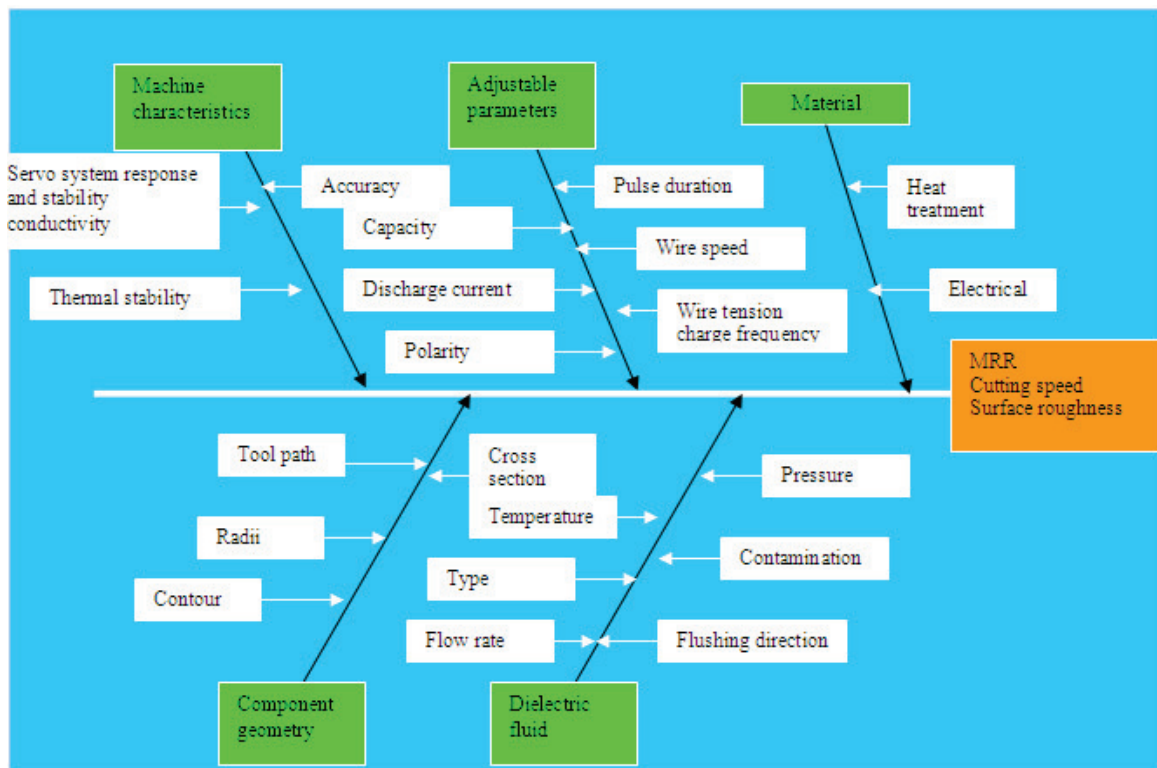


Figure 3.3 Cause and effect diagram for WEDM process

As can be seen from **Figure 3.3**, the machining performance of WEDM depends on many factors including the physical, chemical, thermal, and mechanical properties of the workpiece and tool electrode materials. There are five major categories that we identified:

- Material
- Dielectric fluid

- Machine characteristic
- Adjustable parameter
- Component geometry

From these five major categories, there are controllable and uncontrollable factors. A controlled nuisance factor is one whose levels may be set by the experiment. Uncontrollable factor can be controlled for purposes of an experiment. **Figure 3.4** shown the controllable and uncontrollable factors affecting WEDM.

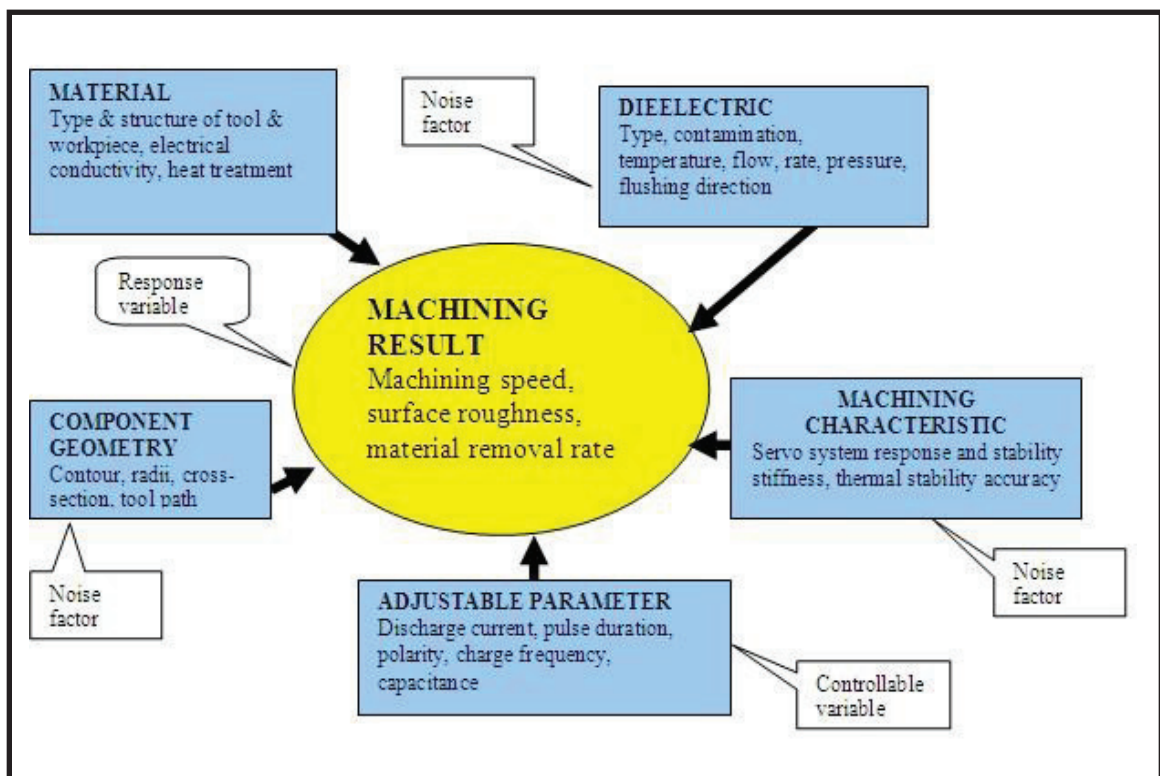


Figure 3.4: The controllable and uncontrollable factors affecting WEDM.

Based on literature, adjustable parameters are the categories of controllable factors and the others are uncontrollable factors. Six controllable factors discharge current, pulse duration, charge frequency, capacitance, wire tension and wire speed are consider as input parameters as initial step. Seven factors and two levels are selected in this experiment.

3.4.3 Dry run the planned experiment

The main reason for dry run was to find range of input parameters and each combination of factors are run on the machine WEDM for a short duration to ensure successful run in the full fledged experiments.

3.4.4 Select appropriate working range

Through dry run step, the levels have been selected such the wide range of value are covered. The allowable WEDM machine range and working range for seven factors is selected as shown in **table 3.4**.

Table 3.4: Input parameter and their level

Factor	Description	Level 1	Level 2
A	On time, ON (μ s)	2	6
B	Off time, OFF (μ s)	10	30
C	Interaction ON x OFF		
D	Peak Current, IP (A)	10	15
E	Servo Feed Rate, SF (mm/min)	10	20
F	Interaction OFF x Peak Current		
G	Servo Reference Voltage, SV (V)	10	50

3.4.5 Selection of response variable

The performance measures for this experiment are cutting speed in mm/min, material removal rate (MRR) in g/min and surface roughness in micron.

3.4.5.1 Material removal rate

Material removal rate (MRR) can be expressed as the volume of work piece loss divided by machining time. The unit for MRR is in g/min.

$$\text{MRR} = \frac{X_b - X_a}{t}$$

Where,

- MRR = material removal rate (g/min)
- X_b = Weight of specimen before cutting (g)
- X_a = Weight of specimen after cutting (g)
- t = machining time (min)

MRR is totally measured using a digital weighing machine, Precisa Balances series XT that only measured workpiece loss. The average result of MRR are calculated and recorded.

3.4.5.2 Surface roughness

It is direct transform as surface roughness of the workpiece after machining and the unit of Ra is μm . Ra is measured by using a Portable Surface Roughness Tester, series Talysurf. The Ra values are measured three times for each trial and get the average. Result of Ra can get direct from the machined process so no calculation needed.

3.4.5.3 Cutting speed

Cutting speed (CS) can be expressed as the length of cutting divided by machining time. The unit of cutting speed is mm/min.

$$CS = \frac{L}{t} \quad (\text{mm/min})$$

CS = Cutting Speed (mm/min)

L = length of cutting (mm)

t = time was taken (minutes)

Note : The time are already recorded by the machine timer indicator.

3.4.5.4 Width of Cut (Kerf)

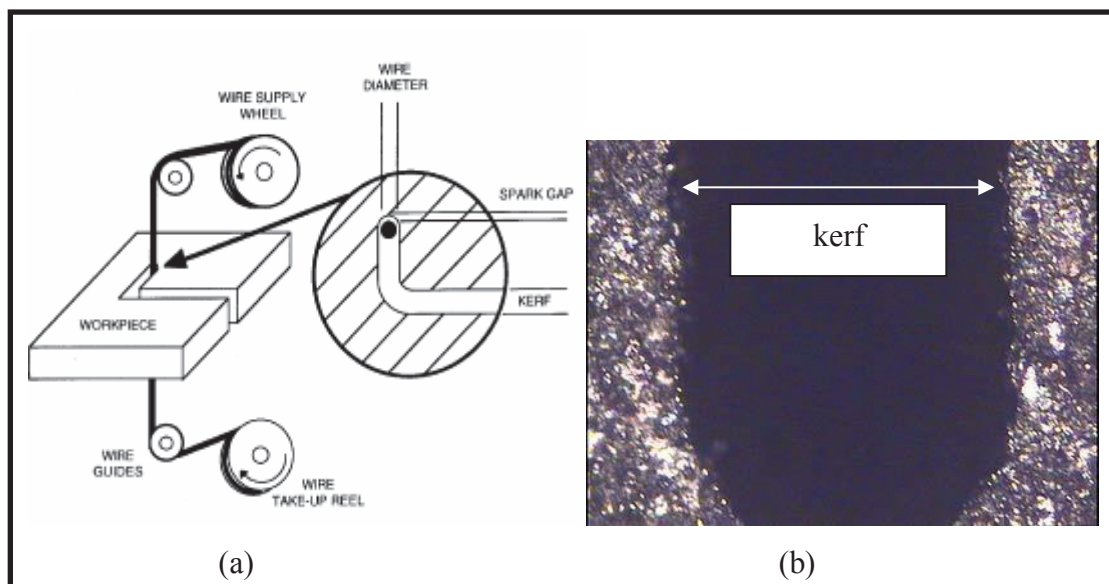


Figure 3.5(a) and (b): Kerf profile [45].

Kerf or width of cut was measured three time at the different point along the kerf width left by the wire pass using the profile projector. Figure 3.5(a) and (b) shown kerf profile.

3.4.6 Selection of the Orthogonal arrays (OA) for experimentation

The selection of an appropriate set of input parameters from **table 4.4** for optimum cutting speed, MRR and optimum surface finish is not easy, because it is not known which parameter combination will yield the best cutting speed and the best surface finish among all the possible combinations. The main objective of WEDM user is to achieve a higher MRR and better surface finish. Hence, the optimum utilization of the WEDM capability requires the selection of an appropriate set of machining parameters. To solve this problem, it is necessary to apply an optimization technique using an experimental design. Here, all possible combinations require eight different experimental runs. The machine-on-time alone needed for these experiments would be considerable. The basic reasons to choose this kind of array are that the conclusions arrived at from those experiments are valid over an entire region spanned by the control factor levels, and the matrix minimizes the number of experiments (Phadke, 1989) [47]. The experimental design, i.e. L_8 orthogonal array, used in this investigation is shown in **Table 3.5**.

Table 3.5: The experiment design L_8 orthogonal array

Experiment numbers	Factors						
	On Time	Off Time	Int (On x Off)	Peak Current	Servo Feed Rate	Int (Off x Peak Current)	Servo Reference voltage
1	1	1	1	1	1	1	1
2	1	1	1	2	2	2	2
3	1	2	2	1	1	2	2
4	1	2	2	2	2	1	1
5	2	1	2	1	2	1	2
6	2	1	2	2	1	2	1

7	2	2	1	1	2	2	1
8	2	2	1	2	1	1	2

3.4.7 Full fledged of experiments

Each experiment performed with a particular set of input parameters, involved cutting the materials. The machining speed and the actual sparking frequency were monitored by an online monitor system. The surface finish was obtained (min) by measuring the mean absolute deviation, Ra.

3.4.8 Analyze the experimental results

After the trial are conducted, the quality characteristic, for example surface roughness etc, will be measured and recorded on the right most column of the OA of each of the trials. In the Taguchi Method, the results of the experiments are analyzed to achieve one or more of the following objectives:

- To establish the best of the optimum condition for a product or a process
- To estimate the contribution of individual factors.
- To estimate the response under the optimum conditions

In order to determine the optimum condition, the main effects of each of the factor would have to be studied by using minor arithmetic manipulation of the numerical results. By knowing the characteristic of the quality attributes, i.e., whether a higher or lower value is preferred, the levels of factors that produce the best results can be predicted.

The contribution of individual factors can be determined by using analysis of variance (ANOVA) that is most commonly applied to determine the percent contribution of each factor and whether the factors are insignificant to the result and thus, be pooled.

3.4.9 Verification run

All of the data that is collected and calculated are analyzed by using Qualitek 4 – 1 to determine the expected result at optimum conditions. The experiment is run again for each of the specimen at the determined optimum conditions from analyzing the results of Taguchi method to confirm the final optimum condition.

3.5 Investigation Characteristics of the Machined Ti-48Al

The machined material analyzed to investigate the surface influenced during machining by WEDM. The analysis will cover the elements present on the top of surface, recast layer and microcrack induced in the Ti-48Al. The analysis will be divided into two sections. The first section is direct machined surface analysis while the other one is cross-sectional surface analysis.

3.5.1 Direct Machined Analysis

The analysis will be conducted directly to the machined surface to observe the severity of surface roughness resulted by using WEDM and to investigate the elements present in the surface. The first analysis will be done by Field Emission Scanning Electron Microscopy (FESEM) and the second analysis will be used by Energy Dispersive Spectroscopy Microanalysis (EDS/EDX).

3.5.2 Cross Section Surface Analysis

In order to further understand the effect of WEDM on TiAl, the crosssectional analysis was carried out to allow investigation on the layers formed during the WEDM process.

The analysis was done by:

a) FESEM examination

The analysis is carry out to observe the layer on cross sectional after WEDM machined and observed recast layer, microcrack and others substances.

b) EDX line scan and EDX spot scan

The analysis purposes is to define element present in the cross sectional WEDM machined.

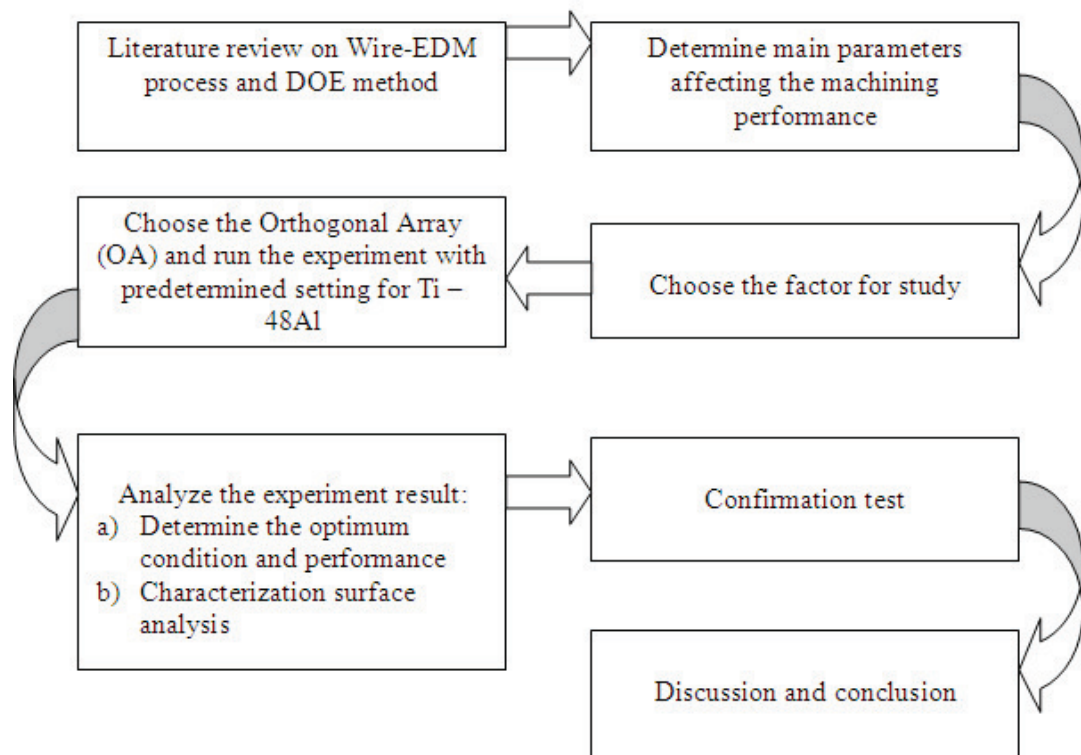


Figure 3.6: The flowchart of process in conducting the experiment

3.6 Measurement equipment

3.6.1 Surface roughness tester

Brand: Taylor Hobson

Model: Sultronic 3+

Code: 1-2-1590 DCN 001

Serial no. : 2052 L

Surface roughness of the machined workpieces will be measured using this machine.



Figure 3.7:Taylor Hobson surface roughness tester

3.6.2 Balance

Brand: Presica

Model: 92SM-202A DR

Resolution: 10 nano gram.

Precision balance will be used to measure the weigh of the workpiece before and after machining process.



Figure 3.8: Presica Balance

3.6.3 Optical microscope (Zeiss)

Brand: Zeiss

Model: Axiotech

The microscope is equipped with various objectives which capable to capture online image of the WEDM workpiece surface.



Figure 3.9: Optical microscope

CHAPTER 4

RESULTS AND ANALYSIS

This chapter presents the experiment result on WEDM of Ti-48Al. Analysis and discussions were focused on cutting speed, material removal rate, surface roughness and width of slit (kerf). An investigation on the effect and optimization of machining parameter due to the machining performances. Finally, analyses for surface characterization of the machined material.

In this study, Taguchi design methodology was used with the aid of the design of experiment (DOE) of Ti-48Al using 0.2mm diameter brass wire. The experimental studies were conducted under varying pulse on time, pulse off time, peak current, servo feed rate and servo reference voltage. The settings of machining parameters were determined using the Taguchi design method. The level of importance of the machining parameters on the cutting speed, material removal rate, surface roughness and kerf are determined by analysis of variance (ANOVA). The optimum machining parameter combination was obtained using the analysis of signal-to-noise (S/N) ratio. The achievable of this experiment produced the fastest cutting speed, higher material removal rate, finest surface finish and smaller kerf. Verification run will be conducted to compare the generated optimum result with the actual experiment results. The sequence of this chapter covered; Experiment results of WEDM of Ti-48Al, Analyzed data using the Taguchi Method, Confirmation test results and Surface characterization of machined Ti-48Al.

4.2 Experimental Results of WEDM of Ti-48Al

Tables 4.1 to 4.4 present the experiment results for wire electrical discharge machining of Ti-48Al in terms of cutting speed, material removal rate, kerf and surface roughness. For each trial condition, three repetitions were run and the average data were calculated. The cutting speed as shown in Table 4.1 was computed based on the time required to cut across the material for a distance of 14 mm (Equation 4.1). In Table 4.2, the material removal rates for each sample was computed using Equation 4.2. The width of the kerf results as shown in table 4.3 was measured by using equation 4.3, after three readings from each slot to obtain the average value.

Measurements of roughness were carried out three times for each sample to obtain an average value (as shown in Table 4.4). During observation on machining of Ti-48Al no wire ruptured were encountered for all trial.

$$\begin{aligned} \text{Cutting Speed} &= \frac{\text{Cutting Distance (mm)}}{\text{Times (minutes)}} \\ &= \frac{14 \text{ mm}}{\text{Time (minutes)}} \end{aligned} \quad \begin{array}{l} \mathbf{\text{Equation}} \\ \mathbf{4.1} \end{array}$$

$$\text{Material Removal Rate} = \frac{\text{Weight before machined} - \text{weight after machined (mg)}}{\text{Times (minutes)}}$$

Equation 4.2

$$\text{Kerf} = \text{Wire Diameter} + \text{Overcut}(\mu\text{m})$$

Equation 4.3

Table 4.1: Experimental results of WEDM of Ti-48Al in term of cutting speed.

Trial	Trial Condition					Cutting Speed (mm/min)			
	On Time (μ s)	Off Time (μ s)	Peak Current A	Servo Feed Rate (mm/min)	Servo Reference Voltage (V)	Result 1	Result 2	Result 3	Average
1	2	10	10	10	10	0.9901	0.9900	0.9900	0.9900
2	2	10	15	20	50	1.9272	1.6837	1.5624	1.7244
3	2	30	10	10	50	0.9622	0.7842	0.8820	0.8761
4	2	30	15	20	10	1.9803	1.5322	1.6621	1.7249
5	6	10	10	20	50	1.9802	1.9042	1.9808	1.9551
6	6	10	15	10	10	0.9900	0.9903	0.9910	0.9904
7	6	30	10	20	10	1.9833	1.9803	1.9811	1.9816
8	6	30	15	10	50	0.9738	0.9897	0.9744	0.9793

Table 4.2: Experimental results of WEDM of Ti-48Al in term of material removal rates.

Trial	Trial Condition					Material Removal Rates (mg/min)			
	On Time (μ s)	Off Time (μ s)	Peak Current A	Servo Feed Rate (mm/min)	Servo Reference Voltage (V)	Result 1	Result 2	Result 3	Average
1	2	10	10	10	10	14.2784	11.4354	12.1692	12.6277
2	2	10	15	20	50	21.8397	19.3971	20.8930	20.7099
3	2	30	10	10	50	11.6219	09.2181	10.2829	10.3743
4	2	30	15	20	10	23.5714	17.2277	19.9988	20.2659
5	6	10	10	20	50	22.2286	21.7114	26.5643	23.5014
6	6	10	15	10	10	13.4233	12.5153	13.3498	13.0961
7	6	30	10	20	10	25.7871	23.4083	26.1057	25.1004
8	6	30	15	10	50	13.2084	12.2512	13.0300	12.8299

Table 4.3: Experimental results of WEDM of Ti-48Al in term of kerf.

Trial	Trial Condition					Kerf (μm)			
	On Time (μs)	Off Time (μs)	Peak Current A	Servo Feed Rate (mm/min)	Servo Reference Voltage (V)	Result 1	Result 2	Result 3	Average
1	2	10	10	10	10	327.5	309.82	332.9	323.41
2	2	10	15	20	50	292.86	266.0	292.98	283.95
3	2	30	10	10	50	341.63	316.39	338.33	332.12
4	2	30	15	20	10	300.72	284.96	304.29	296.66
5	6	10	10	20	50	302.7	281.77	298.69	294.39
6	6	10	15	10	10	310.16	293.41	307.45	303.67
7	6	30	10	20	10	335.63	313.29	338.77	329.23
8	6	30	15	10	50	335.07	301.94	326.75	321.44

Table 4.4: Experimental results of WEDM of Ti-48Al in term of Surface roughness.

Trial	Trial Condition					Surface Roughness (Ra)			
	On Time (μs)	Off Time (μs)	Peak Current A	Servo Feed Rate (mm/min)	Servo Reference Voltage (V)	Result 1	Result 2	Result 3	Average
1	2	10	10	10	10	2.43	2.03	2.38	2.28
2	2	10	15	20	50	2.09	2.11	2.13	2.11
3	2	30	10	10	50	2.30	2.09	2.43	2.27
4	2	30	15	20	10	2.06	1.81	2.21	2.027
5	6	10	10	20	50	2.17	1.75	1.97	1.96
6	6	10	15	10	10	2.30	1.88	2.04	2.073
7	6	30	10	20	10	2.63	2.19	2.47	2.43
8	6	30	15	10	50	2.51	2.24	2.57	2.44

4.3 Data Analysis Using Taguchi Method

By using Taguchi method to analyze the data, information such as main effects, percentage contribution of each factor (using ANOVA), and estimation of the optimum result can be produced. As there were three repetitions for each trial conditions, signal to noise ratio (S/N) analysis was employed as recommended by Taguchi [42]. The data analysis was conducted separately for the four performance measures – cutting speed, material removal rate, kerf and surface roughness. In this present research, the Taguchi method of analysis was conducted with the help of software (Qualitek-4). Appendix C briefly shows the application of Qualitek-4 in analyzing the data. In order to provide a better understanding on how the Taguchi method analyzes the data, a set of manual sample calculation is also presented in Appendix B.

4.3.1 Data Analysis for Cutting Speed

a) Signal to Noise (S/N) Ratio

The cutting speed data were first transformed into S/N ratios using Equation 4.4. The greater the values of S/N the better because this indicates that data variance around the target value are smaller. However, the mean squared deviation (MSD) is defined differently for each of the three quality characteristics considered: smaller, nominal or larger. In the case of cutting speed, the larger value is selected as this indicates faster cutting speed. Therefore, the MSD for the larger the better is defined as in Equation 4.5. Table 4.5 shows the S/N ratios converted from the cutting speed data.

$$S/N = -10\log(\text{MSD})$$

where MSD = Mean square deviation from the target value of the quality characteristics

$$\text{MSD} = \frac{1}{n} \left(y_1^2 + y_2^2 + y_3^2 + \dots + y_n^2 \right)$$

Equation 4.4

where y_1, y_2, \dots, y_n = Results of experiment (eg : cutting speed, material removal rates)
 n = Number of repetitions

Equation 4.5

Table 4.5: S/N ratio for cutting speed.

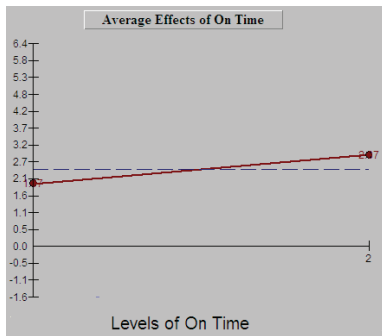
Trail No	Cutting speed data			Signal to Noise Ratio
	Result 1	Result 2	Result 3	
1	0.9901	0.9900	0.9900	-0.088
2	1.9272	1.6837	1.5624	4.633
3	0.9622	0.7842	0.8820	-1.242
4	1.9803	1.5322	1.6621	4.587
5	1.9802	1.9042	1.9808	5.817
6	0.9900	0.9903	0.9910	-0.085
7	1.9833	1.9803	1.9811	5.939
8	0.9738	0.9897	0.9744	-0.189
				2.421

b) Main Effects

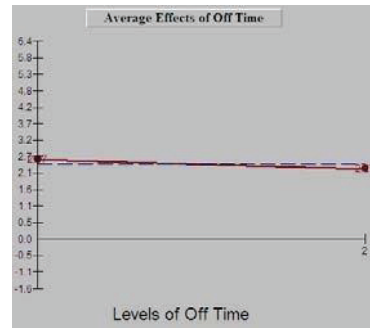
Based on the signal to noise ratio in Table 4.5, the main effects for each factor were generated, as shown in Table 4.6. Since each factor has two levels, the average effect of each level is shown under the three columns marked Level 1 and Level 2. The main effects are the differences between the average effects at Level 1 and Level 2 and they are shown in the fourth column labeled (L2-L1). A minus sign (in the difference column) indicates an increase in noise as the factor changes from Level 1 to Level 2. A positive value, on the other hand, indicates a decrease in noise respectively for the negative value. For a better illustration, the data were plotted into graph as shown in Figures 4.1 (a) to (g). In S/N analysis, the greater value of S/N represents a more desirable condition.

Table 4.6: Main effect of the factors in effecting cutting speed.

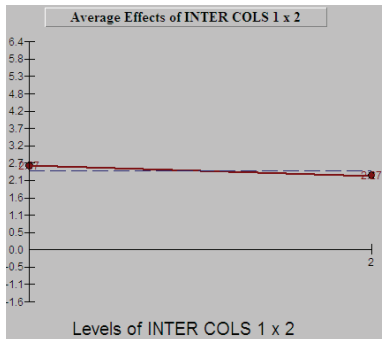
No	Factors	Level 1	Level 2	L2 – L1
1	On Time	1.973	2.870	0.897
2	Off Time	2.569	2.274	-0.295
3	Interaction cols 1x2	2.574	2.269	-0.305
4	Peak Current	2.606	2.237	-0.369
5	Servo Feed Rate	-0.401	5.244	5.644
6	Interaction cols 2x4	2.532	2.311	-0.222
7	Servo Reference Voltage	2.588	2.255	-0.334



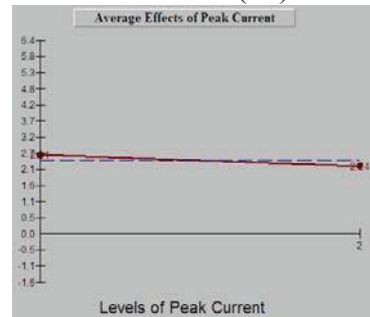
(a)



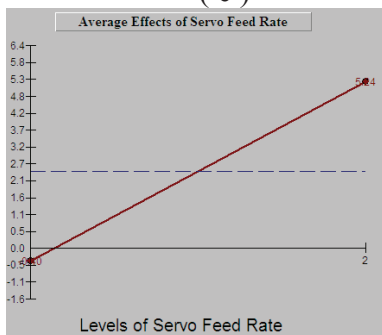
(b)



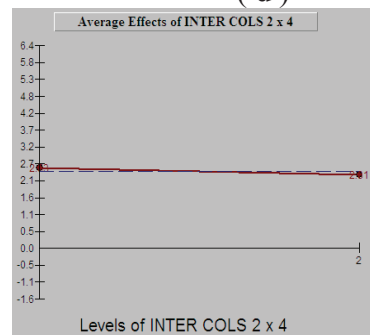
(c)



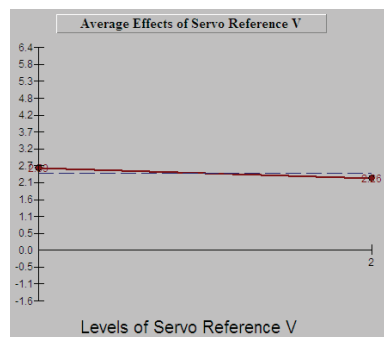
(d)



(e)



(f)



(g)

Figure 4.1: Graphs show average effect of various factor (in affecting cutting speed) at different level (a) On time, (b) Off time, (c) Interaction On and Off time, (d) Peak current, (e) Servo feed rate, (f) Interaction Off time and Peak current, (g) Servo reference voltage.

c) Analysis of Variance (ANOVA)

In order to determine which of the factor/interaction effects are statistically significant, a powerful statistical technique called analysis of variance (ANOVA) was used. Using ANOVA, one is able to identify the active and inactive factor/interaction effects with statistical confidence (Logothetic, 1994). As the S/N ratio is a single performance statistic, it is advisable to pool the insignificant effects to obtain a reasonable estimate of error variance. According to Roy (1990), one should pool the effects (either factor or interaction effects) with low sum of squares in magnitude. Here control factors Off Time, interaction On x Off, Peak Current, interaction Off x Peak current and Servo Reference Voltage have been considered for pooling and the result of the ANOVA on S/N ratio are shown in table 4.7. For better illustration, the percentage contribution of each factor in affecting the WEDM cutting speed is well illustrated through a pie chart as shown in Figure 4.2.

Table 4.7: Pooled ANOVA results for cutting speed at 90 percent confidence level.

No	Factor	DOF	Sum of Squares	Variance	F-Ratio	Pure Sum	Percent (%)
1	On Time	1	1.612	1.612	11.856	1.476	2.227
2	Off Time	(1)	0.174		Pooled		
3	Inter Cols 1x2	(1)	0.185		Pooled		
4	Peak Current	(1)	0.273		Pooled		
5	Servo Feed Rate	1	63.725	63.725	0.000	63.725	95.924
6	Inter Cols 2x4	(1)	0.097		Pooled		
7	Servo Reference Voltage	(1)	0.222		Pooled		
	Other/Error	5	0.952	0.816			1.849
	Total	7	66.291				100.000

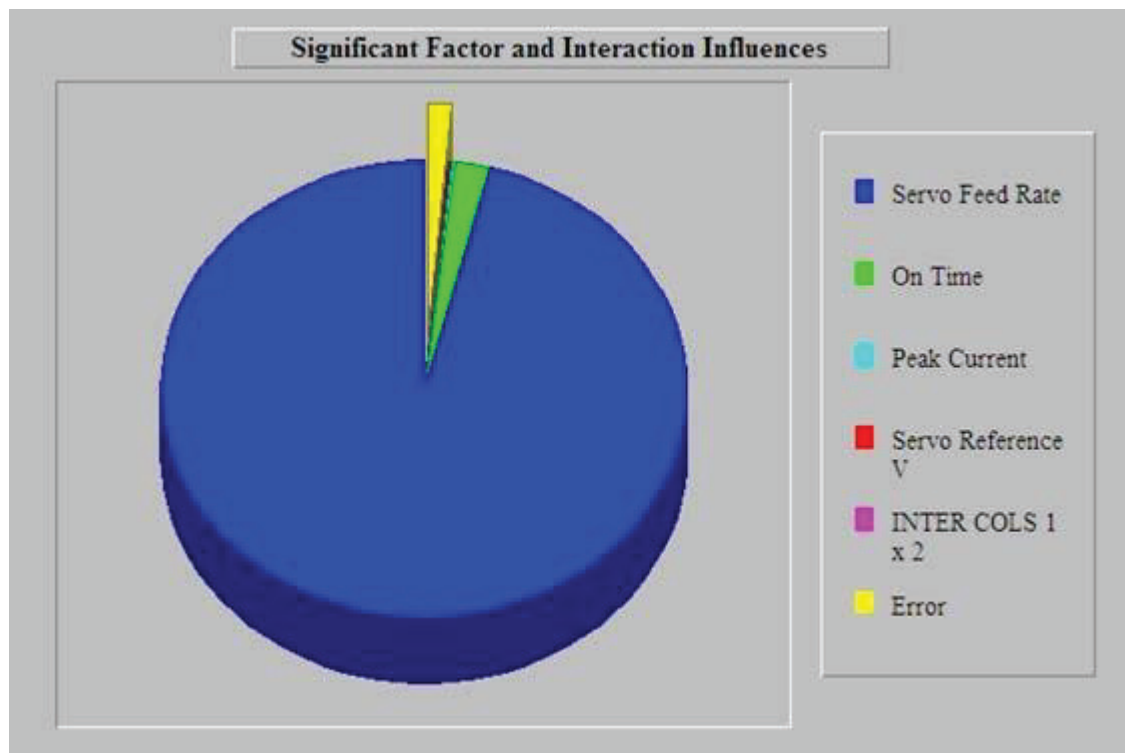


Figure 4.2: Significant factor affecting WEDM cutting speed

d) Estimation of the Optimum Conditions

According to the calculation with the help of software, the fastest cutting speed should be obtained when using condition set as shown in Table 4.8. Besides that, the fastest cutting speed is also able to be predicted. However the estimation result was in S/N ratio. To convert the estimated result to the scale of mm/min, calculation was done. Therefore, the fastest possible cutting speed is 1.926 mm/min with the assumption that the WEDM machine was able to support the speed.

Table 4.8: Estimation of WEDM conditions and predicted performance for fastest cutting speed.

No	Factor	Level Description	Level	Contribution
1	On Time	6	2	0.448
2	Off Time	10	1	pooled
3	Inter Cols 1x2	*Inter*	1	pooled
4	Peak Current	10	1	pooled
5	Servo Feed Rate	20	2	2.822
6	Inter Cols 2x4	*Inter*	1	pooled
7	Servo Reference Voltage	10	1	pooled
Total Contribution From All Factors:				3.270
Current Grand Average Of Performance:				2.421
Expected Result At Optimum Condition				5.691

The equation to estimate of expected result from S/N ratio:

$$S/ N = -10\text{Log}(\text{MSD}) = 5.691$$

$$\text{or MSD} = 10^{(-S/ N) / 10} = 0.269712$$

where

$$\text{MSD} = \frac{1}{n} \left(\frac{1}{y_1^2} + \frac{1}{y_2^2} + \dots + \frac{1}{y_n^2} \right)$$

$$= \frac{1}{Y_{\text{expected}}^2}$$

Therefore,

$$Y_{\text{expected}} = \sqrt{\frac{1}{\text{MSD}}} = \sqrt{\frac{1}{0.269712}} = 1.926 \text{ mm / min}$$

4.3.2 Data Analysis for Material Removal Rate (MRR)

a) Signal to Noise (S/N) Ratio

The material removal rate data were first transformed into S/N ratios using Equation 4.4. The greater the values of S/N the better because this indicates that data variance around the target value are smaller. However, the mean squared deviation (MSD) is defined differently for each of the three quality characteristics considered: smaller, nominal or larger. In the case of material removal rate typically similar to cutting speed, the larger value is selected as this indicates faster cutting speed. Therefore, the MSD for the larger the better is defined as in Equation 4.5. Table 4.9 shows the S/N ratios material removal rate converted from the data.

Table 4.9: S/N ratio for material removal rates.

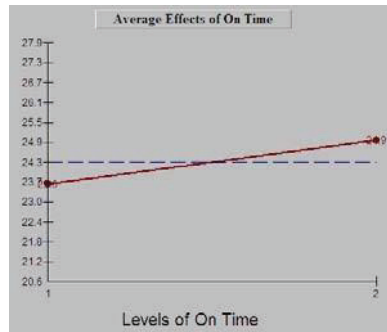
Trail No	Material Removal Rates data			Signal to Noise Ratio
	Result 1	Result 2	Result 3	
1	14.2784	11.4354	12.1692	21.914
2	21.8397	19.3971	20.8930	26.292
3	11.6219	09.2181	10.2829	20.202
4	23.5714	17.2277	19.9988	25.923
5	22.2286	21.7114	26.5643	27.318
6	13.4233	12.5153	13.3498	22.329
7	25.7871	23.4083	26.1057	27.962
8	13.2084	12.2512	13.0300	22.150

b) Main Effects

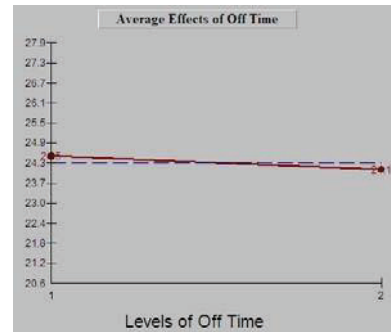
Based on the signal to noise ratio in Table 4.9, the main effects for each factor were generated, as shown in Table 4.10. Since each factor has two levels, the average effect of each level is shown under the two columns marked Level 1 and Level 2. The main effects are the difference between the average effects at Level 1 and Level 2 and they are shown in the fifth column labeled (L2-L1). A minus sign (in the difference column) indicates an increase in noise as the factor changes from Level 1 to Level 2. A positive value, on the other hand, indicates a decrease in noise. For a better illustration, the data were plotted into graph as shown in Figures 4.3 (a) to (g). In S/N analysis, the greater value of S/N represents a more desirable condition.

Table 4.10: Main effect of the factors in effecting material removal rates.

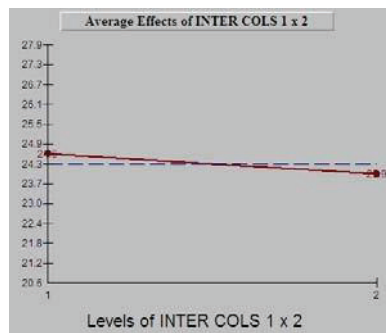
No	Factors	Level 1	Level 2	L2 – L1
1	On Time	23.583	24.940	1.357
2	Off Time	24.463	24.059	-0.404
3	Interaction cols 1x2	24.579	23.943	-0.636
4	Peak Current	24.349	24.173	-0.177
5	Servo Feed Rate	21.649	26.874	5.224
6	Interaction cols 2x4	24.326	24.196	-0.130
7	Servo Reference Voltage	24.532	23.990	-0.543



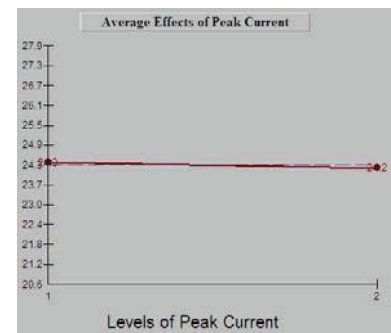
(a)



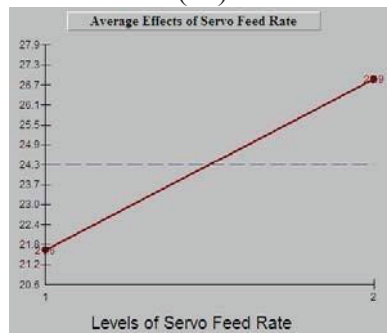
(b)



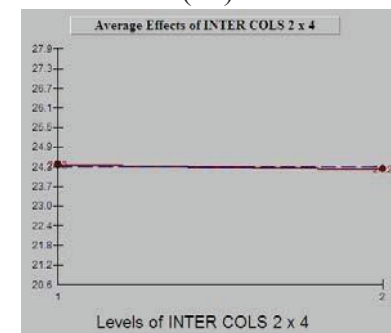
(c)



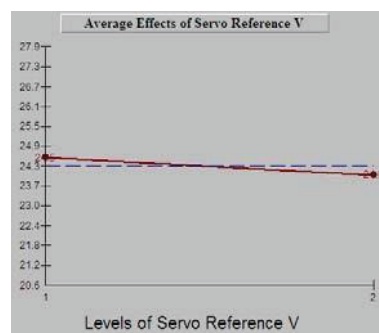
(d)



(e)



(f)



(g)

Figure 4.3: Graphs show average effect of various factor (in affecting material removal rates) at different level (a) On time, (b) Off time, (c) Interaction On and Off time, (d) Peak current, (e) Servo feed rate, (f) Interaction Off time and Peak current, (g) Servo reference voltage.

c) Analysis of Variance (ANOVA)

In order to determine which of the factor/interaction effects are statistically significant, a powerful statistical technique called analysis of variance (ANOVA) was used. Using ANOVA, one is able to identify the active and inactive factor/interaction effects with statistical confidence (Logothetic, 1994). As the S/N ratio is a single performance statistic, it is advisable to pool the insignificant effects to obtain a reasonable estimate of error variance. According to Roy (1990), one should pool the effects (either factor or interaction effects) with low sum of squares in magnitude. Here control factors Off Time, interaction On x Off, Peak Current, interaction Off x Peak current and Servo Reference Voltage have been considered for pooling and the result of the ANOVA on S/N ratio are shown in table 4.11. For better illustration, the percentage contribution of each factor in affecting the WEDM material removal rate is well illustrated through a pie chart as shown in Figure 4.4.

Table 4.11: Pool ANOVA results for material removal rates at 90 percent confidence level.

No	Factor	DOF	Sum of Squares	Variance	F-Ratio	Pure Sum	Percent (%)
1	On Time	1	3.682	3.682	11.955	3.374	5.614
2	Off Time	(1)	0.326		Pooled		
3	Inter Cols 1x2	(1)	0.809		Pooled		
4	Peak Current	(1)	0.061		Pooled		
5	Servo Feed Rate	1	54.598	54.598	177.254	54.290	90.335
6	Inter Cols 2x4	(1)	0.033		Pooled		
7	Servo Reference Voltage	(1)	0.586		Pooled		
	Other/Error	5	1.187	0.893			4.051
	Total	7	60.099				100.000

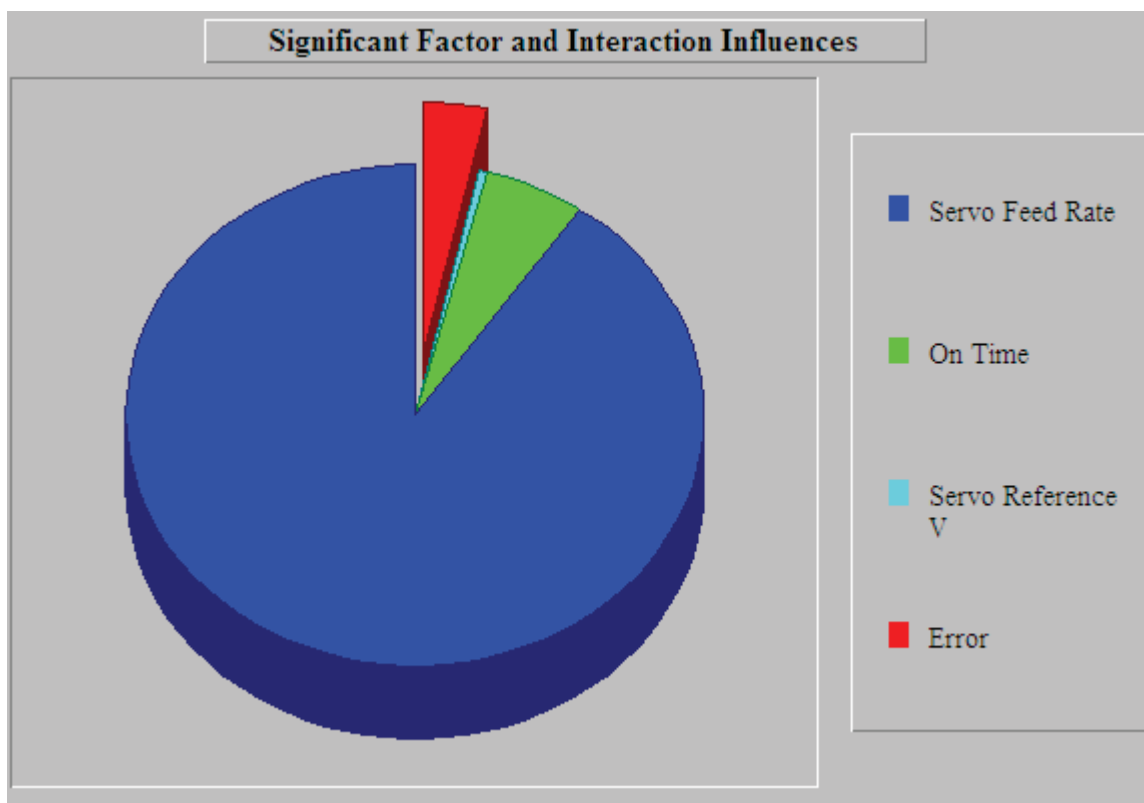


Figure 4.4: Significant factor affecting WEDM material removal rates.

a) Estimation of the Optimum Conditions

According to the calculation with the help of software, the higher material removal rate should be obtained when using condition set as shown in Table 4.12. Besides that, the fastest cutting speed is also able to be predicted. However the estimation result was in S/N ratio. To convert the estimated result to the scale of mg/min, calculation was done below. Therefore, the higher possible material removal rate is 23.853mg/min with the assumption that the WEDM machine was able to support the remove of material from the workpiece during machining.

Table 4.12: Estimation of WEDM conditions and predicted performance for higher material removal rates

No	Factor	Level Description	Level	Contribution
1	On Time	6	2	0.678
2	Off Time	10	1	pooled
3	Inter Cols 1x2	*Inter*	1	pooled
4	Peak Current	10	1	pooled
5	Servo Feed Rate	20	2	2.612
6	Inter Cols 2x4	*Inter*	1	pooled
7	Servo Reference Voltage	10	1	pooled
Total Contribution From All Factors:				3.290
Current Grand Average Of Performance:				24.261
Expected Result At Optimum Condition				27.551

The equation to estimate of expected result:

$$S/N = -10\log(\text{MSD}) = 27.551$$

$$\text{or MSD} = 10^{(-S/N)/10} = 0.001758$$

where

$$\text{MSD} = \frac{1}{n} \left(\frac{1}{y_1^2} + \frac{1}{y_2^2} + \dots + \frac{1}{y_n^2} \right)$$

$$= \frac{1}{Y_{\text{expected}}^2}$$

Therefore,

$$Y_{\text{expected}} = \sqrt{\frac{1}{\text{MSD}}} = \sqrt{\frac{1}{0.001758}} = 23.853 \text{ mg / min}$$

4.3.3 Data Analysis for Surface Roughness

a) Signal to Noise (*S/N*) Ratio

As mention earlier, the mean squared deviation (MSD) is defined differently for each of the three quality characteristics considered, smaller, nominal or larger. In the case of surface roughness, the smaller value is selected as this indicates better surface finish. Therefore, the MSD for the smaller the better is defined as in Equation 4.6. Table 4.13 shows the *S/N* ratio converted from the surface roughness data.

$$\text{MSD} = \left(y_1^2 + y_2^2 + y_3^2 + \dots + y_n^2 \right) / n$$

Where y_1, y_2, \dots, y_n = Results of experiments (eg : Surface roughness, ker f)

Equation 4.6

Table 4.13: *S/N* ratio for surface roughness

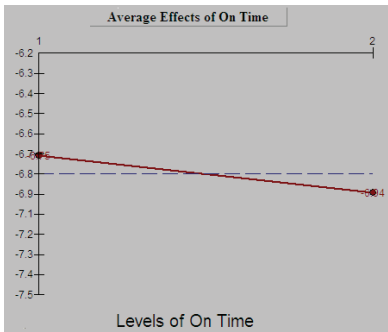
Trail No	Surface Roughness data			Signal to Noise Ratio
	Result 1	Result 2	Result 3	
1	2.43	2.03	2.38	-7.184
2	2.09	2.11	2.13	-6.486
3	2.30	2.09	2.43	-7.150
4	2.06	1.81	2.21	-6.165
5	2.17	1.75	1.97	-5.893
6	2.30	1.88	2.04	-6.364
7	2.63	2.19	2.47	-7.737
8	2.51	2.24	2.57	-7.763

b) Main Effects

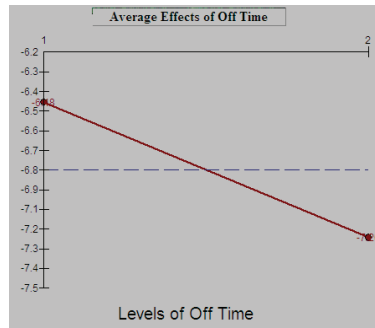
Likewise, the main effects for each of the factors were generated using the Qualitek-4 software, as shown in Table 4.14. Graphs for the main effects were plotted as shown in Figures 4.5 (a) to (g). As mention earlier, a greater value of S/N ratio represents a more desirable condition.

Table 4.14: Main effects of the factor in effecting surface roughness.

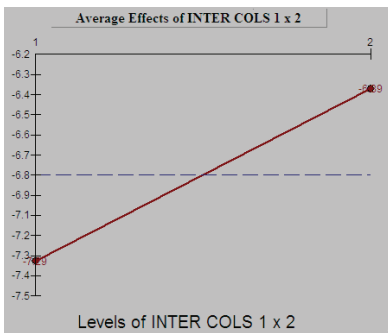
No	Factors	Level 1	Level 2	L2 – L1
1	On Time	-6.746	-6.939	-0.193
2	Off Time	-6.482	-7.204	-0.722
3	Interaction cols 1x2	-7.293	-6.393	0.900
4	Peak Current	-6.991	-6.695	0.295
5	Servo Feed Rate	-7.116	-6.570	0.545
6	Interaction cols 2x4	-6.751	-6.934	-0.183
7	Servo Reference Voltage	-6.863	-6.823	0.040



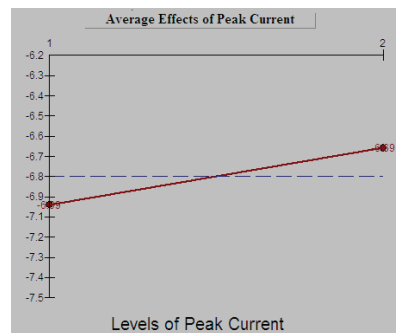
(a)



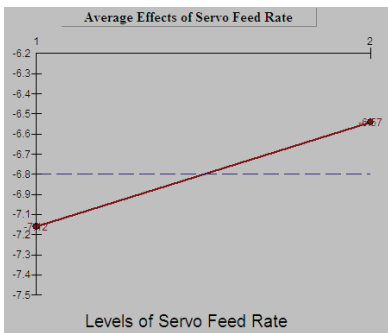
(b)



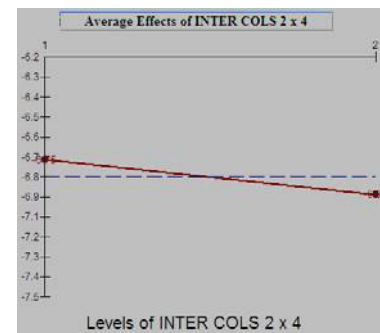
(c)



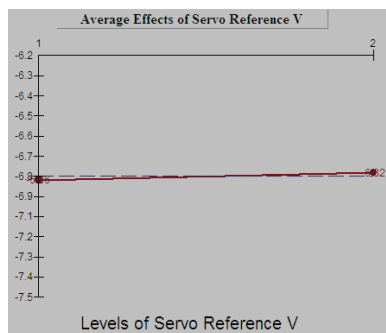
(d)



(e)



(f)



(g)

Figure 4.5: Graphs show average effect of various factor (in affecting surface roughness) at different level (a) On time, (b) Off time, (c) Interaction On and Off time, (d) Peak current, (e) Servo feed rate, (f) Interaction Off time and Peak current, (g) Servo reference voltage.

c) Analysis of Variance (ANOVA)

In order to determine which of the factor/interaction effects are statistically significant, a powerful statistical technique called analysis of variance (ANOVA) was used. Using ANOVA, one is able to identify the active and inactive factor/interaction effects with statistical confidence (Logothetic, 1994). As the S/N ratio is a single performance statistic, it is advisable to pool the insignificant effects to obtain a reasonable estimate of error variance. According to Roy (1990), one should pool the effects (either factor or interaction effects) with low sum of squares in magnitude. Here control factors On Time, Peak Current, interaction Off x Peak current and Servo Reference Voltage have been considered for pooling and the result of the ANOVA on S/N ratio are shown in table 4.15. For better illustration, the percentage contribution of each factor in affecting the surface roughness produced by WEDM is illustrated through a pie chart as shown in Figure 4.6.

Table 4.15: ANOVA results for surface roughness at 90 percent confidence level.

No	Factor	DOF	Sum of Squares	Variance	F-Ratio	Pure Sum	Percent (%)
1	On Time	(1)	0.074		pooled		
2	Off Time	1	1.041	1.041	29.748	1.006	28.160
3	Inter Cols 1x2	1	1.618	1.618	46.221	1.583	44.297
4	Peak Current	(1)	0.175		pooled		
5	Servo Feed Rate	1	0.594	0.594	16.971	0.559	15.645
6	Inter Cols 2x4	(1)	0.066		pooled		
7	Servo Reference Voltage	(1)	0.003		pooled		
	Other/Error	4	0.318				11.898
	Total	7	3.575				100.000

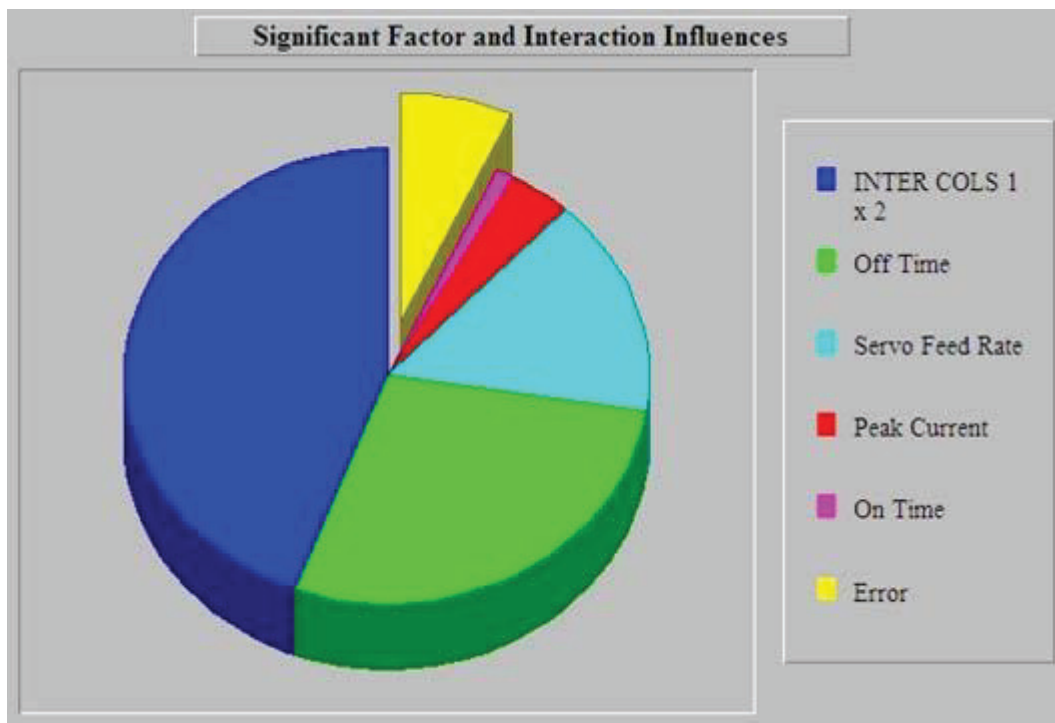


Figure 4.6: Significant factor affecting WEDM surface roughness

d) Estimation of the Optimum Conditions

The finest surface finish for WEDM of Ti-48Al should be obtained when condition set as shown in Table 4.16 is applied. Besides that, the finest surface finish is also able to be predicted. However the estimation result was in S/N ratio. To convert the estimated result to the scale of μm , calculation was done and shown below. Therefore, the finest possible surface finish can be obtained is $1.941\mu\text{m}$.

Table 4.16: Estimation of WEDM conditions and predicted performance for finest surface roughness.

No	Factor	Level Description	Level	Contribution
1	On Time	2	1	pooled
2	Off Time	10	1	0.36
3	Inter Cols 1x2	*Inter*	2	0.449
4	Peak Current	15	2	pooled
5	Servo Feed Rate	20	2	0.272
6	Inter Cols 2x4	*Inter*	1	pooled
7	Servo Reference Voltage	50	2	pooled
Total Contribution From All Factors:				1.080
Current Grand Average Of Performance:				-6.843
Expected Result At Optimum Condition				-5.762

The equation to estimate of expected result:

$$S/N = -10\log(\text{MSD}) = -5.762$$

$$\text{or MSD} = 10^{(-S/N)/10} = 3.768773$$

Where,

$$\text{MSD} = \left(y_1^2 + y_2^2 + y_3^2 + \dots + y_n^2 \right) / n$$

$$\text{MSD} = Y_{\text{expected}}^2$$

Therefore,

$$Y_{\text{expected}} = \sqrt{\text{MSD}} = \sqrt{3.768773} = 1.941 \mu\text{m}$$

4.3.4 Data Analysis for kerf

a) Signal to Noise (*S/N*) Ratio

As mention before, the mean squared deviation (MSD) is defined differently for each of the three quality characteristics considered, smaller, nominal or larger. In the case of kerf, definitely similar to the surface finish characteristic. Therefore, the smaller value is selected as this indicates better kerf. The MSD for the smaller the better is defined as in Equation 4.6. Table 4.17 shows the *S/N* ratio converted from the kerf data.

Table 4.17: *S/N* ratio for kerf

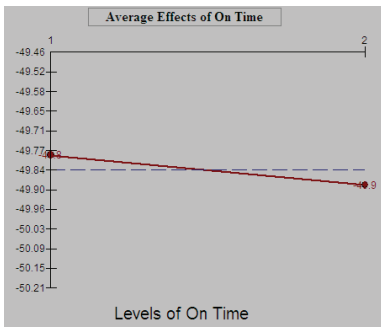
Trail No	Kerf data (mm) x 10 ⁻³			Signal to Noise
	Result 1	Result 2	Result 3	Ratio
1	327.5	309.82	332.90	-50.200
2	292.86	266.00	292.98	-49.074
3	341.63	316.39	338.33	-50.431
4	300.72	284.96	304.29	-49.449
5	302.7	281.77	298.69	-49.383
6	310.16	293.41	307.45	-49.651
7	335.63	313.29	338.77	-50.356
8	335.07	301.94	326.75	-50.146

b) Main Effects

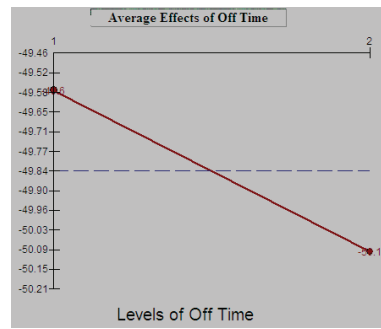
Similarly, the main effects for each of the factors were generated using the Qualitek-4 software, as shown in Table 4.18. Graphs for the main effects were plotted as shown in Figures 4.7(a) to (g). As mention earlier, a greater value of S/N ratio represents a more desirable condition.

Table 4.18: Main effects of the factor in effecting kerf.

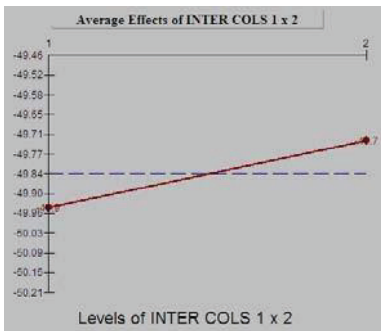
No	Factors	Level 1	Level 2	L2 – L1
1	On Time	-49.788	-49.884	-0.097
2	Off Time	-49.577	-50.095	-0.519
3	Interaction cols 1x2	-49.944	-49.729	0.215
4	Peak Current	-50.092	-49.580	0.512
5	Servo Feed Rate	-50.107	-49.585	0.542
6	Interaction cols 2x4	-49.794	-49.878	-0.085
7	Servo Reference Voltage	-49.914	-49.758	0.155



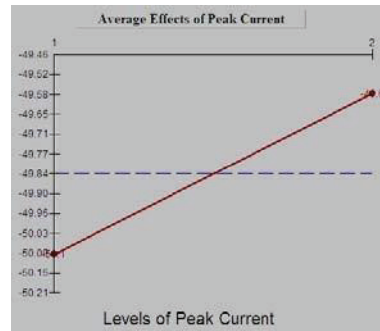
(a)



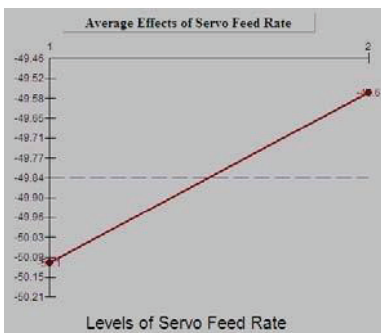
(b)



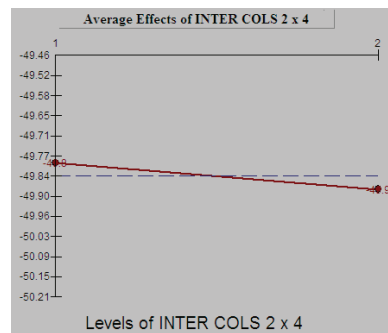
(c)



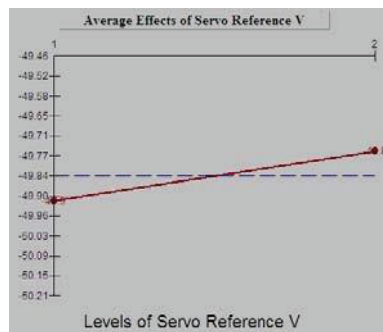
(d)



(e)



(f)



(g)

Figure 4.7: Graphs show average effect of various factor (in affecting kerf) at different level (a) On time, (b) Off time, (c) Interaction On and Off time, (d) Peak current, (e) Servo feed rate, (f) Interaction Off time and Peak current, (g) Servo reference voltage.

c) Analysis of Variance (ANOVA)

In order to determine which of the factor/interaction effects are statistically significant, a powerful statistical technique called analysis of variance (ANOVA) was used. Using ANOVA, one is able to identify the active and inactive factor/interaction effects with statistical confidence (Logothetic, 1994). As the S/N ratio is a single performance statistic, it is advisable to pool the insignificant effects to obtain a reasonable estimate of error variance. According to Roy (1990), one should pool the effects (either factor or interaction effects) with low sum of squares in magnitude. Here control factors On Time, interaction On x Off, interaction Off x Peak current and Servo Reference Voltage have been considered for pooling and the result of the ANOVA on S/N ratio are shown in table 4.19. For better illustration, the percentage contribution of each factor in affecting the kerf produced by WEDM is illustrated through a pie chart as shown in Figure 4.8.

Table 4.19: ANOVA results for kerf at 90 percent confidence level.

No	Factor	DOF	Sum of Squares	Variance	F-Ratio	Pure Sum	Percent (%)
1	On Time	(1)	0.019		pooled		
2	Off Time	1	0.539	0.539	33.473	0.523	28.714
3	Inter Cols 1x2	(1)	0.094		pooled		
4	Peak Current	1	0.523	0.523	32.494	0.507	27.848
5	Servo Feed Rate	1	0.584	0.584	36.310	0.568	31.222
6	Inter Cols 2x4	(1)	0.012		pooled		
7	Servo Reference Voltage	(1)	0.046		pooled		
	Other/Error	4	0.173	0.156			12.216
	Total	7	1.822				100.000

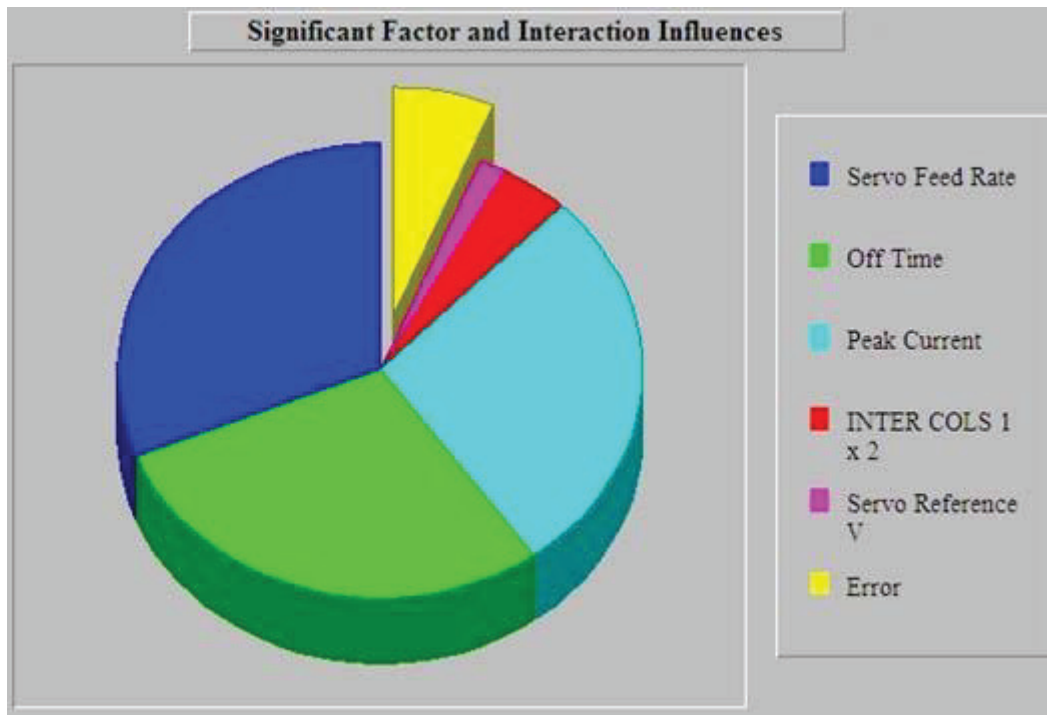


Figure 4.8: Significant factor affecting WEDM of kerf.

d) Estimation of the Optimum Conditions

The finest surface finish for WEDM of Ti-48Al should be obtained when condition set as shown in Table 4.20 is applied. Besides that, the better kerf is also able to be predicted. However the estimation result was in S/N ratio. To convert the estimated result to the scale of μm , calculation was done and shown below. Therefore, the finest possible surface finish can be obtained is $274.758\mu\text{m}$.

Table 4.20: Estimation of WEDM conditions and predicted performance for better kerf.

No	Factor	Level Description	Level	Contribution
1	On Time	2	1	pooled
2	Off Time	10	1	0.259
3	Inter Cols 1x2	*Inter*	2	pooled
4	Peak Current	15	2	0.256
5	Servo Feed Rate	20	2	0.270
6	Inter Cols 2x4	*Inter*	1	pooled
7	Servo Reference Voltage	50	2	pooled
Total Contribution From All Factors:				0.785
Current Grand Average Of Performance:				-49.836
Expected Result At Optimum Condition				-49.051

The equation to estimate of expected result:

$$S/N = -10\log(\text{MSD}) = -49.051$$

$$\text{or MSD} = 10^{(-S/N)/10} = 80371.09$$

Where,

$$\text{MSD} = \left(y_1^2 + y_2^2 + y_3^2 + \dots + y_n^2 \right) / n$$

$$\text{MSD} = Y_{\text{expected}}^2$$

Therefore,

$$Y_{\text{expected}} = \sqrt{\text{MSD}} = \sqrt{75491.83} = 283.498 \mu\text{m}$$

4.4 Interaction

The term interaction, expressed by inserting “X” mark between the two interacting factors, is used to describe a condition in which the influence of one factor upon the result is dependent on the condition of the other [42]. Two factors A and B are said to interact (written as A x B) when the effects of changes in the level of A, determines the influence of B and vice versa. From the experiment data, a graphical method can be used to reveal the existence of interaction. Assuming there are 2 factors with two levels at each factor, and the experiment data are plotted into a graph. This experiment is carried out as to determine the interaction since the factors cross lines, and no interaction was occurred when the line parallel. The interaction between two factors for cutting speed, material removal rate, kerf and surface roughness will be described as bellow.

4.4.1 Interaction between two factors for cutting speed

The significant interacting factors for cutting speed between two factors are as follows (shown in table 4.21) while the plotted graph of interaction is on figure 4.9. The interaction severity index shown in figure 4.10 determine the significant percentage for interaction between two factors influences the cutting speed.

Table 4.21: Interacting between two factors for cutting speed.

Rank	Interacting factor	Columns	SI (%)	Col	Opt.
1	Off Time x Servo reference voltage	2 x 7	94.41	5	[2,1]
2	On Time x Peak current	1 x 4	86.27	5	[2,1]
3	Peak current x Servo reference voltage	4 x 7	43.33	3	[1,1]
4	Off Time x Peak current	2 x 4	33.18	6	[1,1]
5	On Time x Off Time	1 x 2	25.33	3	[2,2]
6	On Time x Servo reference voltage	1 x 7	17.92	6	[2,1]
7	Peak current x Servo feed rate	4 x 5	13.72	1	[1,2]
8	On Time x Servo feed rate	1 x 5	5.64	4	[2,2]

9	Off Time x Servo feed rate	2 x 5	5.58	7	[2,2]
10	Servo feed rate x Servo reference voltage	5 x 7	4.94	2	[2,1]

Columns of chart explained:

Columns – Indicates the column of the interacting

SI – Interaction severity index (100% for 90 degrees, 0% for parallel)

Col – Column number that should be reserved for interacting effect

Opt – Indicates the optimum levels of the interacting

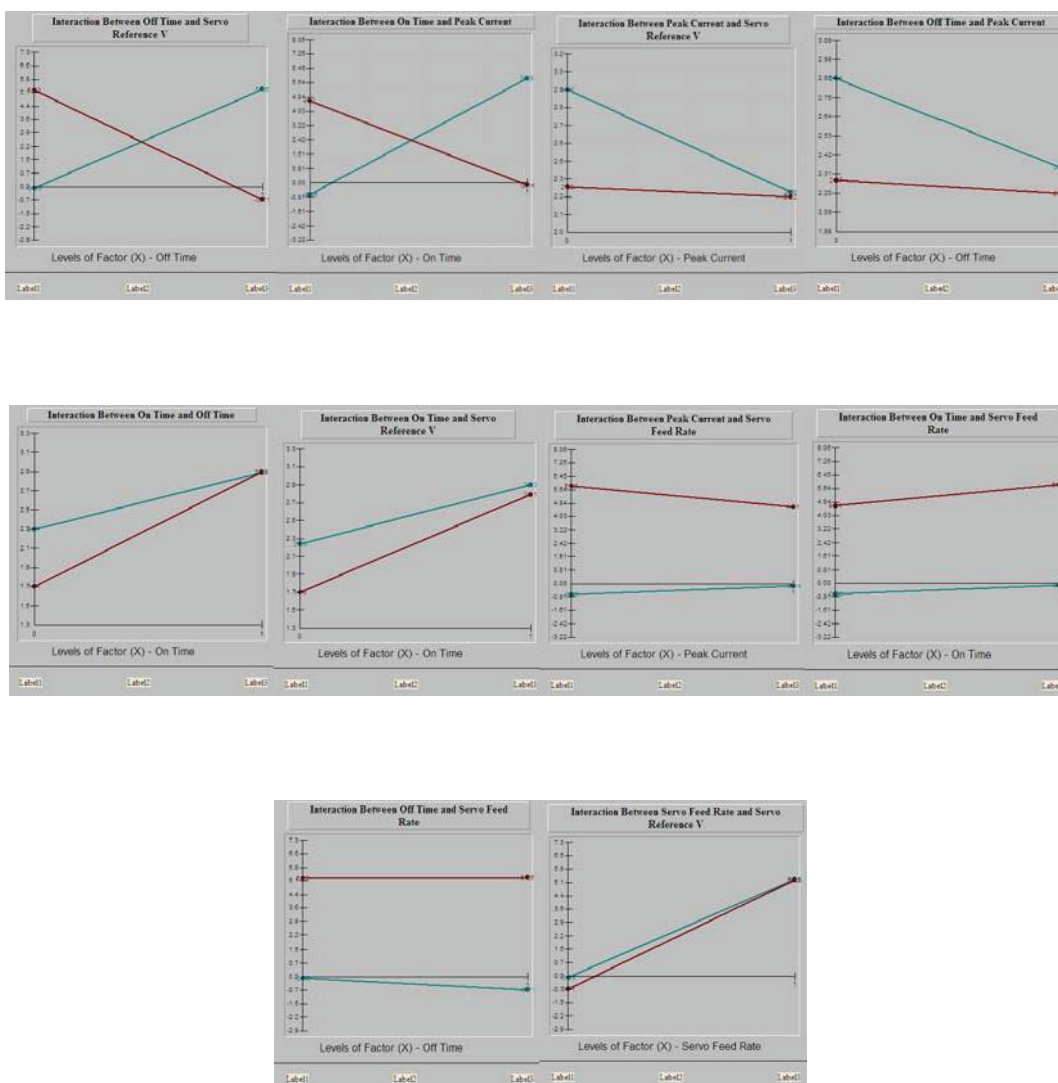


Figure 4.9: Interacting between 2 factors for cutting speed

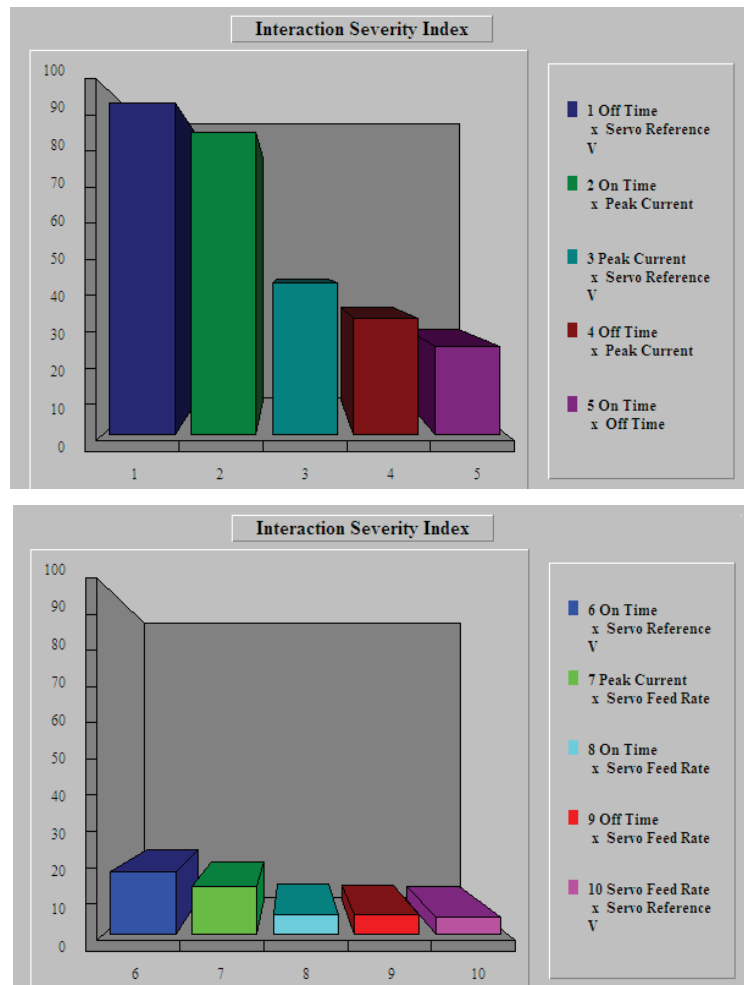


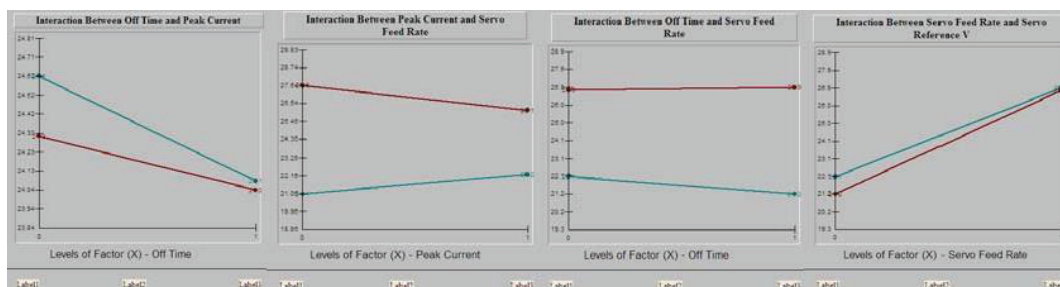
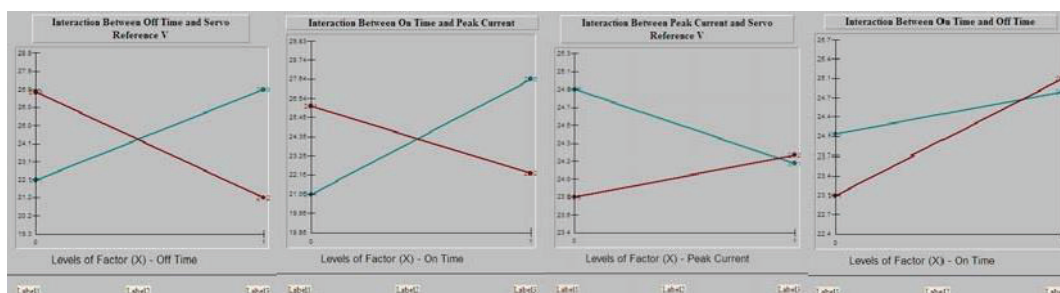
Figure 4.10: Interaction severity index for cutting speed.

4.4.2 Interaction between two factors for material removal rate

Interaction between two factors for material removal rate consequently to the interaction of cutting speed because the fastest the cutting speed at the same time, more material will be removed from the workpiece during machining. The significant interaction rank by severity index (SI) shown in table 4.22 and will describe on plotted graph in figure 4. 11 and figure 4.12 show the histogram of interaction by percentage influence the material removal rate.

Table 4.22: Interacting between two factors for material removal rate.

Rank	Interacting factor	Columns	SI (%)	Col	Opt.
1	Off Time x Servo reference voltage	2 x 7	90.61	5	[2,1]
2	On Time x Peak current	1 x 4	79.38	5	[2,1]
3	Peak current x Servo reference voltage	4 x 7	54.03	3	[1,1]
4	On Time x Off Time	1 x 2	31.92	3	[2,2]
5	Off Time x Peak Current	2 x 4	22.43	6	[1,1]
6	Peak current x Servo feed rate	4 x 5	20.61	1	[1,2]
7	Off Time x Servo feed rate	2 x 5	9.38	7	[2,2]
8	Servo feed rate x Servo reference voltage	5 x 7	7.0	2	[2,1]
9	On Time x Servo reference voltage	1 x 7	6.84	6	[2,1]
10	On Time x Servo feed rate	1 x 5	2.66	4	[2,2]



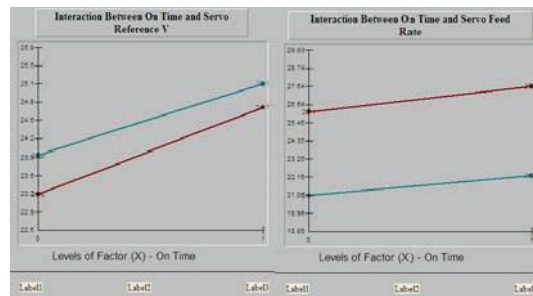


Figure 4.11: Interacting between 2 factors for material removal rate.

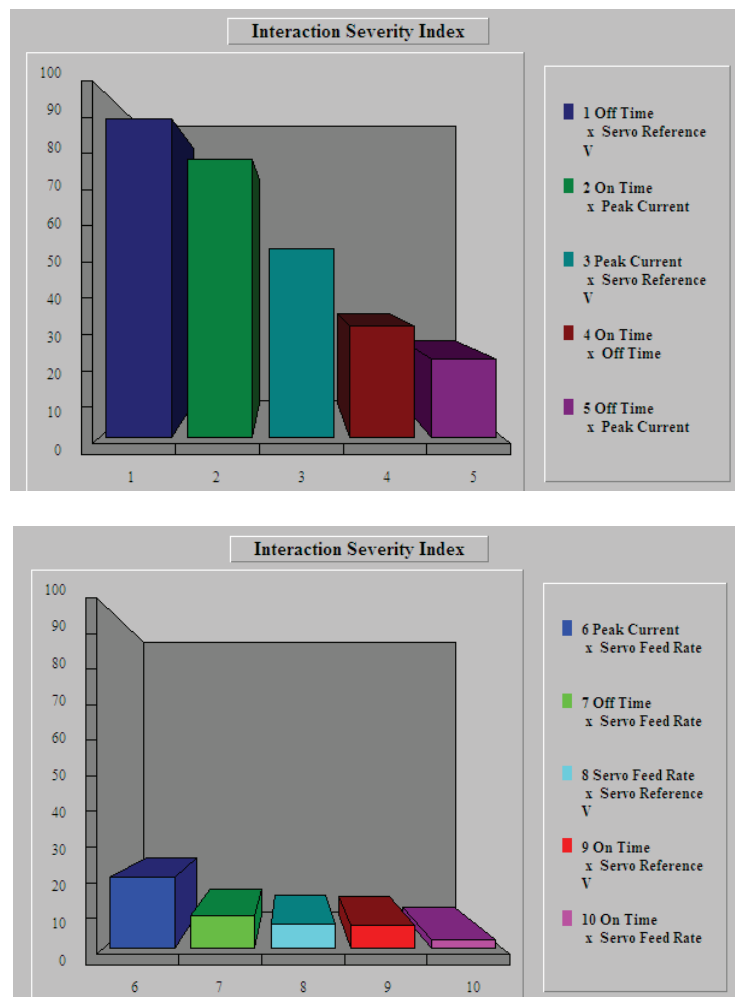


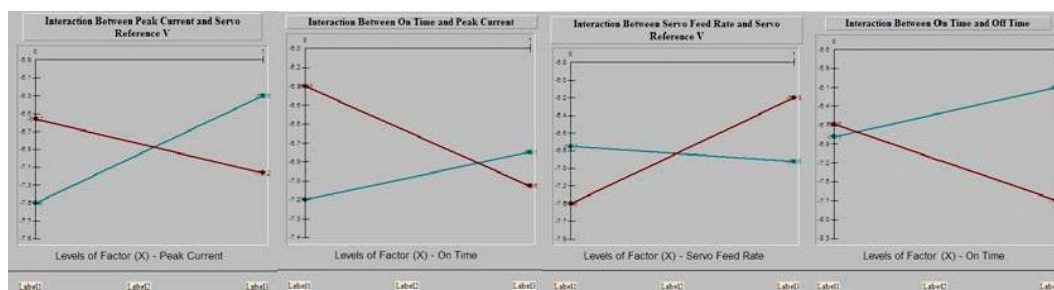
Figure 4.12: Interaction severity index for material removal rate.

4.4.3 Interaction between two factors for surface roughness

The interaction between two factors influences in surface roughness during machining shown in table 4.23, where the direction for and which is the optimum condition will be defined in each interaction. The plotted graph in figure 4.13 explained the significant interaction occurred from the experiment. The histogram of severity index in figure 4.14 describes the percentage contributed in surface roughness.

Table 4.23: Interacting between two factors for surface roughness.

Rank	Interacting factor	Columns	SI (%)	Col	Opt.
1	Peak current x Servo reference voltage	4 x 7	75.2	3	[2,1]
2	On Time x Peak current	1 x 4	64.76	5	[1,2]
3	Servo feed rate x Servo reference voltage	5 x 7	56.97	2	[2,2]
4	On Time x Off Time	1 x 2	55.48	3	[2,1]
5	On Time x Servo reference voltage	1 x 7	48.66	6	[1,1]
6	Off Time x Servo reference voltage	2 x 7	43.02	5	[1,2]
7	On Time x Servo feed rate	1 x 5	35.23	4	[1,2]
8	Peak current x Servo feed rate	4 x 5	22.92	1	[2,2]
9	Off Time x Peak current	2 x 4	17.95	6	[1,2]
10	Off Time x Servo feed rate	2 x 5	3.09	7	[1,2]



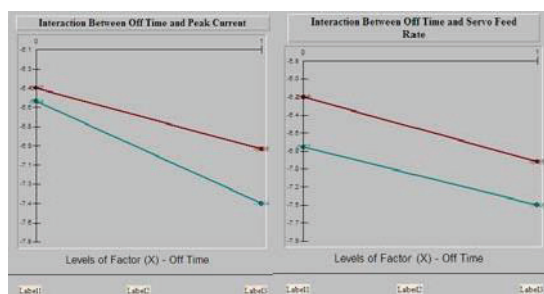
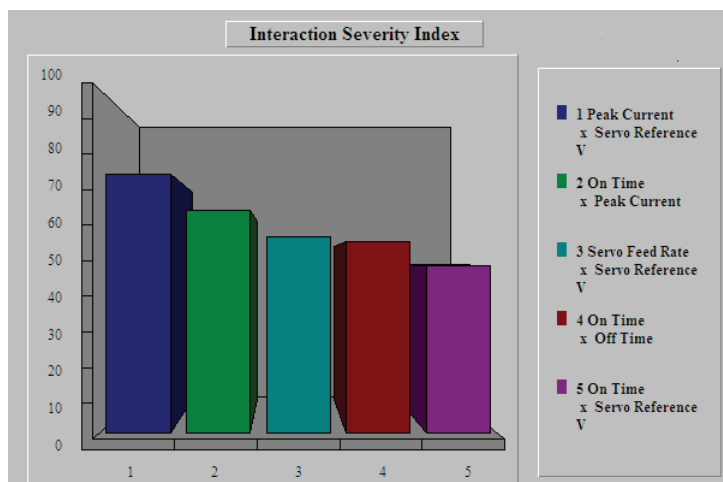


Figure 4.13: Interacting between 2 factors for surface roughness.



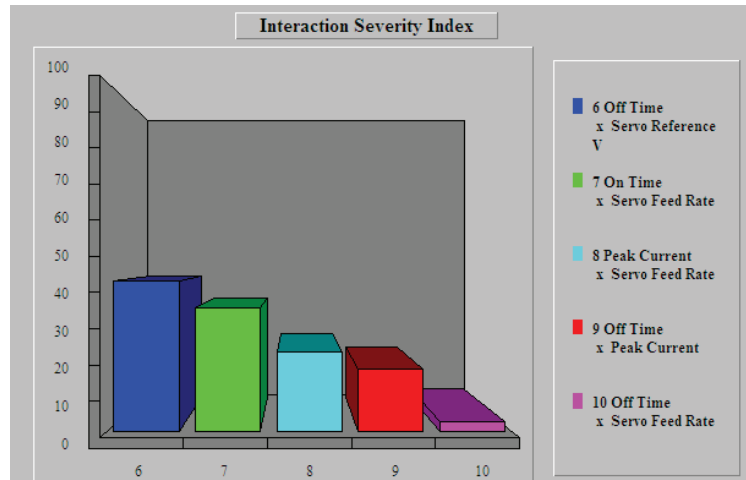


Figure 4.14: Interaction severity index for surface roughness.

4.4.4 Interaction between two factors for Kerf

Referring to table 4.24, shows the percentage interaction between two factors will influence the kerf. The plotted graph in figure 4.15 explained the significant interaction, while the histogram in figure 4.16 describes the detail of the contribution of each interaction.

Table 4.24: Interacting between two factors for kerf.

Rank	Interacting factor	Columns	SI (%)	Col	Opt.
1	On Time x Peak current	1 x 4	51.38	5	[1,2]
2	Off Time x Servo reference voltage	2 x 7	51.08	5	[1,2]
3	Servo feed rate x Servo reference voltage	5 x 7	48.91	2	[2,2]
4	On Time x Servo feed rate	1 x 5	48.61	4	[1,2]
5	On Time x Servo reference voltage	1 x 7	33.35	6	[1,2]
6	Peak current x Servo reference voltage	4 x 7	29.56	3	[2,1]
7	On Time x Off Time	1 x 2	29.31	3	[2,1]
8	Off Time x Servo feed rate	2 x 5	14.65	7	[1,2]
9	Peak current x Servo feed rate	4 x 5	9.05	1	[2,2]
10	Off Time x Peak current	2 x 4	8.11	6	[1,2]

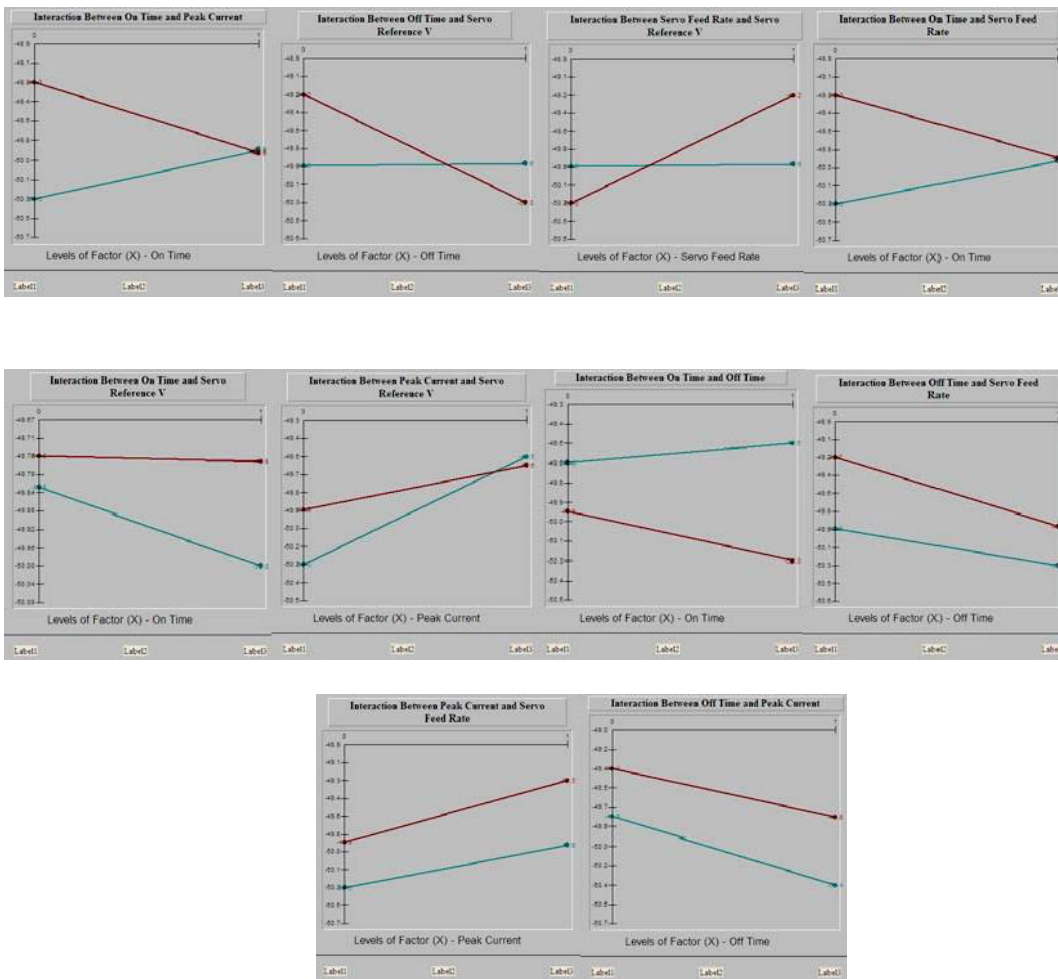
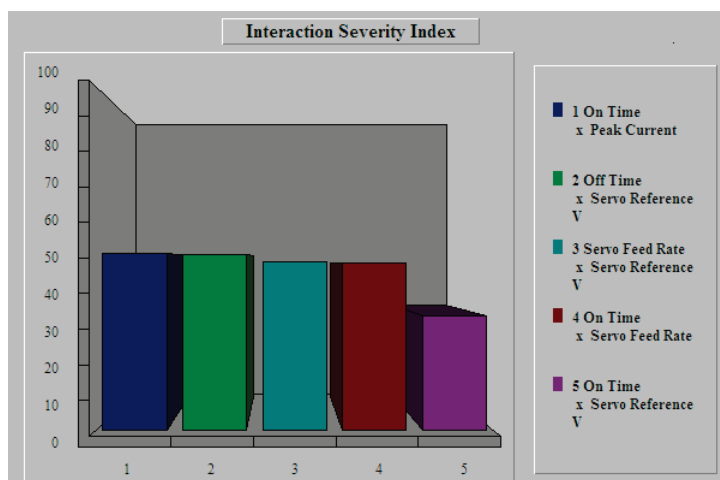


Figure 4.15: Interacting between 2 factors for kerf.



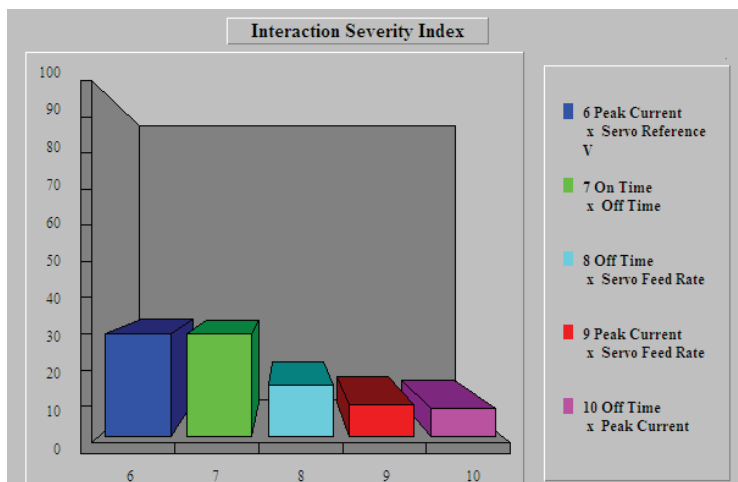


Figure 4.16: Interaction severity index for kerf.

4.5 Confirmation Test Results

Once the optimum parameter settings were identified and the prediction results were also generated, the confirmation test needs to be carried out. Confirmation testing is a necessary and important step in the Taguchi method as it is a direct proof of the methodology. The following tables show the experimental results and the condition sets that produce fastest cutting speed, higher material removal rate, finest surface finish and better kerf respectively. The experimental results were then compared with the predicted results generated by the Taguchi method, as shown in Table 4.25 to 4.28. The percentage of error was calculated using Equation 4.7.

$$\text{Percentage of Error} = \frac{[\text{Theoretical Result} - \text{Experimental Result}]}{\text{Theoretical Result}} \times 100\%$$

Equation 4.7

Table 4.25: Comparison between the theoretical result and the experimental result for fastest cutting speed.

Cutting Speed (mm/min)					Percentage of Error (%)
Theoretically	Experimentally				
	Repeat 1	Repeat 2	Repeat 3	Average	
1.9260	1.9809	1.9816	1.9833	1.9819	2.90
<u>Setting Factors:</u> On Time = 6 μ s Off Time = 10 μ s Peak Current = 10A Servo Feed Rate = 20 mm/min Servo Reference Voltage = 10 V					

Table 4.26: Comparison between the theoretical result and the experimental result for higher material removal rates (MRR).

Material Removal Rates (mg/min)					Percentage of Error (%)
Theoretically	Experimentally				
	Repeat 1	Repeat 2	Repeat 3	Average	
23.8530	25.3129	26.2171	26.1048	25.8783	8.50
<u>Setting Factors:</u> On Time = 6 μ s Off Time = 10 μ s Peak Current = 10A Servo Feed Rate = 20 mm/min Servo Reference Voltage = 10 V					

Table 4.27: Comparison between the theoretical result and the experimental result for finest surface roughness.

Surface Roughness (Ra)					Percentage of Error (%)
Theoretically	Experimentally				
	Repeat 1	Repeat 2	Repeat 3	Average	
1.941	2.05	1.86	1.96	1.957	0.8
<u>Setting Factors:</u> On Time = 2 μ s Off Time = 10 μ s Peak Current = 15A Servo Feed Rate = 20 mm/min Servo Reference Voltage = 50 V					

Table 4.28: Comparison between the theoretical result and the experimental result for smaller kerf.

Kerf (mm)x 10⁻³					Percentage of Error (%)
Theoretically	Experimentally				
	Repeat 1	Repeat 2	Repeat 3	Average	
283.498	289.152	288.426	280.048	285.875	0.83
<u>Setting Factors:</u> On Time = 2 μ s Off Time = 10 μ s Peak Current = 15A Servo Feed Rate = 20 mm/min Servo Reference Voltage = 50 V					

4.3 Analysis of Surface Characterization of Machined Ti-48Al

The analyses were separated by direct machined surface and the cross sectional surface of the specimen.

4.3.1 Direct machined surface

Firstly, the analysis was done on the pre machining surface to define the severity of the surface roughness and to identify the element present on the surface and the microstructure of Ti-48Al. Figure 4.17 shows microstructure before machined by wire-cut processes by using Zeiss optical microscope model axiotech with the different magnification.

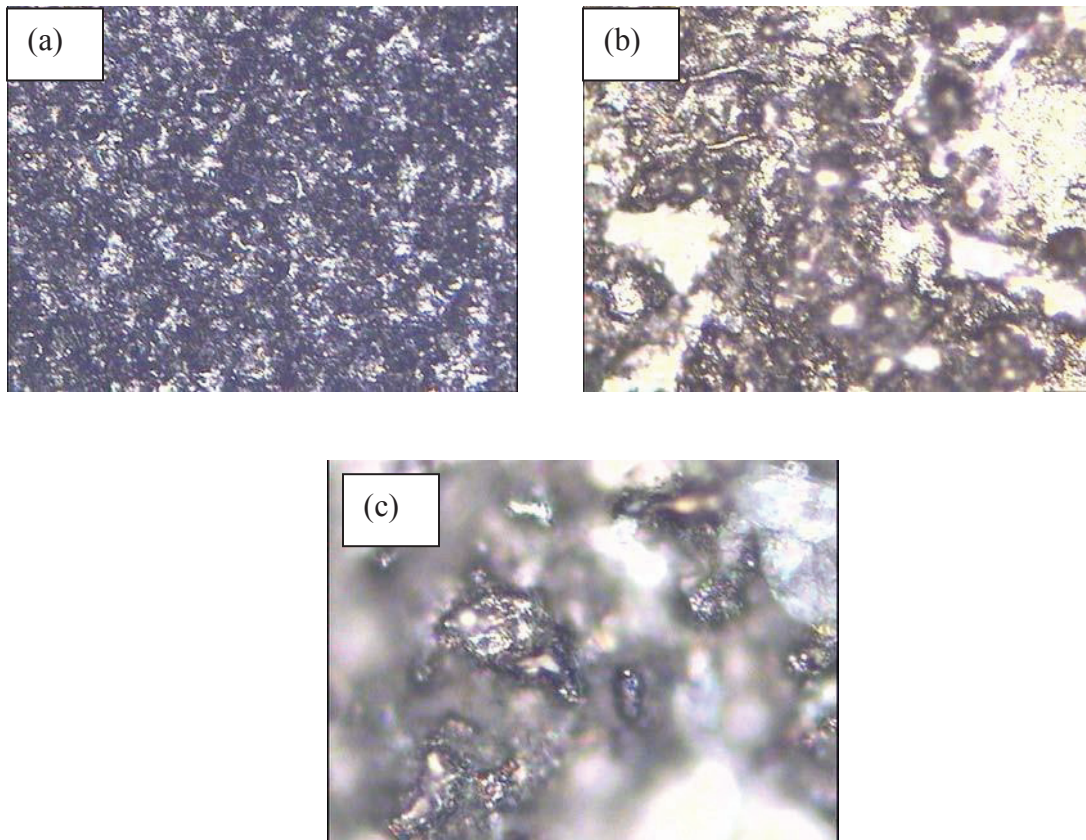


Figure 4.17 (a), (b) and (c): Microstructure of Ti-48Al before machining at magnification of 10x, 20x and 50x before machined by wire-cut process.

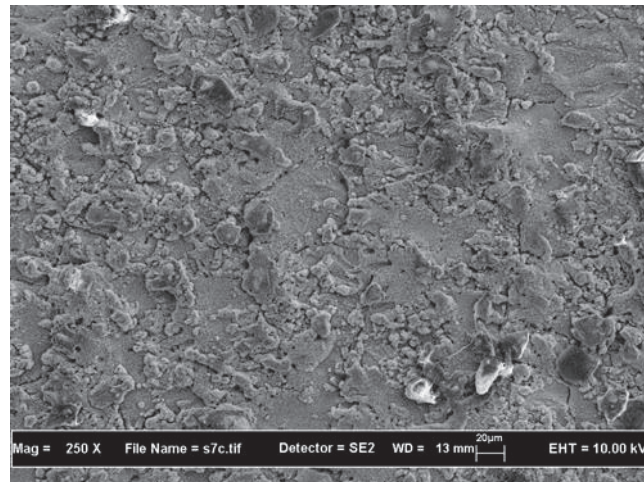
a) Field Emission Scanning Electron Microscopy (FESEM)

FESEM is used to observe the severity of the surface roughness resulted by the wire-cut process and to identify the element present on the machined surface. Figure 4.18 (a) illustrates micrograph of the surface morphology of machined surface which contributed to higher material removal rate. Figure 4.18 (b) shows surface morphology that contributed finest surface finish. Both the figure elaborated more crack but (a) is more significant than (b). At magnification 250x, it can be observed where the surface produced by wire-cut process was rough.

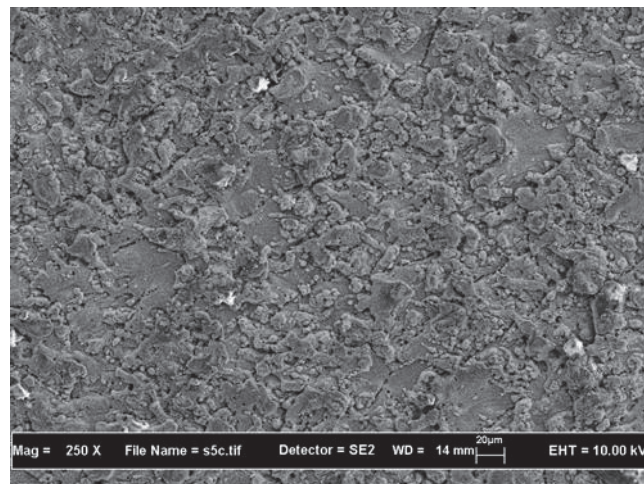
Figure 4.19 illustrates micrograph with difference magnification. Upon observation, it is found that crystal formed on top of the surface.

b) Energy Dispersive Spectroscopy Microanalysis (EDS)

Analyzed to identify the element present on top of the machined surface by wire-cut was done by using energy dispersive spectroscopy microanalysis (EDS). The results of the various features are illustrated in figure 4.20 (contributed higher MRR) and figure 4.21 (contributed finest surface finish and smaller kerf) showing the significant element exist on top of the machined surface.



(a)



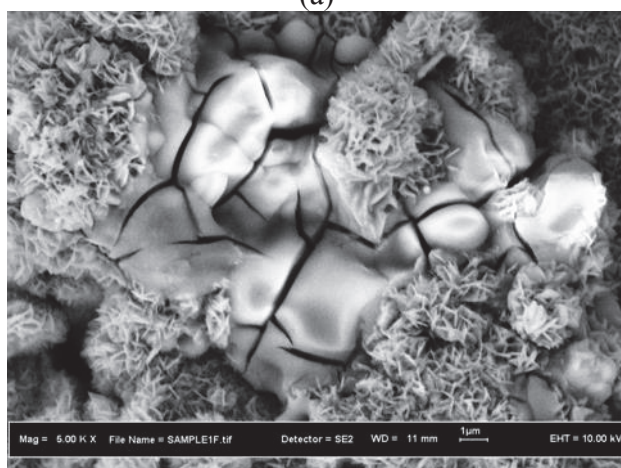
(b)

Figure 4.18: FESEM micrographs of surface morphology of WEDM Ti-48Al at 500x with WEDM condition:

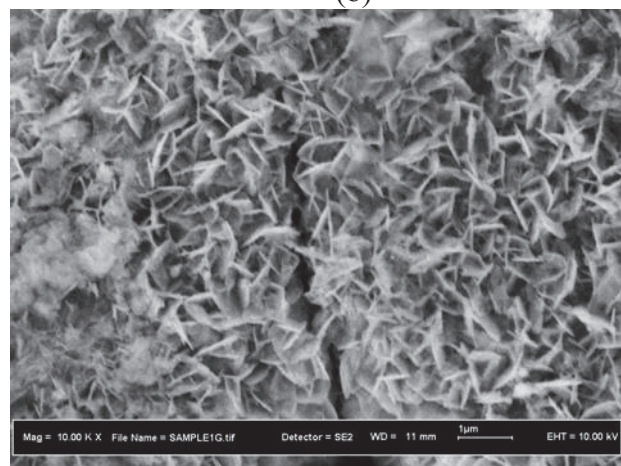
- a) On Time= $6\mu\text{s}$, Off Time= $10\mu\text{s}$, Peak Current=10A, Servo Feed Rate=20mm/min and Servo Reference Voltage=10V (Contributed to higher MRR=25.8783mg/min)
- b) On Time= $2\mu\text{s}$, Off Time= $10\mu\text{s}$, Peak Current=15A, Servo Feed Rate=20mm/min and Servo Reference Voltage=50V (Contributed to finest surface finish=1.957Ra)



(a)



(b)



(c)

Figure 4.19: FESEM micrographs of surface morphology of WEDM Ti-48Al at various magnifications where crystal observed on the top surface machined. (a) 2,500x (b) 5,000x (c) x10,000. (Machining Condition: On Time=6 μ s, Off Time=10 μ s, Peak Current=10A, Servo Feed Rate=20mm/min and Servo Reference Voltage=10V (Contributed to higher MRR=25.8783mg/min))

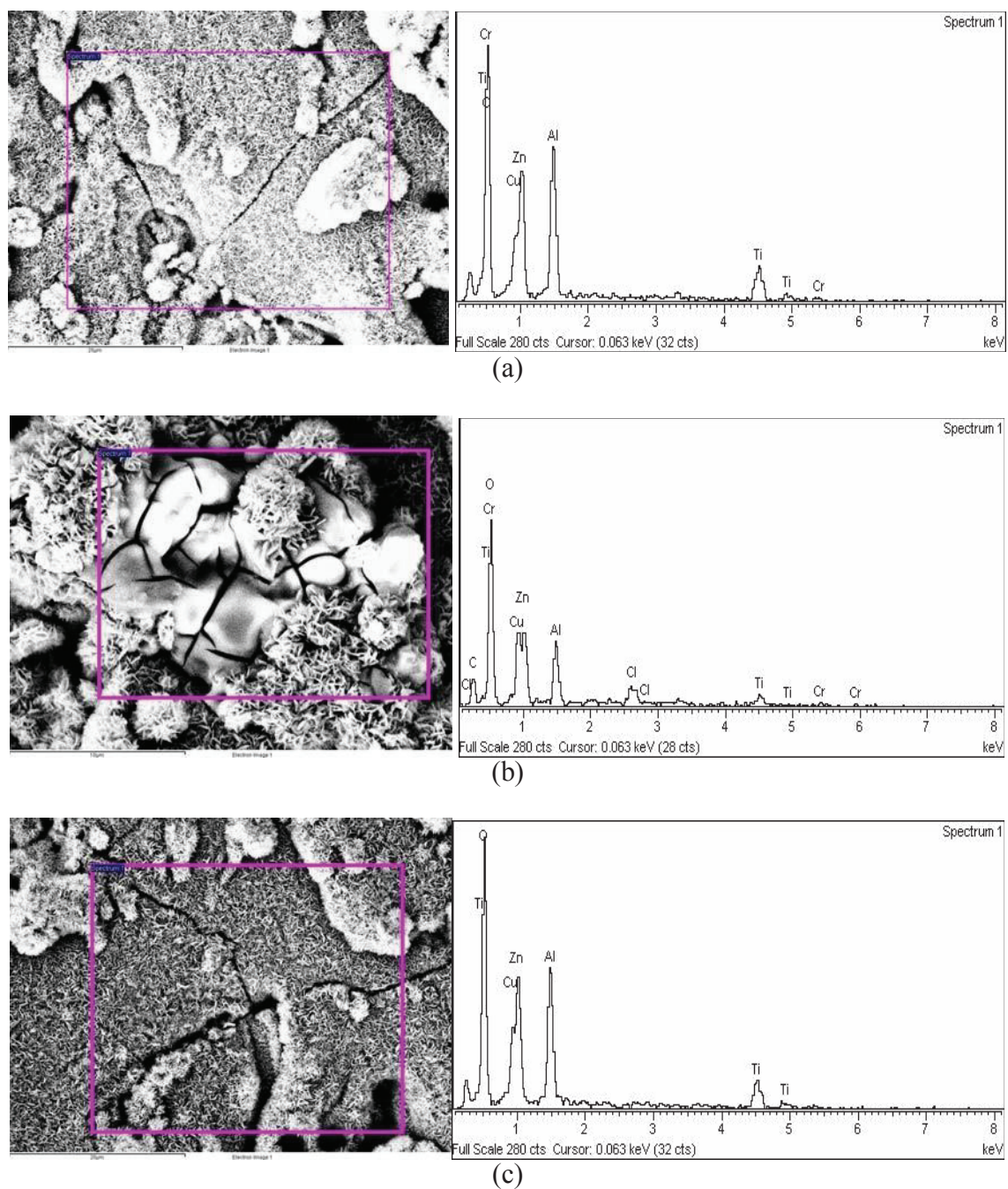


Figure 4.20: FESEM micrographs of WEDM Ti-48Al surface with corresponding EDX spectrum at various features with machining Condition: On Time=6 μ s, Off Time=10 μ s, Peak Current=10A, Servo Feed Rate=20mm/min and Servo Reference Voltage=10V (Contributed to higher MRR=25.8783mg/min)

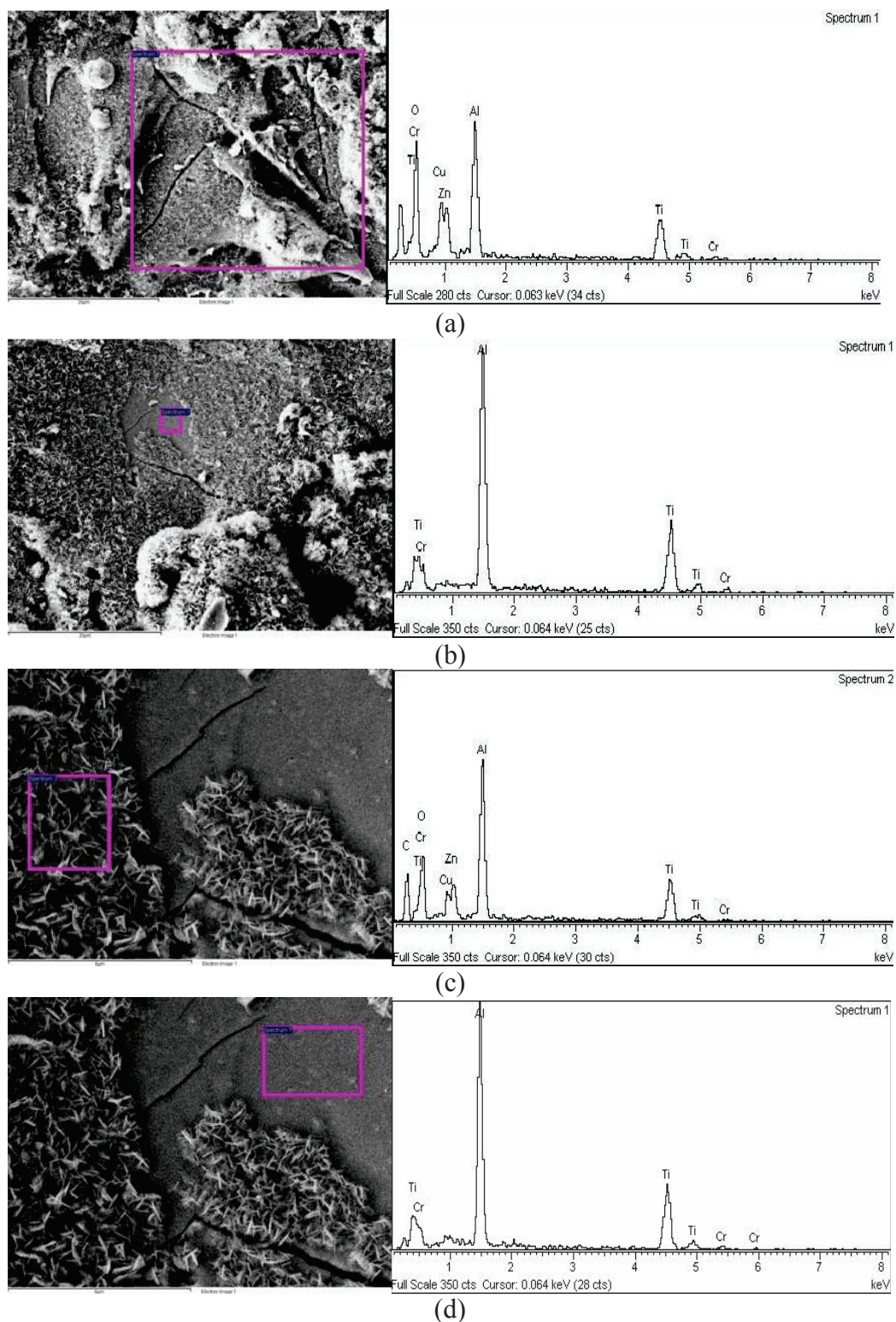


Figure 4.21: FESEM micrographs of WEDM Ti-48Al surface with corresponding EDX spectrum at various features with WEDM condition On Time=2 μ s, Off Time=10 μ s, Peak Current=15A, Servo Feed Rate=20mm/min and Servo Reference Voltage=50V (Contributed to finest surface finish=1.957Ra)

4.3.2 Cross Sectional Analysis of the Specimen

The cross sectional analyses were done in this study to investigate through the layers formed during wire-cut process.

a) Field Emission Scanning Electron Microscopy (FESEM)

Figure 4.22 and figure 4.23 show the micrographs of the cross sectioned specimen with the difference response of wire-cut performance. Figure 4.22 describes the higher material removal rate while figure 4.23 illustrates the machining condition for finest surface finish produced by WEDM process. It can be observed that there are hardened layer on top of the base –alloy. This layer is called recast layer. The thickness of this recast layer for the higher material removal rate (figure 4.22) ranges from $5\mu\text{m}$ to $12\mu\text{m}$. However, the thickness recast layer for the finest surface finish (figure 4.23) is from $2\mu\text{m}$ to $6\mu\text{m}$.

Micro crack was identified in this study and to prove this figure 4.24 and 4.25 will describe cracks that occurred during cutting the Ti-48Al by WEDM. In figure 4.24 illustrates the microcracks penetrate deeper than recast layer, as deep as $25\mu\text{m}$, it was observed in machining condition; On Time= $6\mu\text{s}$, Off Time= $10\mu\text{s}$, Peak Current= 10A , Servo Feed Rate= $20\text{mm}/\text{min}$ and Servo Reference Voltage= 10V (Contributed to higher MRR= $25.8783\text{mg}/\text{min}$). Likewise, in figure 4.23 shows microcracks penetration as deep as $7\mu\text{m}$ occurred in the machining condition; On Time= $2\mu\text{s}$, Off Time= $10\mu\text{s}$, Peak Current= 15A , Servo Feed Rate= $20\text{mm}/\text{min}$ and Servo Reference Voltage= 50V (Contributed to finest surface finish= 1.957Ra).

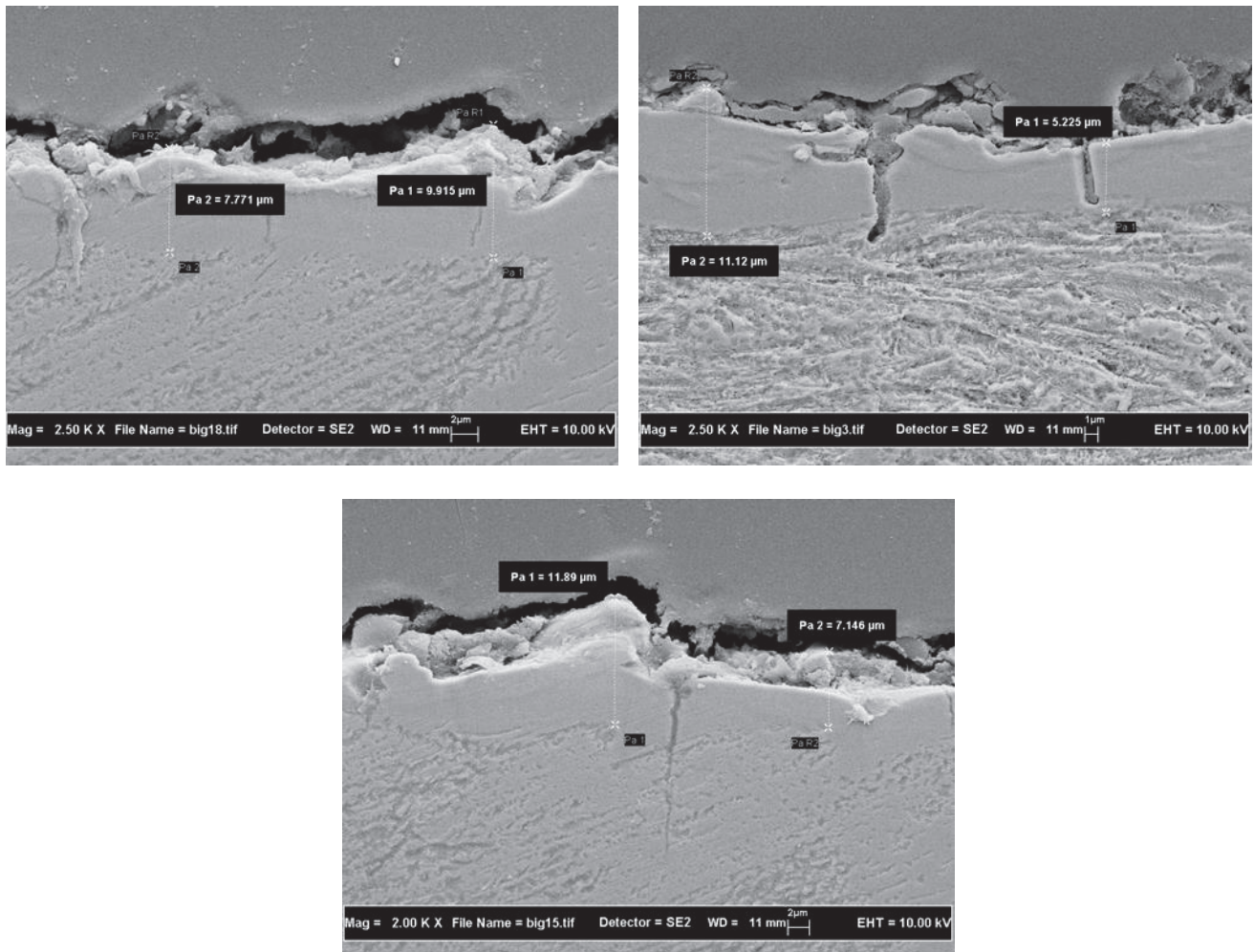


Figure 4.22: FESEM micrographs of cross sectioned specimen identify the recast layer with the thickness ranging from 5 μm to 12 μm (Machining Condition: On Time=6 μs , Off Time=10 μs , Peak Current=10A, Servo Feed Rate=20mm/min and Servo Reference Voltage=10V (Contributed to higher MRR=25.8783mg/min))

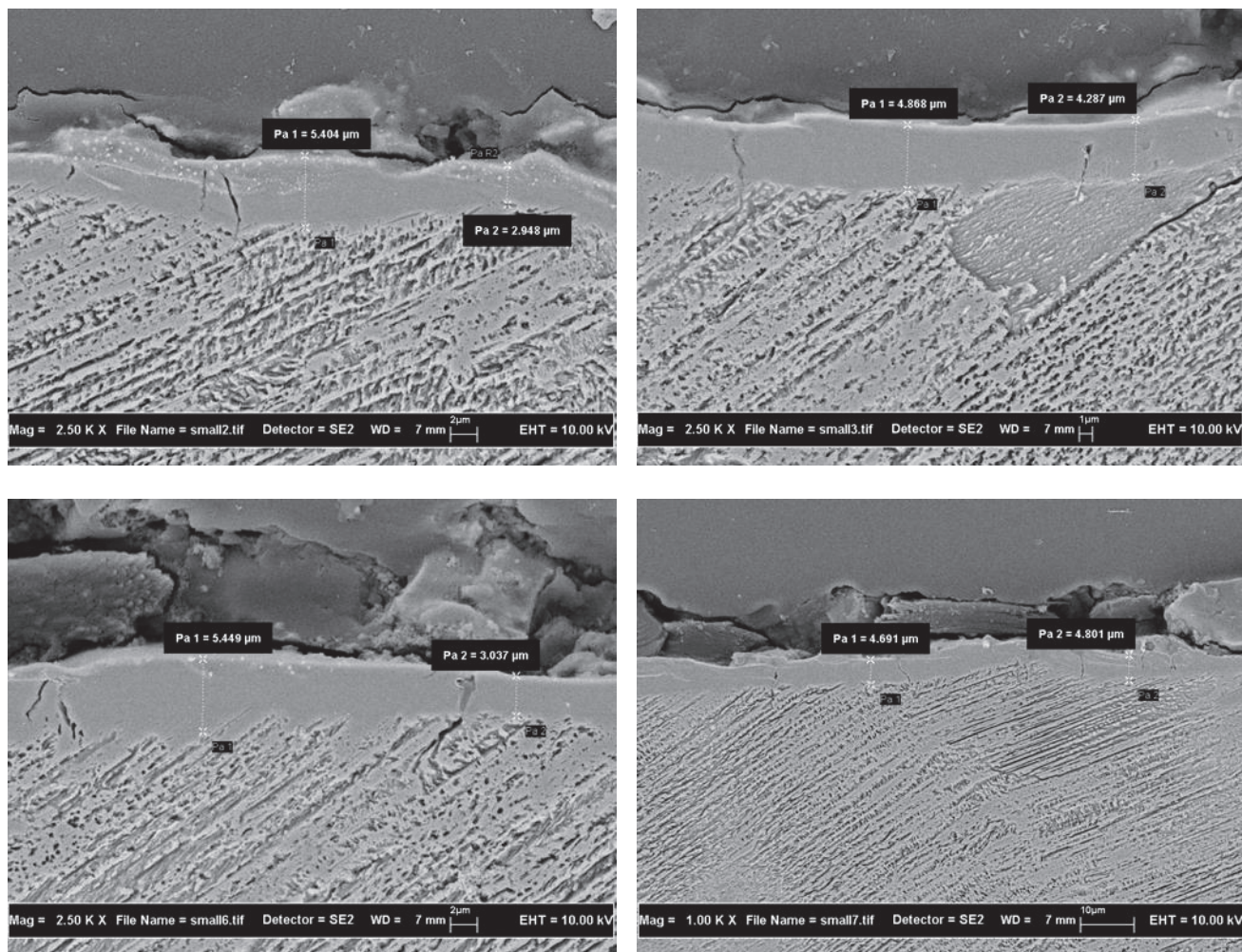


Figure 4.23: FESEM micrographs of cross sectioned specimen identify the recast layer with the thickness ranging from 2 μm to 6 μm , WEDM condition On Time=2 μs , Off Time=10 μs , Peak Current=15A, Servo Feed Rate=20mm/min and Servo Reference Voltage=50V (Contributed to finest surface finish=1.957Ra)

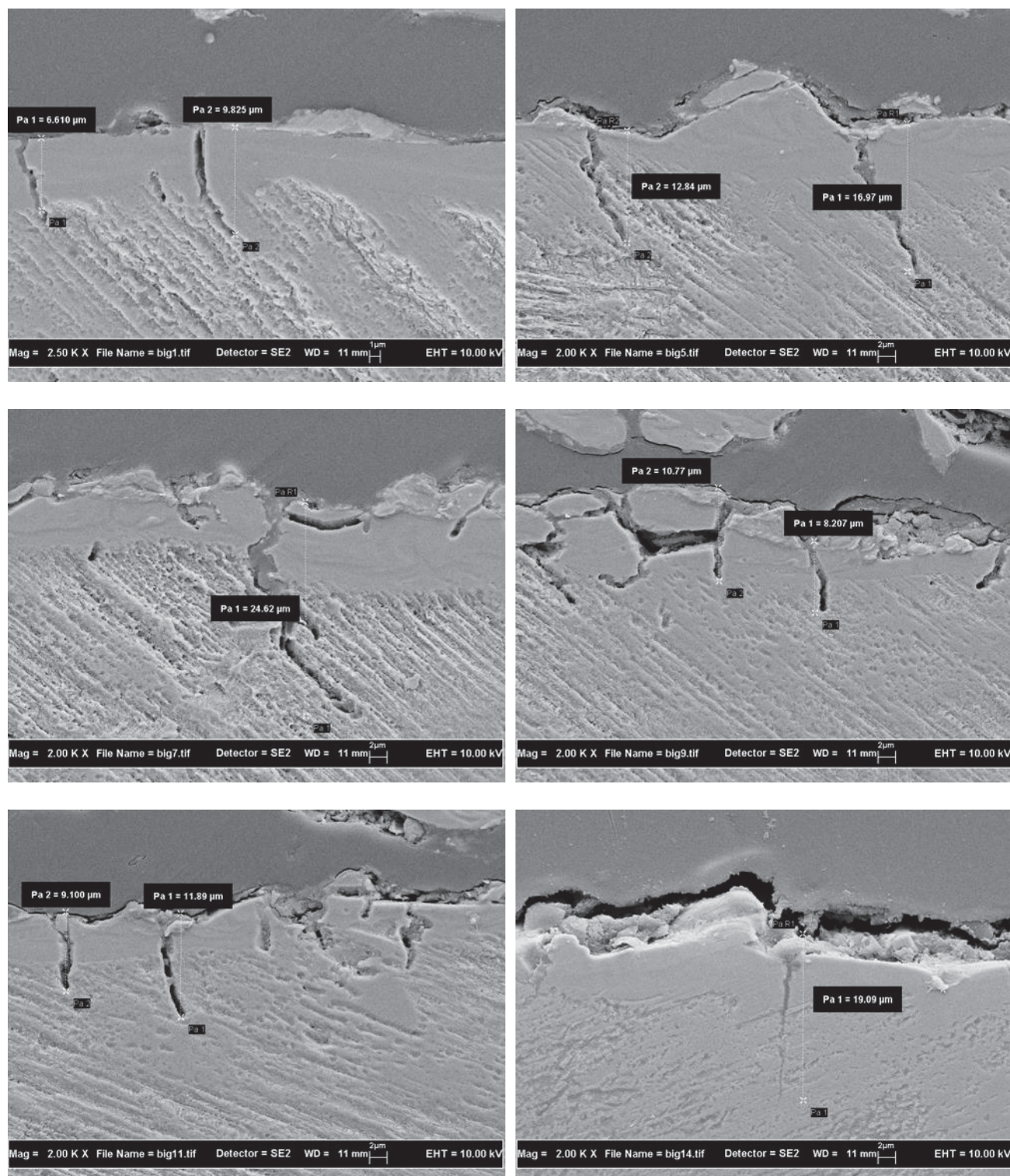


Figure 4.24: FESEM micrographs of cross sectioned specimen observed the micro crack penetrate deeper than recast layer as deep as 25 μm . Machining Condition: On Time=6 μs , Off Time=10 μs , Peak Current=10A, Servo Feed Rate=20mm/min and Servo Reference Voltage=10V (Contributed to higher MRR=25.8783mg/min)

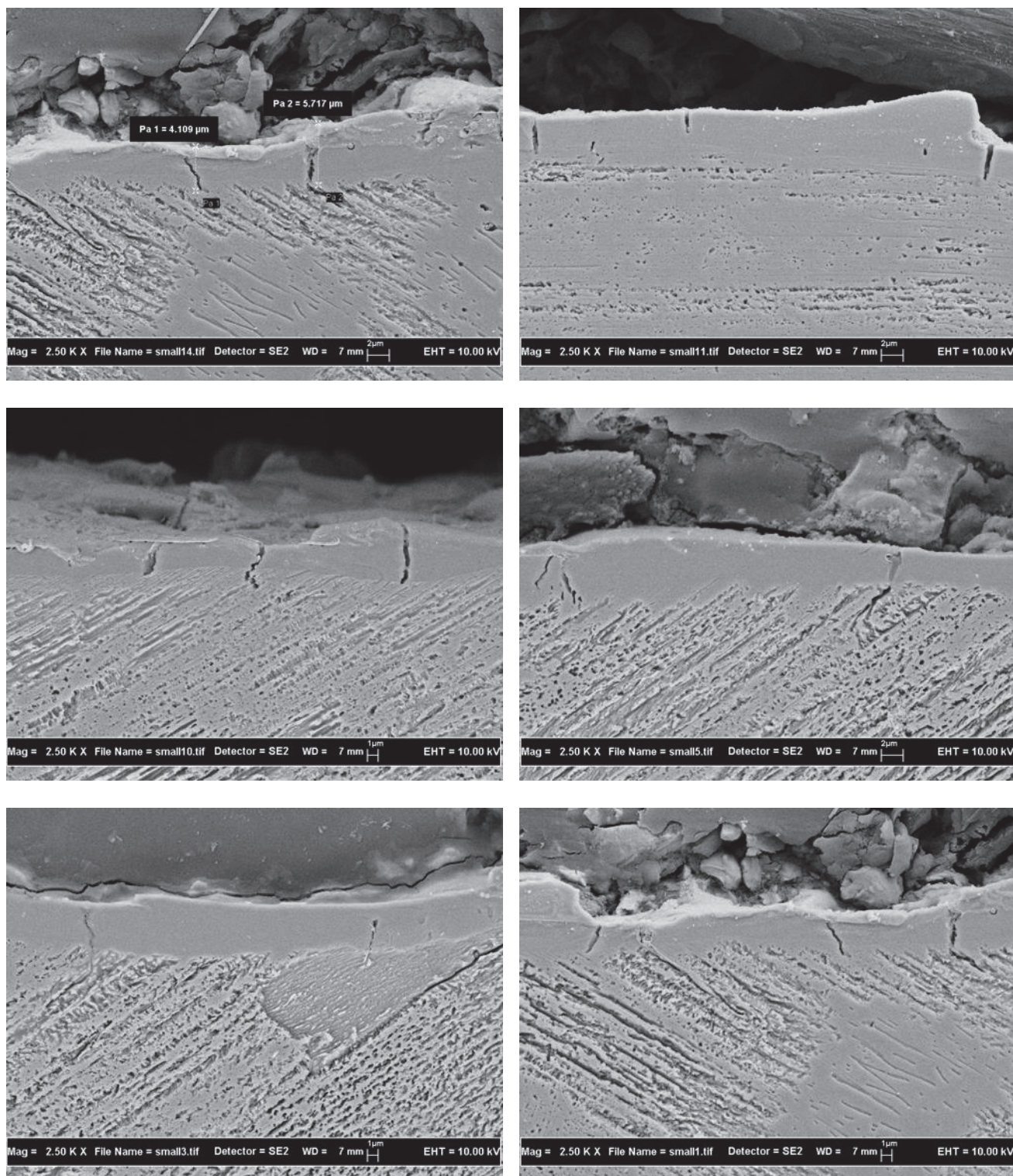


Figure 4.25: FESEM micrographs of cross sectioned specimen observed the micro crack penetrate deeper than recast layer as deep as $7\mu\text{m}$, WEDM condition On Time= $2\mu\text{s}$, Off Time= $10\mu\text{s}$, Peak Current= 15A , Servo Feed Rate= $20\text{mm}/\text{min}$ and Servo Reference Voltage= 50V (Contributed to finest surface finish= 1.957Ra)

b) EDX Line Scan Analysis

EDX line-scan analysis was performed along the cross-section of the specimen. Line scanning is able to plot the elements profile in atomic percentage across the layer to the base-alloy. Figure 4.26 – figure 4.29 illustrate the result of line-scan on the specimen cross-section. The result shows that the recast layer was mainly dominated by copper (Cu) and zinc (Zn). Figure 4.26 and figure 4.29 show the line scan analyses in the machining condition which resulted in finest surface finish. While figure 4.28 and figure 4.29 illustrate the analyses in the machining condition which contributed to higher material removal rate.

c) Spot Scan Analysis

Spot scan used to investigate and analyze the element present in the point of this specimen was taken. By taking any point in the cross sectioned machined of wire-cut illustrated the existence of element in the point taken. Figure 4.30 – figure 4.33 show the analyses were done with the difference point, also configure an element present in each point.

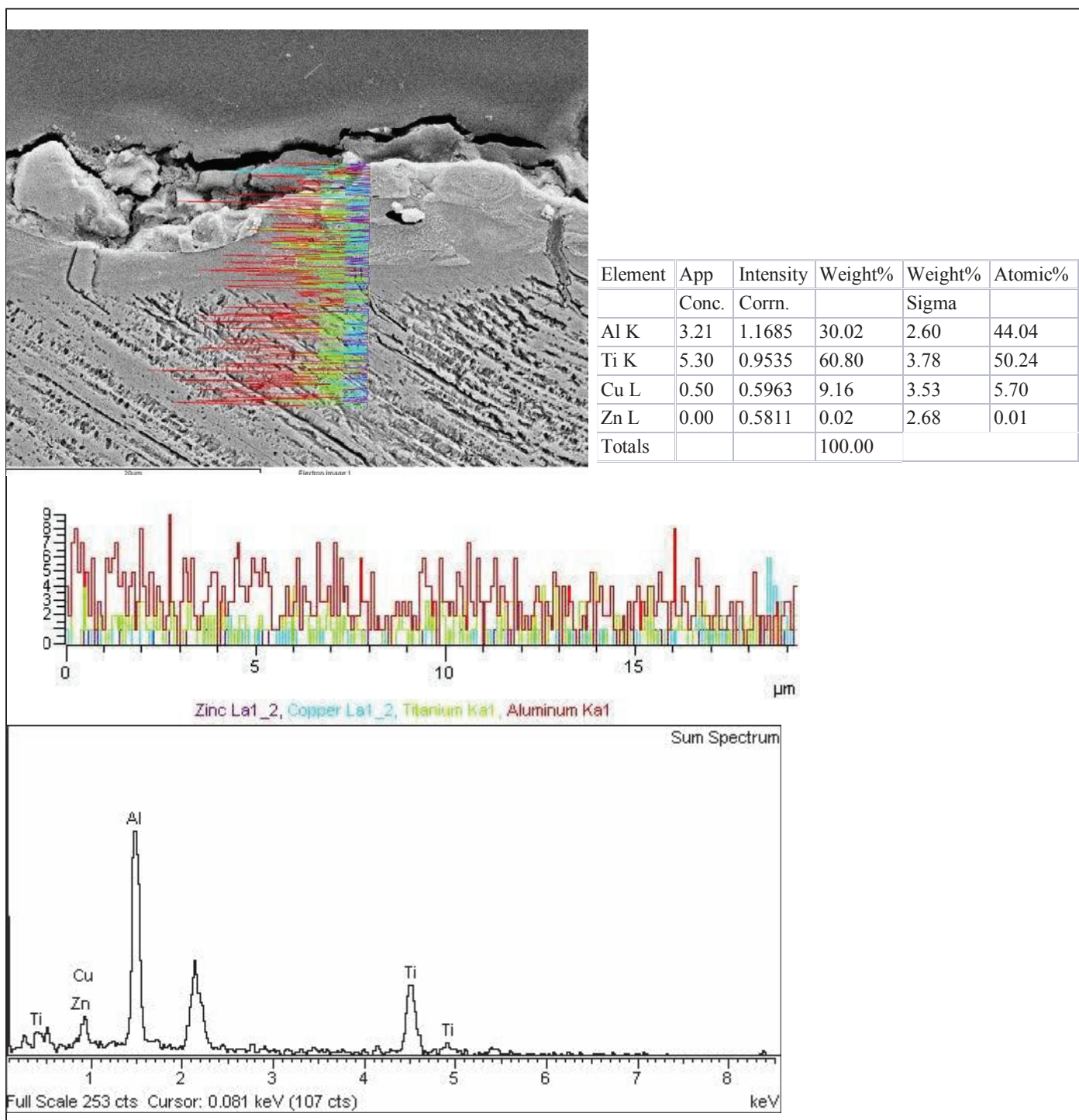


Figure 4.26: EDX line-scan profile of the elements present along the recast layer and base-alloy of the cross-sectional surface of WEDM Ti-48Al. WEDM condition On Time=2 μ s, Off Time=10 μ s, Peak Current=15A, Servo Feed Rate=20mm/min and Servo Reference Voltage=50V (Contributed to finest surface finish=1.957Ra)

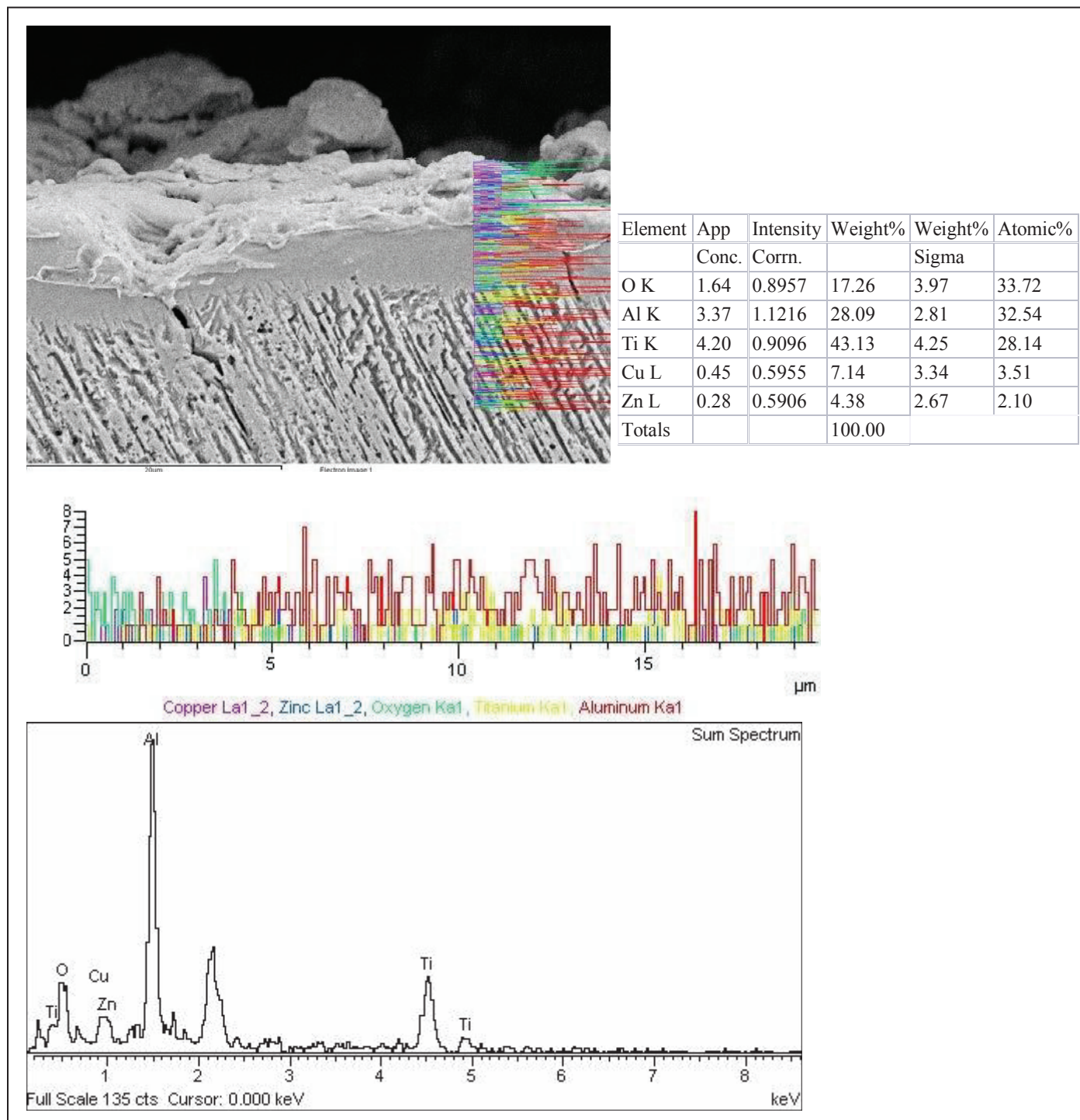


Figure 4.27: EDX line-scan profile of the elements present along the recast layer and base-alloy of the cross-sectional surface of WEDM Ti-48Al. WEDM condition On Time=2 μ s, Off Time=10 μ s, Peak Current=15A, Servo Feed Rate=20mm/min and Servo Reference Voltage=50V (Contributed to finest surface finish=1.957Ra)

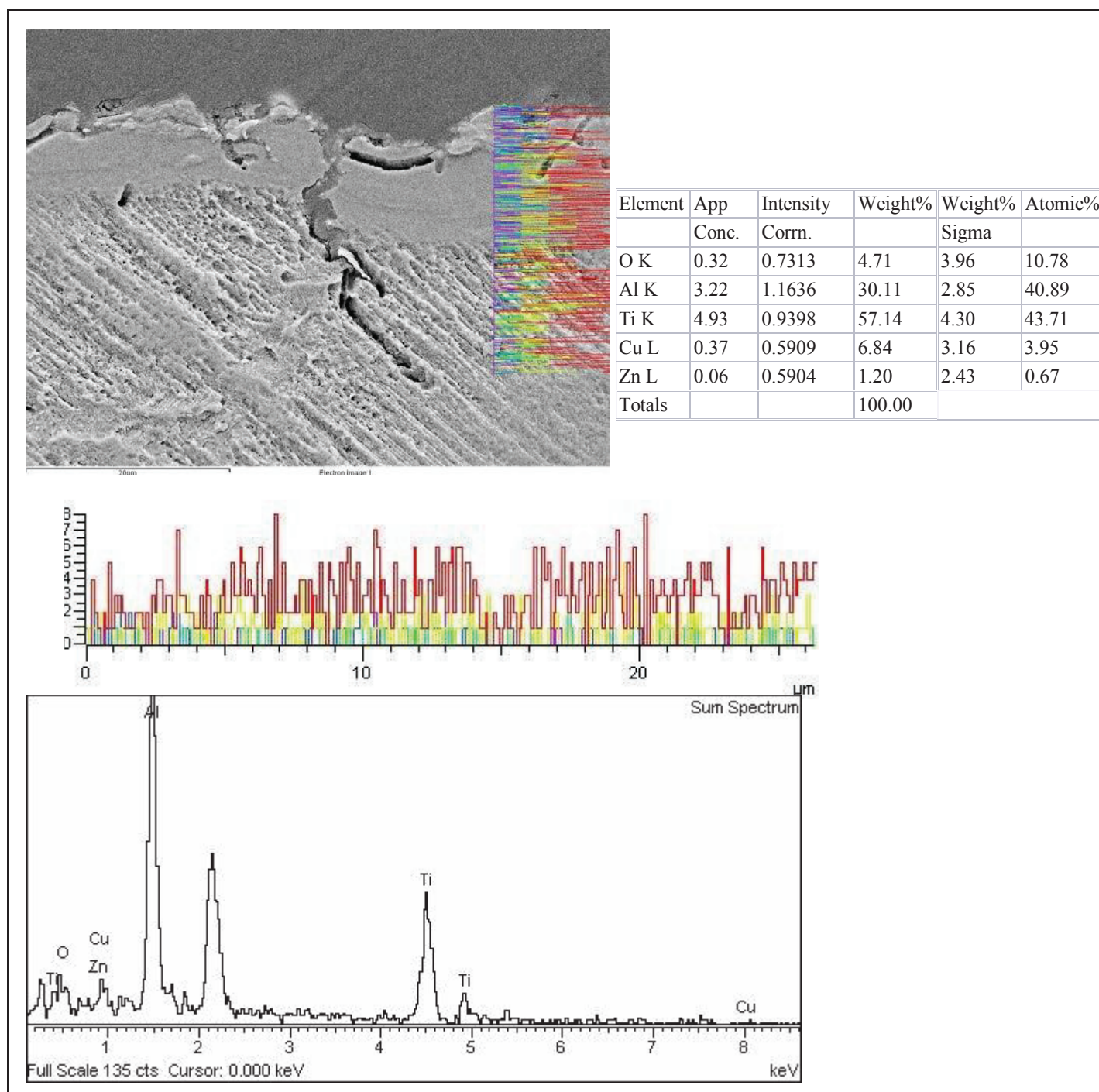


Figure 4.28: EDX line-scan profile of the elements present along the recast layer and base-alloy of the cross-sectional surface of WEDM Ti-48Al. Machining Condition: On Time=6 μ s, Off Time=10 μ s, Peak Current=10A, Servo Feed Rate=20mm/min and Servo Reference Voltage=10V (Contributed to higher MRR=25.8783mg/min)

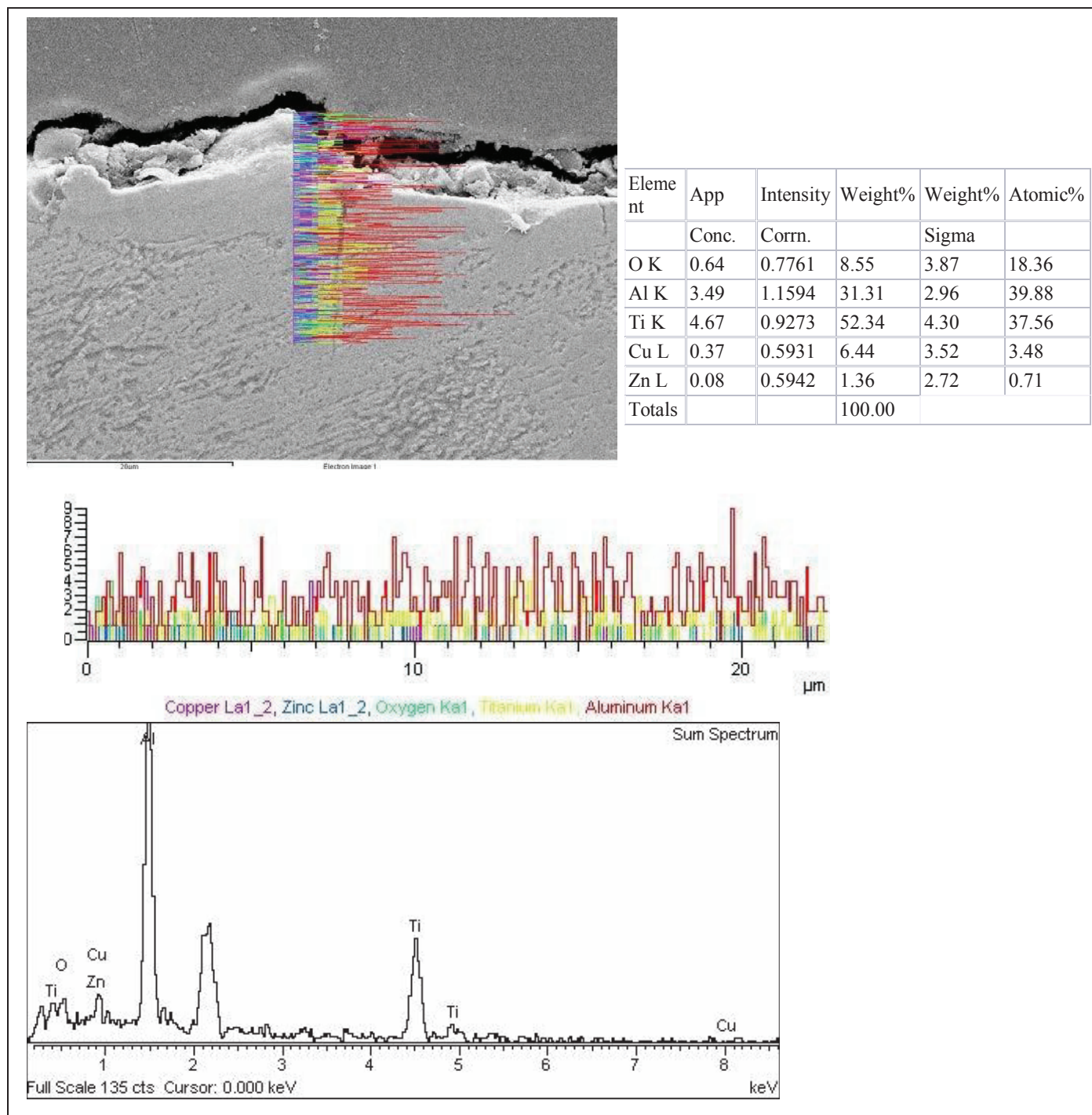


Figure 4.29: EDX line-scan profile of the elements present along the recast layer and base-alloy of the cross-sectional surface of WEDM Ti-48Al. Machining Condition: On Time=6µs, Off Time=10µs, Peak Current=10A, Servo Feed Rate=20mm/min and Servo Reference Voltage=10V (Contributed to higher MRR=25.8783mg/min).

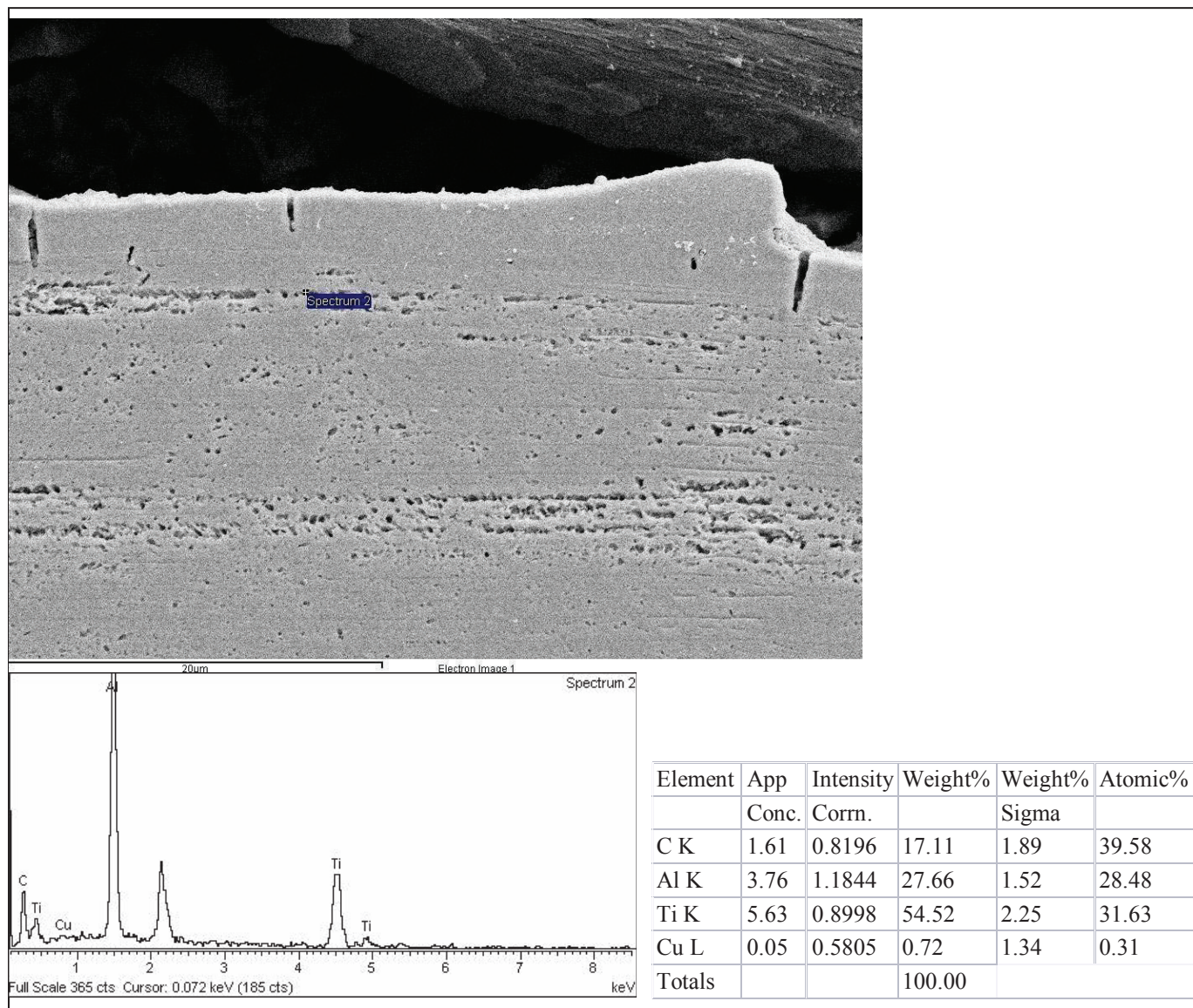


Figure 4.30: EDX spot-scan profile of the element present in the point was taken on the in the cross-sectional surface of WEDM Ti-48Al. The point mainly dominated carbon (C), Aluminum (Al), Titanium (Ti) and Copper (Cu).

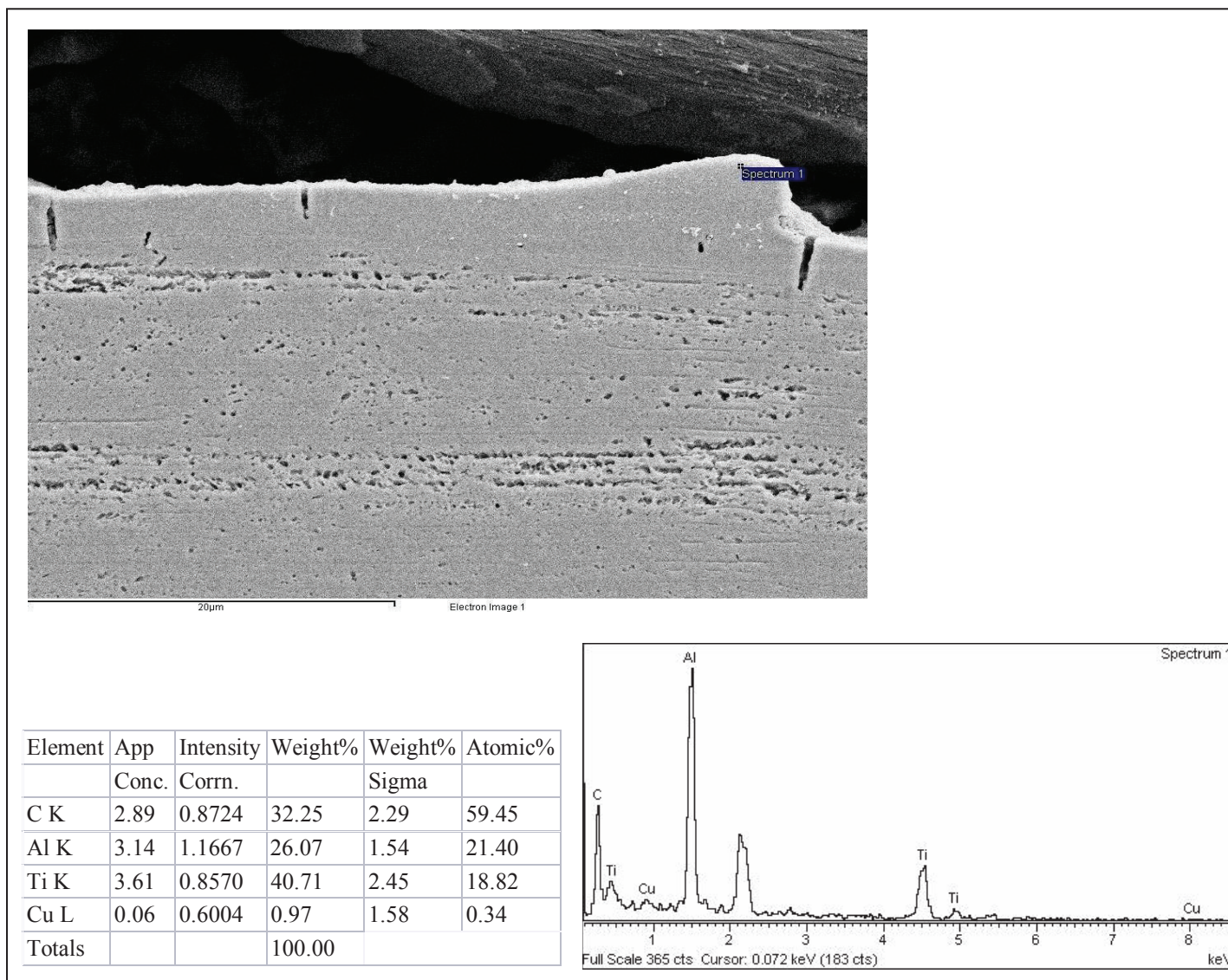


Figure 4.31: EDX spot-scan profile of the element present in the point was taken on the cross-sectional surface of WEDM Ti-48Al. The point mainly dominated carbon (C), Aluminum (Al), Titanium (Ti) and Copper (Cu).

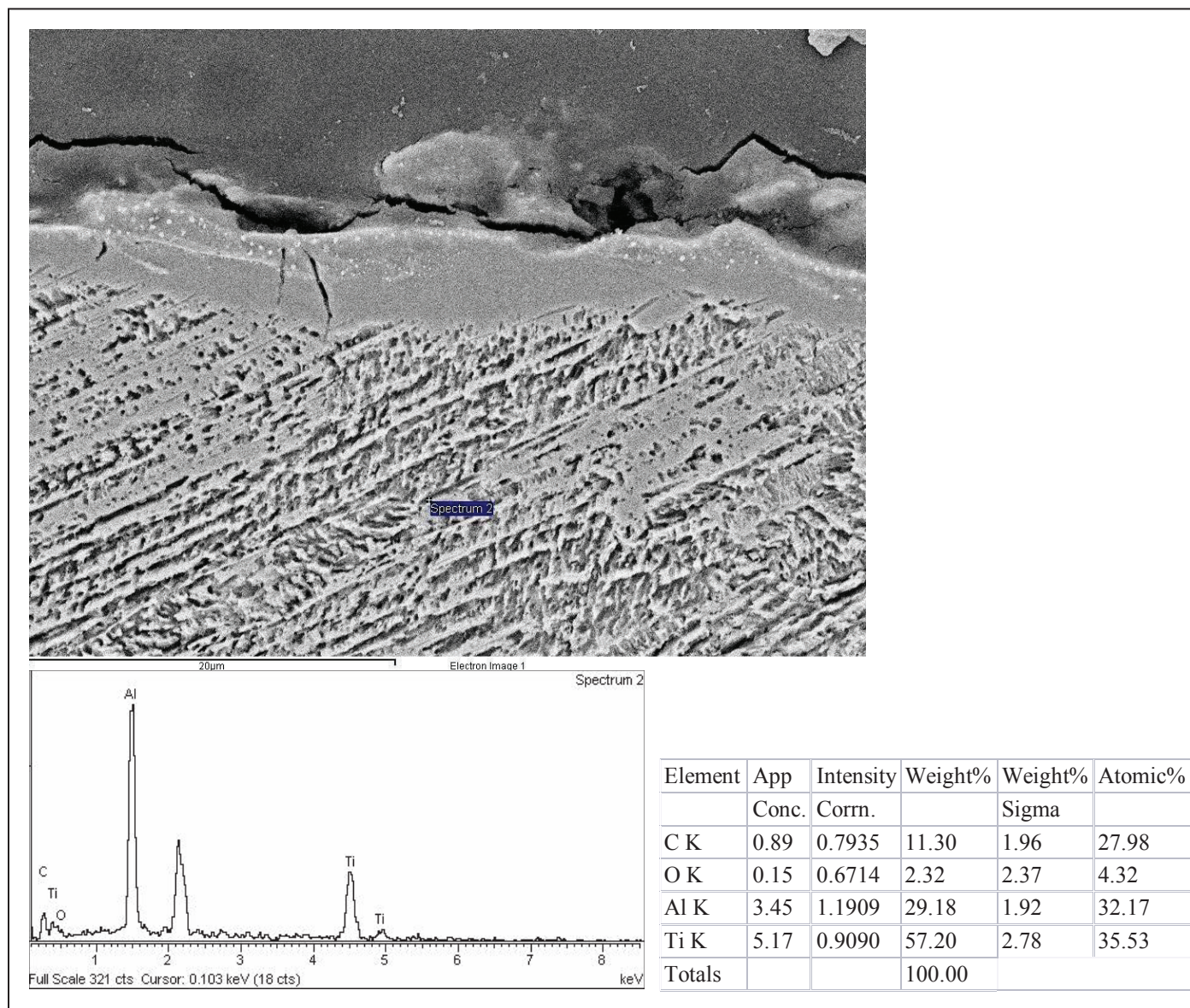


Figure 4.32: EDX spot-scan profile of the element present in the point was taken on the in the cross-sectional surface of WEDM Ti-48Al. The point mainly dominated carbon (C), Aluminum (Al), Titanium (Ti) and oxygen (O).

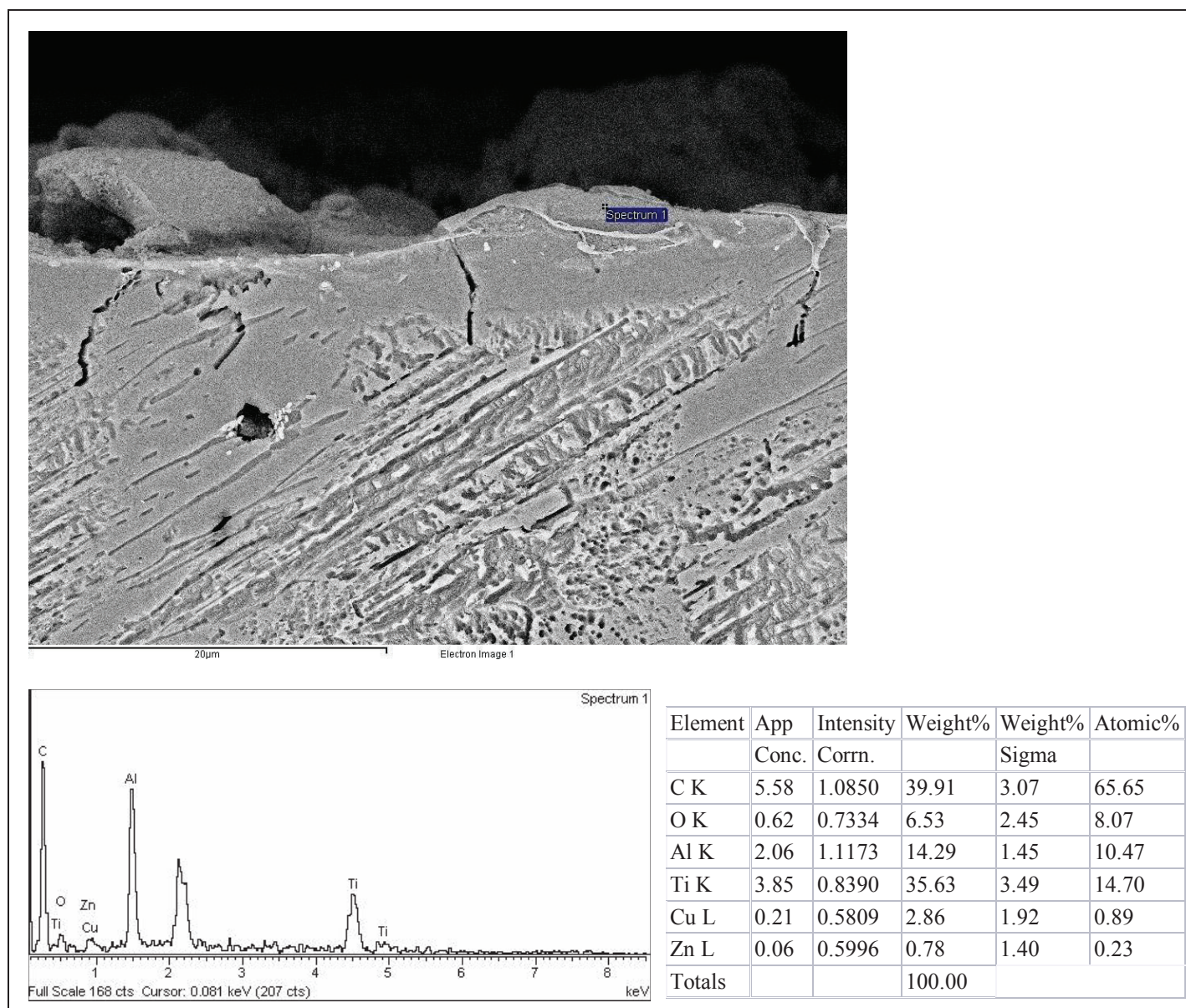


Figure 4.33: EDX spot-scan profile of the element present in the point was taken on the in the cross-sectional surface of WEDM Ti-48Al. The point mainly dominated carbon (C), Aluminum (Al), Titanium (Ti) and oxygen (O), copper (Cu) and Zink (Zn).

CHAPTER 5

DISCUSSION

This chapter will elaborate clearly about the relationship between the performance measure to the main parameters and it's influenced. The performance measures to be discussed will be cutting speed, material removal rate, surface roughness and kerf while the parameter including on time, off time, peak current, servo feed rate and servo reference voltage.

Further discussion scope will cover the surface properties induced by WEDM process on Ti-48Al. This will consist of oxidation on the top of machined surface, recast layer; microcracks and substances formed during machining by WEDM.

5.1 Parameters and Performance Measures

5.1.1 Cutting Speed and Material Removal Rate

The most important performance measure in wire-cut is cutting speed (material removal rate). Based on this study there are two significant factors observed during machining Ti-48Al. There are servo feed rate and pulse on time. Based on table 4.7 and figure 4.2, after pooled the insignificant factor at 90 percent confidence level servo feed rate contributed 95.924 % and followed by pulse on time (2.227 %). The sequence of significance of each factor was computed by Analysis of Variance (ANOVA). The percentage for error is 1.85% in the ANOVA computation due to no remaining degree of freedom (DOF) after assigning one DOF to each of the factor as shown in table 4.7. However, when signal to noise ratio (S/N) is employed, an L_8 orthogonal array there is only 7 DOF and it is described in equation 5.1.

$$\text{Degree of Freedom (DOF) with S/N ratio} = \text{number of trial condition} - 1$$

(i.e., Number of repetitions is reduced to 1)

Equation 5.1

Servo feed rate is found to be the dominant factor influencing the machining speed. According to the experiment done, it can be observed that servo feed rate obviously set the maximum cutting speed of wire-cut machine. For instance, if servo feed rate is set as 20mm/min, the wire-cut machine try to achieve this speed. However, it is constrained by other factors such as on time, off time, peak current and servo reference voltage and surrounding environment factors. Therefore, the cutting speed drastically increase when the servo feed rate is increasing, as described in figure 4.1(e).

The percentage contribution of on time in affecting machining speed is 2.227 %. When the on time increasing, the cutting speed slightly increase, as shown in figure 4.4(a). It is proved by other researchers [31, 49]. Increasing pulse on time means lengthen the time for material removal and amplifying the peak current added more power and sparks during discharging: hence improving speed. While increasing pulse duration (off

time) and servo reference voltage will slowed the cut. Analogously, higher pulse off time caused less time for machining and slowed the cut. Increasing both servo feed rate (table feed) and pulse on time while reducing both of pulse interval (off time) and servo reference voltage directly improved the machining speed (table 4.1 will describe for this).

The second part for this topic discussed about material removal rate (MRR). This response requires opposite consideration from surface roughness (Ra) and cut-width (kerf) in term of determining optimization settings for all the five factors. This is due to the fact that surface finish and kerf optimization objectives is to obtain as minimum as possible where design of Taguchi methodology define it as “the smaller the better” while MRR and cutting speed optimizations are to maximize both responses or “ the bigger the better”.

Based on the table 4.11 and figure 4.4, servo feed rate contributed 90.335 % and pulse on time contributed 5.614% after pooled the insignificant factor at 90 percent confidence level. Servo feed rate is found to be the dominant factor affecting the material removal rate. From this experiment, it can be observed that servo feed rate obviously set the higher material removal rate for the WEDM machine. MRR increased drastically as servo feed rate was amplified, as in figure 4.3(e). Similarly to cutting speed response, if servo feed rate is set as 20mm/min; the machine will try to achieve this removal rate. However, is constrained by other factors (on time, off time, servo reference voltage and peak current) and the surrounding environment influence factors.

The percentage contribution of on time in affecting MRR is 5.614%. When the on time is increased, the MRR slightly increased as shown in figure 4.3(a). This result corresponds to previous researchers' finding. It is obvious that increasing on time caused longer time for machining and logically higher MRR was achieved. Analogously, increasing off time (OFF) and servo reference voltage (SV) resulted in a shorter time machining thus smaller MRR was achieved.

5.1.2 Surface Finish and Kerf

Figure 4.6 shows that “interaction ON x OFF” contributed 44.297% followed by pulse off time (28.16%) and servo feed rate (15.645%). “Interaction ON x OFF”, off time and servo feed rate are the significant factors which influenced the surface finish while peak current, on time and interaction OFF x Peak current insignificant factor. Once again, there is 11.898% of error in ANOVA computation due to four remaining of DOF after assigning one DOF to each of the seven factors. Otherwise, for more detail on surface roughness, refer to table 4.15, 4.16, 4.4 and figure 4.5.

According to the table 4.27, the finest surface finish generated by Taguchi method is 1.941 μm . In actual experiment, the finest surface finish obtained was 1.957 μm when machining at optimum WEDM condition suggested by the Taguchi method as followed; on time=2 μm , off time=10 μm , peak current=15A, servo feed rate=20mm/min and servo reference voltage=50V. Therefore, the percentage of error is only 0.8% so it is proved as evidence that the Taguchi method is reliable in improving the surface finish.

As mentioned before, surface roughness and kerf optimization objectives is to obtain as minimum as possible where Taguchi method defines it as “the smaller the better” opposite to both of cutting speed and MRR defined as “the bigger the better”. By referring to figure 4.8 illustrate that the contribution factor on kerf as a response. Servo feed rate contributed as 31.22% followed by off time (28.714%) and Peak current (27.85%). It was determined that the servo feed rate, off time and peak current are the significant factors as compared to others. Likewise, refer to table 4.3, 4.19, and 4.20 and figure 4.7 for detailed description.

As show in table 4.28 the smaller kerf generated by Taguchi method is 283.498 μm . In the actual experiment, the smaller kerf obtained was 285.875 μm . The condition of WEDM machined to achieve the optimization are on time =2 μs , off time=10 μs , peak current, servo feed rate=20mm/min and servo reference voltage=50V.

Consequently, the percentage of error 4.05%, Taguchi method is reliable in improving the kerf.

5.1.3 Response optimization

After completed analyzing and discussing all the four responses, the factor need to be optimized must correlate accordance to the objective and the goal. The optimization process can be divided into different parts which:

- a) Minimizing or “the smaller the better” for surface roughness, Ra and width of cut, kerf.
- b) Maximizing or “the bigger the better” for cutting speed and material removal rate, MRR.

The value of each response, which is required for optimization, can be calculated from each response’s from the ANOVA analysis. In ANOVA, the relationship equations and coefficient under coded units between factors affecting each response can be determined. From those calculations, the result values were forwarded as target value for optimization.

Table 5.1: The factors and its level after analyze by ANOVA

Factor	WEDM Condition (Level)			
	Maximizing		Minimizing	
	Cutting speed	MRR	Surface roughness	Kerf
On time	2	2	1	1
Off time	1	1	1	1
Interaction (On x Off)	1	1	2	2
Peak current	1	1	2	2
Servo Feed Rate	2	2	2	2
Interaction (Off x Peak Current)	1	1	1	1
Servo reference voltage	1	1	2	2

Based on the parameter condition shown in table 5.1, verification run were done according to the response to be analyzed. The results for this verification elaborated in table 5.2.

Table 5.2: Comparison responses between experiments (confirmation run) with the predicted.

Result	Responses			
	Maximizing		Minimizing	
	Cutting Speed (mm/min)	MRR (mg/min)	Surface Roughness (μm)	Kerf (μm)
Theoretical	1.9260	23.8530	1.941	283.498
Experiment	1.9819	25.8783	1.957	285.875
Error (%)	2.90	8.50	0.80	0.83

After calculated followed by the equation 4.4, the purpose is to make comparison between theoretical results and experimental results. By solving the calculation, the margin of error percentage for cutting speed is 5.67%, material removal rate will be 2.67%, surface roughness 5.0% and the kerf is 4.05%. Actually, this is an evidence to prove that this experiment was succeeded because the aim of the margin error percentage less than 10%.

Table 5.3: Summary of the responses obtained throughout this experiment.

Performance Measure	Data Range
Cutting Speed (mm/min)	0.8820 – 1.9833
Material Removal Rate (mg/min)	10.2829 – 26.5643
Surface Roughness (μm)	1.75 – 2.63
Kerf (μm)	281.77 – 341.63

Table 5.2 summarizes the range of cutting speed, material removal rate, kerf and surface roughness obtained throughout this research. It can be observed that the cutting speed lowest value of 0.8820mm/min to highest value of 1.9833mm/min. However, the

range for the material removal rate is 10.2829 mg/min (lowest) to 26.5643mg/min (highest). While the surface roughness values are fall between 1.75 μ m to 2.63 μ m followed by width of cut (Kerf) as lowest 281.77 μ m to 341.63 μ m. Understanding that the surface finish is varying not much, one can increase the cutting speed to the maximum for roughing cut as long as there is no wire breakage problem. Anyway, the selection of the WEDM conditions is much dependant on the surface finish desired to be obtained. If surface finish better than 2 μ m is desired, more than one cutting pass is necessary in order to obtain the desired surface finish. On the other hand, if surface finish is not a concern, WEDM conditions should be set for fastest cutting speed.

5.2 Surface Morphology and Characterization of Ti-48Al

5.2.1 Direct Machined Surface

Figures 4.16 (a) and (b) show the FESEM micrographs of the surface morphology of Ti-48Al after WEDM process under various parameter settings. At magnification of 250x, it can be observed that they show almost the same roughness pattern, with many small spherical bumps and hollows which in turn contain numerous micro holes. In addition, there are cracks along the surface. WEDM process resulted a multidirectional or no lay surface finish on the surfaces instead of the directionally pattern of a conventionally machined surface. However, it can be observed that surface in Figure 4.16 (b) apparently illustrates a better surface topography with less denser compared to surfaces shown in Figure 4.16 (a). In fact, surface finish shown in Figure 4.16 (b) is the finest surface finish obtained in this research, with a surface roughness of $1.957\mu\text{m}$ (measured by Taylor-Hobson).

The surface texture is composed of a random array of overlapping craters or cusps, as shown in Figure 4.16, after machining. During each electrical discharge, intense heat is generated, causing local melting or even evaporation of the workpiece material. With each discharge, a crater is formed on the workpiece. Some of the molten material produced by the discharge is carried away by the dielectric circulation. The remaining melt resolidifies to form an undulating terrain.

At magnification of 2500x and higher, it can be actually observed that there are fine crystals formed on top of the surface produced by WEDM process, as shown in Figure 4.17 (a) to (c). The crystals can only be observed under high magnification and covering the entire surface. The crystals are believed to be the “oxide layer” formed during the WEDM process which involved high temperature (up to $12,000^{\circ}\text{C}$). This assumption is made based on the EDS result (see Figure 4.18 (a) to (c)) showing the evidence of the present of oxygen element. See also figure 5.1 that illustrates the presence of oxide layer on the top of machined surface analyzed by EDX line scan. It is noticed

that a mixture of oxides is formed on the surface, due to the machining process, as the heat concentration on the machined surface is not uniform.

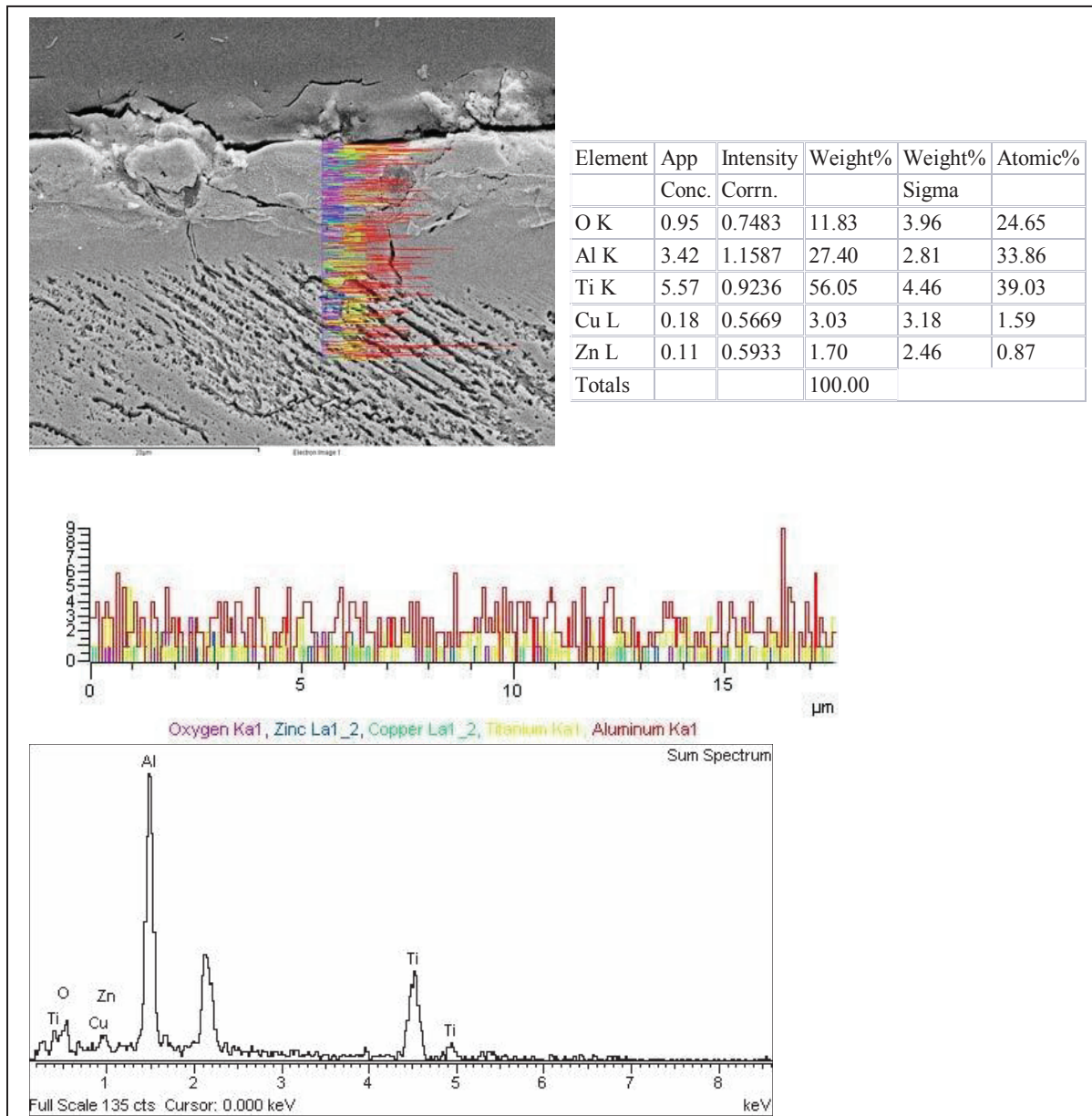


Figure 5.1: The existence of oxide layer on the top of machined surface analyzed by EDX line scan.

Each specimen is machined at different combinations of parameter. According to the previous researchers [50, 45], titanium and its alloys have very high affinity to oxygen. In normal condition, a natural oxide layer of few nanometers thickness is always

present on the surface. This acts as a protective layer and prevents further oxidation. A thicker oxide layers will be formed due to thermal oxidation during machining.

From the FESEM micrograph in Figure 5.2, it can be found that pores with diameter ranging from $0.5\ \mu\text{m}$ to $2\ \mu\text{m}$ are formed on the surface. Actually the pores are the craters produced by the spark during the WEDM process. The actual depth of the crater is not known at the present level, but it is believed to be varying, depending on the machining factors such as on time, peak current, servo reference voltage etc; and also the hardness of material at that particular spot. Many substances with different sizes and shapes were also found to be scattered around the surface (as shown in Figure 4.17). With the help of the EDS analysis (as shown in Figure 4.18), it is known that the elements were present in the substances.

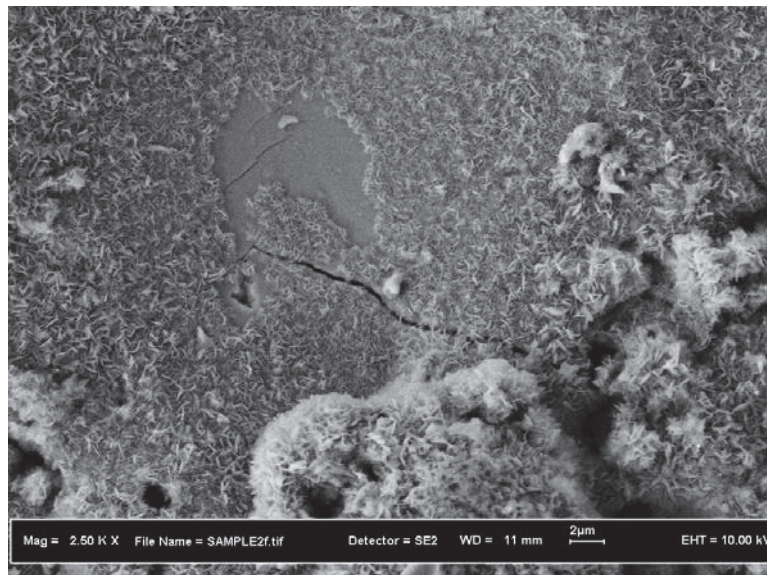


Figure 5.2: Pores or voids found and formed on the surface.

Figures 4.18 (a) to (c) illustrate EDS spectrum for various features found on the surface of the machined Ti-48Al. The common elements found in the EDS results were titanium, aluminum, copper, zinc and oxygen. The presence of titanium and aluminum can be easily understood as they are from the base-alloy of Ti-48Al. The existence of copper and zinc were probably contributed by the brass wire which was used to cut the

material. Under high temperature during the WEDM process, the base-alloy (titanium and aluminum) and some of the wire material (copper and zinc) were fused together and resolidify to form a recast layer. At the same time, oxidation process occurred where titanium and aluminum reacted with oxygen to form aluminum titanium oxide teolite (Al_2TiO_5). This explains the existence of oxygen element in the EDS result and also the formation of crystals (oxide layer).

5.2.2 Cross Sectional Analysis

The cross sectional analysis obviously to investigate the microcrack and the layer affected due the condition of machining Ti-48Al. As expected, recast layer and microcrack were found in the cross section of the specimen. According to other researcher (Ahmet Hascalyk *et al.*, 2004) [51], the formation of the recast layer is due to resolidification process of the base-alloy (titanium and aluminum) and the wire material (brass). During the WEDM process, not all of the workpiece material melted by the spark is expelled into the dielectric. Some of the workpiece material together with material from the wire will quickly chilled, primarily by heat condition into the bulk of the base-alloy, resulting in formation of recast layer.

As shown in figure 4.20, for the higher material removal rate (25.878mg/min) will contributed more thickness recast layer as compared to the finest surface finish (see figure 4.21). MRR has higher range of thickness of recast layer i.e. $5\mu\text{m}$ to $12\mu\text{m}$ whereby finest surface finish ranges between $2\mu\text{m}$ to $6\mu\text{m}$. The differences of both situations are caused by the condition of machining parameters. The thickness of the recast layer is believed to be depending on the parameters will be taken for the responses, the real time temperature and surrounding environment condition during the cutting process.

Likewise, the microcrack penetration for the higher MRR influencing the deeper penetrate as deep as $25\mu\text{m}$ but for the finest surface finish the depth of penetration as deep as $7\mu\text{m}$ (see figure 4.22 and 4.23 for proven and comparison). Similarly, the depth of penetration of microcracks is believed to be depending on the parameters will be taken for the responses, the real time temperature and surrounding environment condition during the cutting process. Both recast layer and microcrack has negative effect. It will affect the precision of desired dimension and will result in visual imperfection in the final product. Therefore, it is necessary to grind and polish the machined material in order to remove the recast layer before service.

Figure 4.24 to figure 4.27 shown the line scanning analysis result that illustrate the element profile along the scanning performed. It can be observed that there is significant difference of element composition. The difference is mainly due to the presence of recast layer. The recast layer is mainly built up by zinc and copper, which are the wire material (brass). Besides that, oxygen element was found in the recast layer due to oxidation process during the WEDM of Ti-48Al (see figure 5.3).

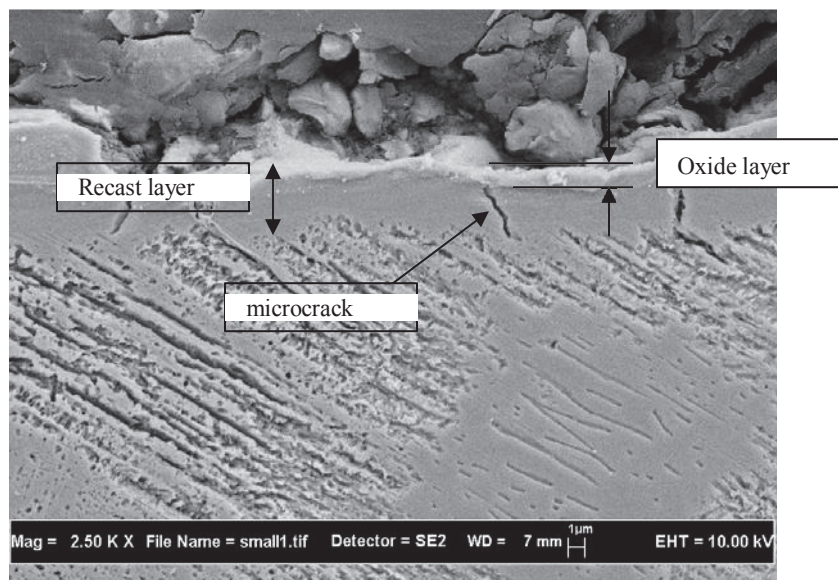


Figure 5.3: Oxide layer formed on the top surface

Spot scanning analysis result (as shown in Figure 4.28 to Figure 4.31) illustrates the element profile on the point where the scanning was performed. Likewise, to the line

scanning, spot scan is focused only on the point which was selected on the cross sectional surface. The point determines the presence of elements using the EDX spot scan. Based on figure 4.28 and 4.29, the point was taken in the recast layer mainly dominated by Carbon (C), Aluminum (Al), Titanium (Ti) and Copper (Cu). However, referring to Figure 4.30, Copper is not present in that point because the point was taken away from the machined surface obviously not affected by the wire material (brass). But figure 4.31 illustrates that oxide was present because the point taken is near the top surface where oxide exists.

CHAPTER 6

CONCLUSIONS AND RECOMMENDATIONS

6.1 Conclusion

Reviewing all the objectives stated at the beginning of this study, it is infallible that all the goals determined are achieved accordingly. The study was conducted using 0.2mm diameter brass wire and the workpiece used was Ti-48Al while all experiment runs, planning and analysis were done using Taguchi Design Methodology. All experiment runs was performed on a linear motored AQS37L Fine Sodick 5-Axis. The following conclusions can be drawn the study:

- a) In WEDM of Ti-48Al, the fastest cutting speed obtained is 1.982mm/min when the WEDM conditions are set accordingly (on time= 6 μ s, off time=10 μ s, peak current= 10A, servo feed rate= 20mm/min servo reference voltage= 10V). ANOVA result shows that servo feed rate is the most significant factor in affecting the cutting speed, with percentage contribution of 95.93%. The experimental findings show that the cutting speed increases with servo feed rate and on time, but decreases with servo reference voltage and peak current.

- b) The higher material removal rate is 25.8783mg/min with the percentage of error 8.5% compare to the theoretical result when the WEDM conditions are set accordingly (on time= 6 μ s, off time=10 μ s, peak current= 10A, servo feed rate= 20mm/min servo reference voltage= 10V). Servo feed rate is the significant factor with the percentage contribution 90.34% followed by on time (5.62%), other factors are not significant.
- c) The finest surface finish obtained in this research is 1.957 μ m and was achieved when the WEDM conditions are set at: on time= 2 μ s, off time=10 μ s, peak current= 15A, servo feed rate= 20mm/min and servo reference voltage= 50V. It was found that interaction ON x OFF, off time and servo feed rate is the significant factor in affecting the surface finish. The contribution of other three factors (peak current, on time, interaction OFF x peak current and servo reference voltage) are not significant.
- d) Servo feed rate with 31.22%, Off time (28.72%) and Peak current(27.85%) are the significant factor affecting the smaller width of slit (kerf) as 285.875 μ m with the error 0.83% compared to theoretical result. The condition of WEDM is similarly with the surface roughness machining condition.
- e) Servo feed rate is the most significant factor of all the seven parameters (including interaction ON x OFF and interaction OFF x peak current) used in this study since servo feed rate appeared to be the main effect for all four responses.
- f) Void, crater and crack were found on the WED machined surface of Ti-48Al. At high magnification, the surface appeared too many substances and hollow contain numerous micro holes. Oxide layer is present on the top of the machined surface.
- g) Recast layer formed during WEDM of Ti-48Al with different ranging thickness depending on machining condition was taken. For contribution higher MRR and fastest cutting speed the recast ranging from 5 μ m to 12 μ m while for finest surface finish and smaller kerf the recast thickness is between 2 μ m to 6 μ m(finest surface

finish will reduce the recast thickness during WED machined). Obviously, recast layer is build of wire material (copper and zinc).

- h) Microcrack was found, the deeper crack penetrate depends on machine condition while the WEDM condition contributed fastest cutting speed and higher MRR the penetration of crack exceeding $25\mu\text{m}$ while the WEDM condition contributed finest surface finish and smaller kerf will reduce the crack penetrates as deep as $7\mu\text{m}$.
- i) Both the fastest cutting speed and finest surface finish cannot be achieved simultaneously with single WEDM condition set. When the cutting speed increases, the surface finish will deteriorate and vice versa. Therefore, both of this performance measures need to compromise each other. Depending on the WEDM conditions, the cutting speed can range from 0.8820 mm/min – 1.9833mm/min , whereas surface roughness only varies from $1.75\mu\text{m}$ to $2.63\mu\text{m}$. If surface finish is not a major concern (greater than $2.63\mu\text{m}$), WEDM conditions can be set for maximum cutting speed. On the other hand, surface finish is better than $1.75\mu\text{m}$ requires more than a single cutting pass, with proper WEDM condition settings.
- j) Material and metallurgical properties of Ti6Al4V contributed to the overall machining performance in terms of all the four responses focused in this study. Any adjustment of the parameter settings must correlate to the properties. Poor conductivity of Ti-48Al contributed to wire pitting and breakage, poor heat dissipation, poor sparks distribution and large crater. While the extreme hardness of titanium alloys resulted in difficulties of particles chipping; requires repetitive cuts in order to obtain the best settings.

6.2 Recommendation for further studies.

From the performed experiments, the observations and analyzing the findings, some shortcomings were encountered and from the optimization solutions, a few suggestions for further study were proposed as follows:

- a) Different wire materials need to be considered for better understanding of the effect on surface characteristics of wire material plunged into the workpiece surface consequent upon wire pitting. For example, a study using two different wires with zinc coated and uncoated brass wires. Besides, the effects and interactions between wire material and Ti-48Al can be identified.
- b) The minimum and maximum level for each of the factor should be wider in range and selected in such a manner that there will be no wire breakage problem when the levels of the factors are combined together during the actual cutting process. This can be done by conducting preliminary run to test the machine limit.
- c) Different orthogonal arrays (OA) by using Taguchi Methodology may will be used in the experiment such as L_{18} or L_{27} so that more trial can be run and more factors can be investigated to find more significant parameters as to get a better performance results.
- d) In WEDM Sodick AQ537L the setting MAO can be changed to finding the difference result during machining.
- e) The effect of parameters due to recast layer and microcrack will be further analyzed in term of proven the performance results if “the bigger the better” will give more deeper crack penetration and more thicker recast layer as compared to “the smaller the better” respectively.

REFERENCES

1. S.Sarkar, S. Mitra, B. Bhattacharyya, (2005), Parametric Analysis and Optimization of wire electrical discharge machining of γ -titanium aluminide alloy, Journal of Material Processing Technology
2. B. Pan, D.J. Kim, B.M. Kim, T.A. Dean, (2001), Incremental deformation and the forgeability of γ -titanium aluminide, Int. J. Mach. Tools Manuf. 41: 749–759.
3. T.A. Spedding, Z.Q. (1997), Wang, Study on modeling of wire EDM process, J. Mater. Process. Technol.

4. Scott D, Bovina S, Rajurkar KP (1991) "Analysis and optimization of parameter combinations in wire electrical discharge machining". Int J Prod Res 29(11):2189– 2207.
5. Agietron Corporation (1982), Understanding EDM surface integrity Addison,III
6. Prazda, T.J, Wick C.,(1983). Tool and Manufacturing Engineer Handbook: Vol I Machining and Manufacturing Engineers,
7. Brochure ASSAB Steel
8. Dauw DF, Albert L (1992) "About the evolution of tool wears performance in wire EDM".
9. Indurkha, G., and Rajurkar, K. P., (1995), Artificial Neural Network Approach in Modeling of EDM and Wire-EDM Processes, Special Issue of IIE Transactions on Design and Implementation of Intelligent Manufacturing Systems, Parsaei, H. R., Ed., pp. 161-186
10. Wang, W. M., and Rajurkar, K. P., (1994), Adaptive Control of WEDM by on-Line Identifying Workpiece Height, Transactions of NAMRI/SME, Vol. XXII, pp. 73-78.
11. Rajurkar, K. P., and Wang, W. M., (1993), Thermal Modeling and On-line Monitoring of Wire-EDM," Journal of Materials Processing Technology, Vol. 38: pp. 417-430.
12. Wang, S. Z., and Rajurkar, K. P., (1993), Study of Wire Electrical Discharge Machining of Polycrystalline Diamond, Transactions of the NAMRI, Vol. XXI: pp. 139-1